

# Alternative Methods for Evaluation of Oxygen Transfer Performance in Clean Water

---

Ingrid Fändriks



## **ABSTRACT**

### **Alternative Methods for Evaluation of Oxygen Transfer Performance in Clean Water**

Ingrid Fändriks

Aeration of wastewater is performed in many wastewater treatment plants to supply oxygen to microorganisms. To evaluate the performance of a single aerator or an aeration system, there is a standard method for oxygen transfer measurements in clean water used today. The method includes a model that describes the aeration process and the model parameters could be estimated using nonlinear regression. The model is a simplified description of the oxygen transfer which could possibly result in performance results that are not accurate. That is why many have tried to describe the aeration at other ways and with other parameters. The focus of this Master Thesis has been to develop alternative models which better describe the aeration that could result in more accurate performance results. Data for model evaluations have been measured in two different tanks with various numbers of aerators.

Five alternative methods containing new models for oxygen transfer evaluation have been studied in this thesis. The model in method nr 1 assumes that the oxygen transfer is different depending on where in a tank the dissolved oxygen concentration is measured. It is assumed to be faster in a water volume containing air bubbles. The size of the water volumes and the mixing between them can be described as model parameters and also estimated. The model was evaluated with measured data from the two different aeration systems where the water mixing was relatively big which resulted in that the model assumed that the whole water volume contained air bubbles. After evaluating the results, the model was considered to maybe be useful for aeration systems where the mixing of the water volumes was relatively small in comparison to the total water volume. However, the method should be further studied to evaluate its usability. Method nr 2 contained a model with two separate model parameter, one for the oxygen transfer for the air bubbles and one for the oxygen transfer at the water surface. The model appeared to be sensitive for which initial guesses that was used for the estimated parameters and it was assumed to reduce the model's usability. Model nr 3 considered that the dissolved oxygen equilibrium concentration in water is depth dependent and was assumed to increase with increasing water depth. Also this model assumed that the oxygen was transferred from both the air bubbles and at the water surface. The model was considered to be useful but further investigations about whether the saturation concentrations should be constant or vary with water depth should be performed. The other two methods contained models that were combinations of the previous mentioned model approaches but was considered to not be useful.

**Keywords:** Aeration, oxygenation, oxygen transfer, modeling, wastewater treatment

*Department of Information Technology, Uppsala University, Box 337, SE- 751 05  
Uppsala, ISSN 1401-5765*

## REFERAT

### Alternativa metoder för utvärdering av syreöverföringsprestanda i rent vatten

Ingrid Fändriks

Luftning av avloppsvatten förekommer på många reningsverk för att tillföra syre till mikroorganismer. För att utvärdera en enskild luftare eller ett helt luftningssystem prestanda används idag en standardmetod för syreöverföringsmätningar i rent vatten. Metoden innehåller bland annat en modell som beskriver luftningsprocessen och vars modellparametrar kan skattas genom ickelinjär regression. Modellen är en förenklad beskrivning av syreöverföringen vilket kan medföra att prestandaresultaten inte är korrekta. Därför har många försökt beskriva luftningen på andra sätt och med andra parametrar. Fokus för detta examensarbete har varit att utveckla alternativa modeller som beskriver luftningen bättre vilket gör det möjligt att få mer korrekta prestandaresultat. Data för att utvärdera modellerna har uppmätts i två olika tankar med olika många luftare i.

Fem alternativa metoder innehållande nya modeller för syreöverföringsutvärderingar har studerats i detta examensarbete. Modellen i metod nr 1 utgår ifrån att syreöverföringen är olika beroende på vart i tanken koncentrationen av löst syre mäts. Den antas vara snabbare i volymer där luftbubblorna är. Hur stora de båda vattenvolymererna är och hur stor omblandningen är mellan dem kan beskrivas som modellparametrar och därefter skattas. Modellen utvärderades för mätdata från två olika luftningssystem där omblandningen av vattnet var relativt stor vilket medförde att modellen antog att hela vattenvolymen innehöll luftbubblor. Efter resultatutvärdering antogs den modellen kunna vara användbar för system där omblandningen av vattenmassorna är liten i jämförelse med den totala vattenvolymen. Metoden bör dock studeras vidare för att på så sätt undersöka dess användbarhet. Metod nr 2 innehåller en modell som har två parametrar för dels syreöverföringen via luftbubblorna och dels syreöverföringen via vattenytan. Modellen visade sig vara känslig för vilka initialgissningar som användes för de skattade parametrarna och bedömdes inte vara användbar. Modell nr 3 tog hänsyn till att mättnadskoncentrationen för löst syre i vatten är djupberoende. Mättnadskoncentrationen antas öka med ökande djup. Även denna modell tog separat hänsyn till syreöverföringen via luftbubblorna och via vattenytan. Denna modell ansågs vara användbar men en vidare utredning om huruvida mättnadskoncentrationen ska vara konstant eller variera med djupet bör föras. De andra två metoderna innehöll modeller som var kombinationer av de tidigare nämnda modellerna men bedömdes inte vara användbara i dagsläget.

**Nyckelord:** Luftning, syresättning, syreöverföring, modellering, avloppsvattenrening

*Institutionen för informationsteknologi, Uppsala universitet, Box 337, SE- 751 05  
Uppsala, ISSN 1401-5765*

## **PREFACE**

This Master Thesis was conducted at ITT Water & Wastewater in Sundbyberg and was the final part of my Master of Science in Aquatic and Environmental Engineering program at Uppsala University. Supervisor for the project was Martin Wessman at the Department for Research and Development at ITT Water & Wastewater. Subject reviewer was Bengt Carlsson at the Department of Information Technology at Uppsala University and examiner was Allan Rodhe at the Department of Earth Sciences at Uppsala University.

First of all I would like to thank my supervisor Martin Wessman for supporting me through the whole project. I have always felt that I could ask you questions and you have supported me with everything, both with theoretical discussions and to encourage me to do more things and expand the project.

Great thanks to Bengt Carlsson, my subject reviewer, for good opinions about the project that have helped me a lot. The project had been much more difficult without you and your help.

Lars Uby at ITT Water & Wastewater has helped me with interesting discussions. He and Ulf Arbeus had the original ideas for model nr 1.

I also want to thank Johan Tammelin at ITT Water & Wastewater for helping me with setting up the test instruments in the laboratory. Without your help it would have been impossible for me to do my measurements.

Last but not least I want to thank my family, Jonathan Styrud and my friends for always supporting and believing in me and my knowledge. Thank you so much!

Uppsala, 2011

Ingrid Fändriks

Copyright © Ingrid Fändriks and the Department of Information Technology, Uppsala University.

UPTEC W 11 002, ISSN 1401-5765

Printed at the Department of Earth Sciences, Geotryckeriet, Uppsala University, Uppsala, 2011.

# POPULÄRVETENSKAPLIG SAMMANFATTNING

## Alternativa metoder för utvärdering av syreöverföringsprestanda i rent vatten

Ingrid Fändriks

Luftning av avloppsvatten sker idag i många reningsverk. Syftet med att lufta vattnet är bland annat att mikroorganismerna ska ha möjlighet att tillväxa vilket gör att de kan omvandla kväve till kvävgas, som då frigges till atmosfären. Man förhindrar då att den största delen av kvävet följer med det renade vattnet ut i sjöar. Hur luftarna ser ut varierar beroende på vilket syfte de har. Vanligt är att ha bottentäckande s.k. membranluftare som distribuerar luftbubblor jämt fördelat i hela tanken.

Syre överförs från luftbubblorna till att bli löst i vatten genom diffusion. Ju fler luftbubblor det finns, desto större blir syreöverföringen. Även storleken på bubblorna spelar en betydande roll, fler mindre bubblor istället för få stora bidrar till en större syreöverföring på grund av ytareans storlek. Syre kan även överföras via vattenytan. Syret i luften kommer främst att överföras om vattenytan är något turbulent. Turbulensen skapas av stigande luftbubblor och den påverkas bland annat av hur stort luftflödet är in i tanken. Ju större luftflödet är desto mer turbulent blir vattenytan på grund av snabbare stigande luftbubblor. Luftbubblorna bidrar även till att vattnet i en tank omblandas. Hur stor omblandningen är beror bland annat på luftflödet och tankdimensionerna. Eftersom syre överförs via luftbubblorna är det möjligt att anta att om omblandningen är stor så är syreöverföringen ungefär lika stor i hela tanken.

För att utvärdera en luftares eller ett luftningssystemens prestanda kan man använda en standardmetod för syreöverföringsmätningar i rent vatten. Metoden innehåller en modell som beskriver luftning av vatten samt mätningar som måste göras för att utvärdera modellen. Genom att skatta modellparametrar är det, med hjälp av icke-linjär regression, möjligt att beräkna prestanda för luftare. Modellen är en massbalansekvation som beskriver hur koncentrationen av löst syre i vatten varierar med tiden i en tank med vatten. Den är en förenklad beskrivning av vad som egentligen sker i en luftad volym vatten. Den totala syreöverföringen beskrivs endast av en parameter,  $K_L a$ , som representerar hur snabbt syret överförs till vattnet. Modellen beskriver även att den drivande faktorn för syreöverföringen påverkas av hur stor skillnaden av koncentrationen löst syre är i tanken vid en viss tidpunkt samt hur stor mättnadskoncentrationen av löst syre är,  $C_{ss}$ . Modellen tar inte individuellt hänsyn till att syre överförs både via luftbubblor och vattenytan. Den tar heller inte hänsyn till att mättnadskoncentrationen teoretiskt varierar med djupet. Djupare ner i en tank så kommer mer syre att kunna överföras på grund av det ökande trycket.

Diskussioner har tidigare förts om huruvida standardmodellen kan beskriva luftningen och om prestandaresultaten är korrekta. Man har också funderat på om modellen kan beskriva alla typer av luftningssystem och applikationer. Flera alternativa metoder för utvärdering av syreöverföringsprestanda har utvecklats under årens lopp. Fokus har mest varit på att utveckla alternativa modeller som beskriver luftningen med andra eller fler parametrar. Det finns flera exempel på alternativa modeller där hänsyn har tagits till

att syre överförs både via luftbubblorna och vattenytan. Vissa har även tagit hänsyn till att mättnadskoncentrationen av löst syre är djupberoende. Det finns även modeller som tagit hänsyn till att syreöverföringen kan vara olika beroende på vart i tanken man mäter koncentrationen av löst syre. Tankvolymen har då delats upp i två olika zoner, en zon som innehåller luftbubblor och en zon som inte innehåller luftbubblor. Zonen med luftbubblor antas vara den volym med vatten som är ovanför en luftare eller luftningssystemet.

Med bakgrund från de ovan nämnda infallsvinklarna för en ny modell har fem alternativa metoder för syreöverföringsutvärderingar utvecklats i detta examensarbete. Även här har fokus varit att utveckla alternativa modeller som bättre beskriver vad som egentligen händer i en luftad tank med rent vatten. De nya modellerna har utvärderats med hjälp av s.k. simulerade data som skapats just för modellutvärderingen samt uppmätta data. Mätningarna har utförts i två olika tankar, dels en cylindertank med en membranluftare samt en s.k. racetrack med fyra membranluftare. Modellerna har därefter testats med data för att utvärdera ifall de verkar rimliga samt om de kan användas oberoende av den mänskliga faktorn utan att resultaten skiljer sig åt. Det är ingen idé att skapa en modell som ger olika resultat beroende på vem som analyserat datat.

Teorin för modell nr 1 utgår ifrån att den totala vattenvolymen kan delas upp i två olika volymer, dels en som innehåller luftbubblor, dels en annan som inte innehåller luftbubblor. För att ta hänsyn till de båda vattenvolymerna har modellen delats upp i två olika ekvationer. Utöver de parametrar som skattas i standardmodellen är det med denna modellen möjligt att ta reda på hur stora de båda volymerna är samt hur stor omblandningen mellan dem är. Modellen ansågs inte vara motiverad att använda på luftningssystem där omblandningen var stor i förhållande till den totala volymen.

Modell nr 2 tar hänsyn till att syret överförs både via luftbubblorna och via vattenytan. Eftersom mättnadskoncentrationen av syre i vatten varierar beroende på olika parametrar baseras modellen på att den syreöverföring som sker via ytan drivs av skillnaden av koncentrationen löst syre i vattnet och mättnadskoncentrationen vid atmosfärstryck. Syreöverföringen via luftbubblorna drivs däremot av skillnaden mellan koncentrationen löst syre i vattnet och mättnadskoncentrationen i tanken,  $C_{ss}$ . Modellen verkar dock inte vara användbar eftersom de skattade modellparametrarna varierade beroende på vilka initialgissningar som användes.

Den tredje modellen hittades i litteratur men utvärderades med en liten modifikation eftersom en extra modellparameter skattades. Modellen utgår ifrån att mättnadskoncentrationen för syre i vatten varierar med djupet. Mättnadskoncentrationen beräknades istället för att, som i standardmetoden, skattas. Även denna modell tar hänsyn till att syret överförs både via luftbubblorna och via vattenytan. Efter utvärdering ansågs modell nr 3 vara användbar för utvärdering av syreöverföringsprestanda. Ett frågetecken kvarstår dock om huruvida mättnadskoncentrationen bör vara konstant eller variera med djupet.

De två resterande modellerna som utvecklades i detta projekt är kombinationer av de ovanstående tre modelltyperna. De ansågs inte vara användbara i dagsläget eftersom vidare studier kring de andra tre bör göras först.



## DEFINITIONS

| Symbol                            | Description   | Unit   |
|-----------------------------------|---|--|
| A                                 | Cross sectional area of the tank  | m <sup>2</sup>   |
| C                                 | Dissolved oxygen concentration  | mg/L   |
| C <sub>0</sub>                    | Dissolved oxygen concentration at time zero   | mg/L   |
| C <sub>1</sub>                    | Dissolved oxygen concentration in a water volume with air bubbles   | mg/L   |
| C <sub>1(0)</sub>                 | Dissolved oxygen concentration in a water volume with air bubbles at time zero  | mg/L   |
| C <sub>2</sub>                    | Dissolved oxygen concentration in a water volume without air bubbles  | mg/L   |
| C <sub>2(0)</sub>                 | Dissolved oxygen concentration in a water volume without air bubbles at time zero   | mg/L   |
| C <sub>o</sub> *                  | Dissolved oxygen equilibrium concentration  | mg/L   |
| C <sub>ss</sub>                   | Dissolved oxygen saturation concentration at steady state   | mg/L   |
| C <sub>ss_20</sub>                | Dissolved oxygen saturation concentration at standard conditions (temperature 20°C and pressure 1atm)   | mg/L   |
| C <sub>ss_20i</sub>               | Dissolved oxygen saturation concentration at standard conditions for measurement probe i (temperature 20°C and pressure 1atm)                                 | mg/L   |
| C <sub>surf_sat</sub>             | Dissolved oxygen saturation concentration at ambient atmospheric pressure   | mg/L   |
| C <sub>surf_sat_20i</sub>         | Dissolved oxygen saturation concentration at ambient atmospheric pressure at standard conditions for measurement probe i (temperature 20°C and pressure 1atm) | mg/L   |
| G                                 | Gas flow rate   | kmol N <sub>2</sub> / h  |
| h <sub>d</sub>                    | Depth to aeration system  | m  |
| K <sub>2</sub>                    | Conversion factor   | 3.13·10 <sup>-5</sup> (kmol O <sub>2</sub> · L) / (m <sup>3</sup> ·mg) |
| K <sub>L</sub> a                  | Volumetric mass transfer coefficient  | min <sup>-1</sup>  |
| K <sub>L</sub> a <sub>20</sub>    | Volumetric mass transfer coefficient at standard conditions (temperature 20°C and pressure 1atm)  | min <sup>-1</sup>  |
| K <sub>L</sub> a <sub>20i</sub>   | Volumetric mass transfer coefficient at standard conditions for measurement probe i (temperature 20°C and pressure 1atm)                                      | min <sup>-1</sup>  |
| K <sub>L</sub> a <sub>b</sub>     | Volumetric mass transfer coefficient for air bubbles  | min <sup>-1</sup>  |
| K <sub>L</sub> a <sub>b_20i</sub> | Volumetric mass transfer coefficient for air bubbles at standard conditions for measurement probe i (temperature 20°C and pressure 1atm)                      | min <sup>-1</sup>  |
| K <sub>L</sub> a <sub>s</sub>     | Volumetric mass transfer coefficient at the water surface   | min <sup>-1</sup>  |
| K <sub>L</sub> a <sub>s_20i</sub> | Volumetric mass transfer coefficient at the water surface at standard conditions for measurement probe i (temperature 20°C and pressure 1atm)                 | min <sup>-1</sup>  |
| K <sub>L</sub> a <sub>s1</sub>    | Volumetric mass transfer coefficient at the bubbled water surface   | min <sup>-1</sup>  |

|                  |   |                                   |
|------------------|---|-----------------------------------|
| $K_{La_s1\_20i}$ | Volumetric mass transfer coefficient at the bubbled water surface at standard conditions for measurement probe i (temperature 20°C and pressure 1atm)     | $\text{min}^{-1}$                 |
| $K_{La_s2}$      | Volumetric mass transfer coefficient at the non-bubbled water surface   | $\text{min}^{-1}$                 |
| $K_{La_s2\_20i}$ | Volumetric mass transfer coefficient at the non-bubbled water surface at standard conditions for measurement probe i (temperature 20°C and pressure 1atm) | $\text{min}^{-1}$                 |
| n                | Number of dissolved oxygen probes   | -                                 |
| P                | Atmospheric pressure  | atm                               |
| $P_{wv}$         | Water vapor pressure  | atm                               |
| q                | Liquid flow rate  | $\text{m}^3/\text{min}$           |
| RSS              | Residual sum of squares   | $(\text{mg/L})^2$                 |
| SAE              | Standard aeration efficiency  | kg/kWh                            |
| SOTE             | Standard oxygen transfer efficiency   | %                                 |
| SOTR             | Standard oxygen transfer rate   | kg/h                              |
| t                | Time  | min                               |
| V                | Water volume  | $\text{m}^3$                      |
| $V_1$            | Aerated water volume containing air bubbles   | $\text{m}^3$                      |
| $V_2$            | Non-aerated water volume without air bubbles  | $\text{m}^3$                      |
| $W_{O_2}$        | Oxygen mass flow  | kg/h                              |
| y                | Concentration of oxygen in gas phase  | $\text{kmol O}_2/\text{kmol N}_2$ |
| z                | Water depth (z=0 at the tank bottom and z= $z_s$ at the water surface)  | m                                 |

---

## TABLE OF CONTENTS

|  |     |
|--|-----|
| ABSTRACT .....   | i   |
| REFERAT .....  | ii  |
| PREFACE.....   | iii |
| POPULÄRVETENSKAPLIG SAMMANFATTNING .....               | iv  |
| DEFINITIONS .....                                      | vii |
| 1 INTRODUCTION.....                                    | 1   |
| 1.1 BACKGROUND .....                                   | 1   |
| 1.2 PURPOSE.....                                       | 2   |
| 1.3 GOALS .....  | 2   |
| 2 THE STANDARD METHOD FOR OXYGEN TRANSFER MEASUREMENTS | 3   |
| 2.1 OXYGEN TRANSFER .....                              | 3   |
| 2.2 PRINCIPLE OF THE STANDARD METHOD .....             | 4   |
| 2.3 THE STANDARD MODEL.....                            | 5   |
| 2.4 REQUIRED MEASUREMENTS.....                         | 6   |
| 2.5 OXYGENATION .....                                  | 6   |
| 2.5.1 Principle.....                                   | 6   |
| 2.5.2 Chemical addition.....                           | 7   |
| 2.6 DATA ANALYSIS.....                                 | 7   |
| 2.6.1 Truncation.....                                  | 7   |
| 2.6.2 Nonlinear regression.....                        | 8   |
| 2.7 CALCULATIONS .....                                 | 8   |
| 2.7.1 Standard oxygen transfer rate (SOTR) .....       | 8   |
| 2.7.2 Standard aeration efficiency (SAE).....          | 9   |
| 2.7.3 Standard oxygen transfer efficiency (SOTE) ..... | 9   |
| 3 PREVIOUS MODEL APPROACHES .....                      | 10  |
| 3.1 SEPARATED WATER VOLUMES .....                      | 10  |
| 3.2 INTRODUCING THE WATER SURFACE.....                 | 10  |
| 3.3 DEPTH DEPENDENT SATURATION CONCENTRATION .....     | 11  |
| 4 ALTERNATIVE METHODS FOR OXYGEN TRANSFER MEASUREMENTS | 12  |
| 4.1 METHOD NR 1 .....                                  | 12  |
| 4.1.1 Model nr 1 .....                                 | 12  |
| 4.1.2 Required measurements.....                       | 14  |

|       |  |    |
|-------|--|----|
| 4.1.3 | Data analysis.....                           | 14 |
| 4.1.4 | Calculations .....                           | 15 |
| 4.2   | METHOD NR 2.....                             | 15 |
| 4.2.1 | Model nr 2 .....                             | 15 |
| 4.2.2 | Required measurements.....                   | 16 |
| 4.2.3 | Data analysis.....                           | 17 |
| 4.2.4 | Calculations .....                           | 17 |
| 4.3   | METHOD NR 3.....                             | 17 |
| 4.3.1 | Model nr 3 .....                             | 17 |
| 4.3.2 | Required measurements.....                   | 19 |
| 4.3.3 | Data analysis.....                           | 19 |
| 4.3.4 | Calculations .....                           | 19 |
| 4.4   | METHOD NR 4.....                             | 19 |
| 4.4.1 | Model nr 4: Combining model nr 1 and 2 ..... | 19 |
| 4.4.2 | Required measurements.....                   | 21 |
| 4.4.3 | Data analysis.....                           | 21 |
| 4.4.4 | Calculations .....                           | 21 |
| 4.5   | METHOD NR 5.....                             | 22 |
| 4.5.1 | Model nr 5: Combining model nr 1 and 3 ..... | 22 |
| 4.5.2 | Required measurements.....                   | 23 |
| 4.5.3 | Data analysis.....                           | 23 |
| 4.5.4 | Calculations .....                           | 23 |
| 4.6   | SUMMARY OF THE ALTERNATIVE MODELS.....       | 23 |
| 5     | METHODS AND MATERIALS .....                  | 25 |
| 5.1   | THE CYLINDER TANK .....                      | 25 |
| 5.2   | THE RACETRACK TANK .....                     | 27 |
| 5.3   | MEASUREMENT INSTRUMENTS .....                | 31 |
| 5.3.1 | Dissolved oxygen probes.....                 | 31 |
| 5.3.2 | Velocimeter .....                            | 33 |
| 5.3.3 | Conductivity measurements .....              | 34 |
| 5.3.4 | Other parameters.....                        | 34 |
| 5.4   | CHEMICAL ADDITION .....                      | 34 |
| 5.5   | DATA ANALYSIS.....                           | 35 |

|       |   |    |
|-------|---|----|
| 5.6   | MODEL EVALUATION .....  | 35 |
| 5.6.1 | Simulated data .....  | 35 |
| 5.6.2 | Plotting .....  | 36 |
| 5.6.3 | Residual sum of squares (RSS) .....                               | 36 |
| 5.6.4 | Parameter sensitivity .....                                       | 36 |
| 5.6.5 | Truncation spans.....   | 37 |
| 6     | RESULTS.....  | 38 |
| 6.1   | THE STANDARD MODEL.....   | 38 |
| 6.1.1 | Simulated data .....  | 38 |
| 6.1.2 | Cylinder tank data.....   | 41 |
| 6.1.3 | Racetrack data.....   | 43 |
| 6.2   | MODEL NR 1.....   | 47 |
| 6.2.1 | Simulated data .....  | 47 |
| 6.2.2 | Cylinder tank data.....   | 49 |
| 6.2.3 | Racetrack data.....   | 50 |
| 6.3   | MODEL NR 2.....   | 52 |
| 6.3.1 | Simulated data .....  | 52 |
| 6.4   | MODEL NR 3.....   | 54 |
| 6.4.1 | Simulated data .....  | 54 |
| 6.4.2 | Racetrack data.....   | 57 |
| 6.5   | MODEL NR 4.....   | 59 |
| 6.6   | MODEL NR 5.....   | 60 |
| 7     | DISCUSSION .....  | 61 |
| 7.1   | THE STANDARD METHOD .....   | 61 |
| 7.2   | METHOD NR 1.....  | 62 |
| 7.3   | METHOD NR 2.....  | 64 |
| 7.4   | METHOD NR 3.....  | 64 |
| 7.5   | METHOD NR 4 AND 5 .....   | 68 |
| 7.6   | POSSIBLE IMPROVEMENTS AND RECOMMENDATIONS FOR<br>FUTURE WORK..... | 68 |
| 8     | CONCLUSIONS.....  | 70 |
| 9     | REFERENCES.....   | 71 |
|       | Personal communication .....                                      | 72 |
|       | APPENDIX A .....  | 73 |

|                  |    |
|------------------|----|
| APPENDIX B.....  | 76 |
| APPENDIX C.....  | 79 |
| APPENDIX D ..... | 83 |

# 1 INTRODUCTION

## 1.1 BACKGROUND

The main purpose of aeration in wastewater treatment plants is to supply oxygen to the processes where microorganisms require oxygen for their growth. The aeration process also keeps the water and the microorganisms mixed in a water tank. It is important that the air is present in the whole tank to keep the microorganisms active (Svenskt Vatten, 2007).

There exists devices that aerate the water at the water surface, but the most common way is by ejecting air at the bottom of a tank. In the water, the air turns into bubbles. Some of the oxygen in the air bubbles is then transferred from the bubble by diffusion and becomes dissolved in the water (Svenskt Vatten, 2007). Oxygen transfer also occurs at the water surface (Chern et al., 2001).

Energy consumption from aeration systems is a big part of the total energy cost in a wastewater treatment plant. Therefore it is interesting to know how effective the aeration system is in comparison to the energy consumption (Svenskt Vatten, 2007). This can be done by applying the standard method for oxygen transfer measurements in clean water (ASCE, 2007). Determination of an aeration system's oxygen transfer capacity and efficiency is standardized since a couple of decades (Svenskt Vatten, 2007) but has barely progressed the last 20 years (McWhirter & Hutter, 1989). The standard method is made for measurements in clean water but can be applied to process water by using a conversion factor (Svenskt Vatten, 2007). Different editions of the standard method for oxygen transfer measurements are used in different countries but the standard method evaluated in this project is the American standard (ASCE, 2007).

Using the method it is possible to evaluate the oxygen transfer rate, the aeration efficiency and the oxygen transfer efficiency. These parameters can make it possible to evaluate the aeration performance for aeration devices (ASCE, 2007). It is also possible to detect deficiencies in an aeration system considering both types of aeration devices and their locations in a tank (Svenskt Vatten, 2007).

The American standard method includes both a model that describes how the dissolved oxygen concentration is varying with time and measurements that are required to evaluate the aeration performance. Using the model with measured data makes it possible to estimate model parameters by using nonlinear regression and later calculating the aeration efficiency etc. (ASCE, 2007). The model used today is a rough simplification of how the oxygen in the air is transferred to be dissolved in water. According to the model, the water is assumed to be completely mixed (Boyle, 1983). The dissolved oxygen concentration is to be measured and if the water is not completely mixed, the method recommends that the measurement probes should be placed where the concentration best represents the total water volume (ASCE, 2007). Since the standard model is a rough simplified description of what's really occurs in a tank, the determinations of aeration performance can be quite uncertain (McWhirter & Hutter,

1989). Furthermore, the results are only valid for exactly the same operating conditions as for which it was tested. That makes it difficult to predict aeration performance for different operating sets (McWhirter & Hutter, 1989). The differences in tank geometry, wastewater conditions, water mixing etc. can contribute to uncertainties in the process prediction of nearly 50% (Boyle, 1983). A better and more reliable model which can predict aeration performance is desirable (Chern & Yang, 2003). That could help designing various aeration systems for both lakes and wastewater treatment plants (DeMoyer et al., 2003).

Different mass balance models have been developed to improve the standard method and to get more accurate performance results. By introducing another model it can also be possible to get more information about the oxygen transfer, for example how big the oxygen transfer is at the water surface (DeMoyer et al., 2003). The risk with developing more complicated models is that they become sensitive for initial guesses if using nonlinear regression to estimate parameters. What measurements that should be done to evaluate a new model depend on the model structure.

## **1.2 PURPOSE**

The main purpose of the thesis is to develop an alternative method for evaluation of oxygen transfer performance in clean water. The method should contain both a model and a description of required measurements to evaluate the oxygen transfer performance. A new model should be a more accurate description of the oxygen transfer and it should be more reliable for different types of systems. The model should also be simple enough that anyone could use it and get the same results. Oxygen transfer measurements should be performed to evaluate the new models.

Another purpose of this thesis is to evaluate the standard method for oxygen transfer measurements. It must be defined if the results given by the standard method are reliable. If they are not, a theoretical model that gives better and more reliable results is needed.

The purpose is also to evaluate whether it is possible to decrease the measurement time. By evaluating the models with just the first measured data it is possible to evaluate this.

## **1.3 GOALS**

- Develop an alternative method for evaluation of oxygen transfer performance which contains both a more accurate model and description of measurements which is required to evaluate the model.
- Perform measurements to be able to evaluate the new models.
- Analyze the standard model that is used today and compare the differences between that model and a new model. Care should be taken to both usability and performance.
- Evaluate the impact of oxygen transfer at the water surface.



## 2 THE STANDARD METHOD FOR OXYGEN TRANSFER MEASUREMENTS

The standard method for oxygen transfer measurements in clean water which is presented in this chapter is published by American Society of Civil Engineers (ASCE, 2007). The model which describes the oxygen transfer is made for aeration performance evaluation in clean tap water. There is a conversion factor available for transforming the performance results to process water, but it is not treated in this thesis. Both SI units and other units are used.

This chapter presents how the oxygen transfer occurs and a short summary of the principle of the method. The method includes a model, required measurements, oxygenation and data analysis. When the data analysis is finished it is possible to calculate the performance parameters.

### 2.1 OXYGEN TRANSFER

Aeration in wastewater treatment plants is done for contaminant removal. The air is released from aeration products primarily for the oxygen demanding microorganisms (ASCE & WPCF, 1988). When the air is released to the water it will turn into air bubbles. Some of the oxygen in the air bubbles is diffused and becomes dissolved in water (Figure 1). There is also oxygen transfer at the water surface which mainly is caused by the turbulent surface. Turbulence is induced by rising bubbles (DeMoyer et al., 2002). The tank water will also be turbulent and circulated because of the air lifting force of the rising bubbles (Fujie et al., 1992).

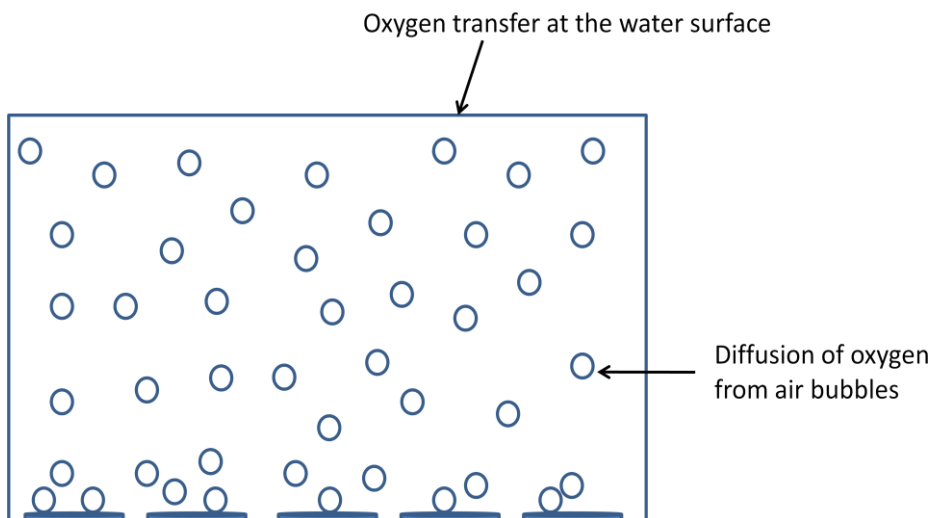


**Figure 1** An aerated tank with five diffusers. Oxygen transfer is possible from the air bubbles and the water surface.

The dissolved oxygen concentration can be affected by many factors, for example by the ambient atmospheric pressure and temperature. More oxygen can be dissolved when the pressure is higher, i.e. with increasing depth, and if the temperature and conductivity is lower (Lewis, 2006). The interface between air and water should be as large as

possible for an effective oxygen transfer (Svenskt Vatten, 2007). The smaller the air bubbles are, the larger is the interface area for oxygen diffusion.

A standard method for oxygen transfer measurements is used for evaluating aeration performance. That makes it possible to evaluate how big the oxygen transfer to water is and how effective the aeration systems are (ASCE, 2007).

## **2.2 PRINCIPLE OF THE STANDARD METHOD**

When it is desired to evaluate aeration device performance there is need for using the standard method for oxygen transfer measurements (ASCE, 2007) and it can be applied for all types of aeration systems (McWhirter & Hutter, 1989). First of all the aeration product should be set in a tank containing clean tap water. Two chemicals should be added to the water while the product is operating which decreases the dissolved oxygen concentration until it reaches almost zero. After a while, the concentration rises to the dissolved oxygen saturation concentration,  $C_{ss}$ , which is a value of how much oxygen that can be dissolved in water. This period is called reoxygenation (ASCE, 2007). The dissolved oxygen concentration should be measured during the whole reoxygenation by probes. They are placed in the tank to represent the total water volume. If there is a small plume with air bubbles, the probes should be positioned in different places in the tank. The measured data should be the dissolved oxygen concentration over time (ASCE, 2007).

Other parameters like air flow and temperatures have to be measured and included in later calculations. Some of them have to be measured both before and after the chemical additions (ASCE, 2007).

When the oxygen transfer measurements are finished it is possible to analyze the data. Data from the reoxygenation should be truncated where the lowest concentration should be lower than 20% of  $C_{ss}$  and the highest concentration should be at least 98% of  $C_{ss}$ . After the truncation, the data with dissolved oxygen concentration over time should be analyzed according to the standard model (ASCE, 2007).

The standard model consists of a mass balance equation which describes the dissolved oxygen concentration in water at various times. It can also be seen as a box with water and air bubbles. The oxygen is transferred to the water by a mass transfer coefficient,  $K_L a$ , which describes how fast the oxygen is transferred to be dissolved in water. That coefficient includes the total oxygen transfer both from the air bubbles and at the water surface (ASCE, 2007).

It is possible to estimate the model parameters by using nonlinear regression. In the standard model there are three parameters that needs to be estimated, the volumetric mass transfer coefficient,  $K_L a$ , the dissolved oxygen saturation concentration at steady state,  $C_{ss}$ , and the dissolved oxygen concentration at time zero,  $C_0$  (ASCE, 2007). The estimated parameters are then calculated to standard conditions which are at an atmospheric pressure of 1atm, water temperature at 20°C and specified gas rate and power conditions (ASCE, 2007).

When the estimated parameters are calculated to standard conditions there are three different performance parameters that could be used to evaluate an aeration device, the standard oxygen transfer rate (SOTR), the standard aeration efficiency (SAE) and the standard oxygen transfer efficiency (SOTE) (ASCE, 2007).

### 2.3 THE STANDARD MODEL

The standard model for oxygen transfer measurements consists of a mass balance equation of how the dissolved oxygen concentration in water is changing over time (ASCE, 2007). The model is quite simplified in comparison with reality mainly because it assumes that the water volume in a tank is completely mixed (Figure 2). Another assumption is that one mass transfer coefficient,  $K_L a$ , describes the whole oxygen transfer, even if oxygen is transferred from both air bubbles and at the water surface. If the air bubbles are evenly distributed in a tank it is reasonable to assume that oxygen transfer occurs in the whole volume, but this is rarely the case in reality. Sometimes there are only bubbles in a small part of the tank. It is also assumed that the mass transfer of other gases in air, other than oxygen, does not affect the oxygen mass transfer (McWhirter & Hutter, 1989).

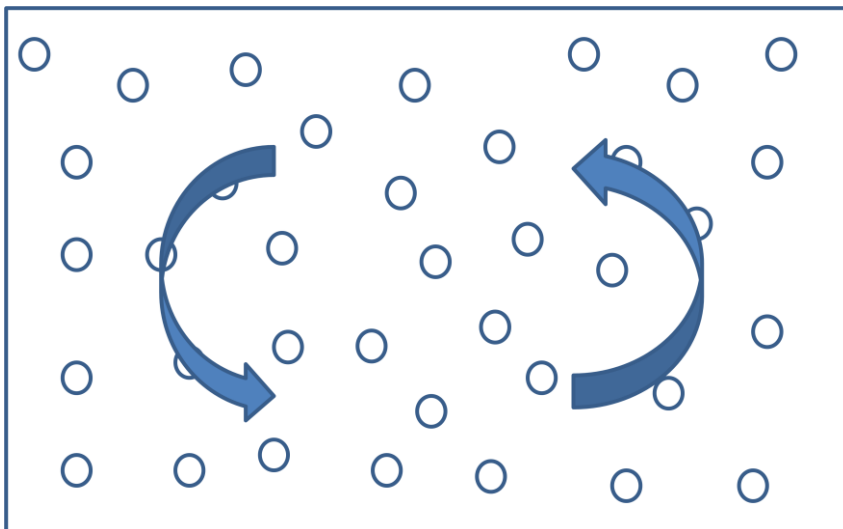


**Figure 2** The standard model which assumes that the water is completely mixed.

The standard model for evaluating oxygen transfer is given by Equation 1.

$$\frac{dC}{dt} = K_L a \cdot (C_{ss} - C) \quad (1)$$

where

- $C$  = dissolved oxygen concentration (mg/L)
- $t$  = time (min)
- $K_L a$  = volumetric mass transfer coefficient ( $\text{min}^{-1}$ )
- $C_{ss}$  = dissolved oxygen saturation concentration at steady state (mg/L)
- $C_0$  = dissolved oxygen concentration at time zero (mg/L)

The equation used for data analysis with nonlinear regression is given in Equation 2 and is a derivation from Equation 1 (Boyle, 1983).  $K_L a$  is constant and the dissolved oxygen concentration varies between  $C_0$  and  $C$ .

$$C = C_{ss} - (C_{ss} - C_0) \cdot e^{(-K_L a \cdot t)} \quad (2)$$

Parameters which have to be estimated for the standard model are the volumetric mass transfer coefficient,  $K_L a$ , the dissolved oxygen saturation concentration at steady state,  $C_{ss}$  and the dissolved oxygen concentration at time zero,  $C_0$  (ASCE, 2007).

## 2.4 REQUIRED MEASUREMENTS

Different parameters have to be measured or estimated to evaluate the results from the oxygen transfer measurements. The dissolved oxygen concentration should be measured at different places in the tank with several probes during the reoxygenation period. Aeration should be performed at least until the dissolved oxygen concentration reaches 98% of  $C_{ss}$ . The probes should be placed where they represent the total volume and at different depths (ASCE, 2007).

Other parameters that have to be measured in the standard method are presented in Table 1. A few parameters should be measured both before and after the test to either ensure that nothing has changed or to calculate an average value (ASCE, 2007). A test is represented by a de- and reoxygenation process which is more described in chapter 2.5.

**Table 1** Parameters that should be measured when the standard method is used.

| <b>Parameter</b>              | <b>Before test</b> | <b>After test</b> |
|-------------------------------|--------------------|-------------------|
| Water depth                   | Yes                | No                |
| Water temperature             | Yes                | Yes               |
| Air flow rate                 | Yes                | No                |
| Conductivity                  | Yes                | Yes               |
| Ambient air temperature       | Yes                | No                |
| Ambient air pressure          | Yes                | No                |
| Bottom floor area of the tank | Yes                | No                |

## 2.5 OXYGENATION

### 2.5.1 Principle

Before starting the oxygen transfer measurements, chemicals must be added for deoxygenation (ASCE, 2007). Deoxygenation means that the dissolved oxygen in water is removed and becomes almost zero (Figure 3). After a while, the dissolved oxygen concentration rises to the saturation concentration due to the aeration. That is called reoxygenation. The aeration device is operating during both the deoxygenation and the reoxygenation, but only the reoxygenation part is interesting for aeration performance evaluation (ASCE, 2007).

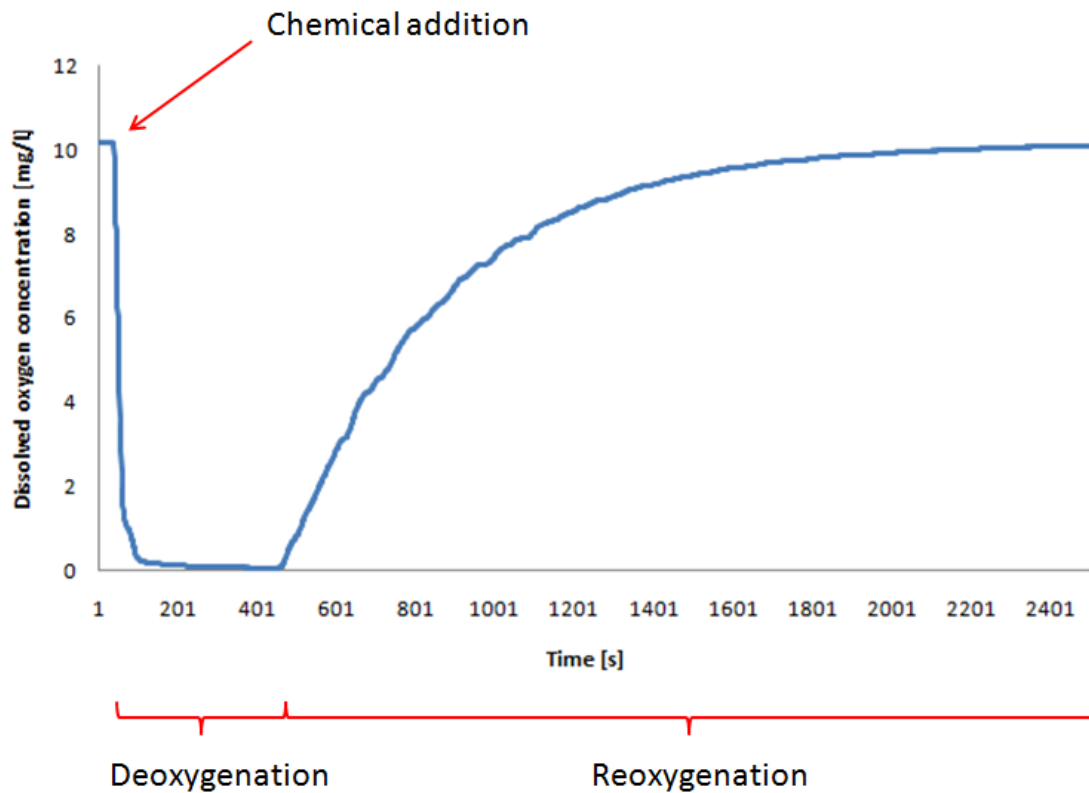


**Figure 3** After chemical addition starts the deoxygenation where the dissolved oxygen concentration decreases. The reoxygenation is where the dissolved oxygen concentration rises to the saturation concentration.

### 2.5.2 Chemical addition

Cobalt salt operates as a catalyst for sodium sulphite and should be added to the water first. Before adding the salt to the test tank it can be dissolved in water to prevent big particles (ASCE, 2007).

Sodium sulphite deoxygenates the water by taking up oxygen molecules (Equation 3) (Larson et al., 2007). Also the sodium sulphite can be dissolved in water before adding it evenly to the test tank. This chemical should be added before starting every new test. Both chemicals should be evenly distributed in the tank while the aeration system is operating (ASCE, 2007).



There are some guidelines in the American standard method for the amounts of chemicals that should be added but the concentration of dissolved oxygen should be lower than 0.5mg/L for at least two minutes (ASCE, 2007).

## 2.6 DATA ANALYSIS

### 2.6.1 Truncation

Only the data from the reoxygenation is used for data analysis. If the data do contain a lot of variations it can be truncated. The lowest dissolved oxygen concentration should not exceed 20% of the dissolved oxygen saturation concentration and the highest

concentration should not be less than 98% of the dissolved oxygen saturation concentration. When the data is truncated, nonlinear regression can be performed (ASCE, 2007).

### 2.6.2 Nonlinear regression

Some model parameters have to be estimated. These parameters cannot be measured or are difficult to measure. By using nonlinear regression it is possible to estimate these parameters (Seber & Wild, 2003). The estimated parameters in the standard method are the dissolved oxygen saturation concentration,  $C_{ss}$ , the mass transfer coefficient,  $K_L a$  and the dissolved oxygen concentration at time zero,  $C_0$ . Each of them are estimated for every data series (ASCE, 2007).

Nonlinear regression is based on a least square method that minimizes the error between the modeled and measured data (ASCE, 2007). Before a nonlinear regression is done, the initial guesses for the estimated parameters have to be defined. To get as correct results as possible the initial guesses should be as good as possible. This is because a problem with using nonlinear regression is that the estimated parameters may get stuck in a local minimum instead of just one global minimum (Seber & Wild, 2003).

## 2.7 CALCULATIONS

There are three different parameters used to evaluate aeration performance, standard oxygen transfer rate (SOTR), standard aeration efficiency (SAE) and standard oxygen transfer efficiency (SOTE). All parameters are expressed as standard parameters which are defined for a water temperature of 20°C and ambient air pressure of 1atm (ASCE, 2007).

All other calculations which are required to calculate the parameters below can be found in the standard method (ASCE, 2007).

### 2.7.1 Standard oxygen transfer rate (SOTR)

The standard oxygen transfer rate (SOTR) describes the rate of oxygen transfer at time zero (Equation 4), i.e. the capacity. For standard conditions, the dissolved oxygen concentration is assumed to be zero at time zero. SOTR is determined by the estimated parameters  $K_L a$  and  $C_{ss}$  and the total water volume and is expressed as mass per time (ASCE, 2007).

$$SOTR = \frac{V}{n} \cdot \sum_{i=1}^n K_L a_{20i} \cdot C_{ss\_20i} \quad (4)$$

where

- V = water volume (m<sup>3</sup>)
- n = number of dissolved oxygen probes (-)
- $K_L a_{20i}$  = volumetric mass transfer coefficient at standard conditions for measurement probe i (temperature 20°C and pressure 1atm) (min<sup>-1</sup>)
- $C_{ss\_20i}$  = dissolved oxygen saturation concentration at standard conditions for measurement probe i (temperature 20°C and pressure 1atm) (mg/L)

### 2.7.2 Standard aeration efficiency (SAE)

Standard aeration efficiency (SAE) is expressed as the oxygen transfer per unit power input (Equation 5). SAE is determined by SOTR and the power input. See the American standard for more details about the power input. SAE is expressed as mass transfer per power unit (ASCE, 2007).

$$SAE = \frac{SOTR}{Power\ input} \quad (5)$$

where        SOTR = standard oxygen transfer rate (kg/h)  
                 Power input = aeration power (W)

### 2.7.3 Standard oxygen transfer efficiency (SOTE)

Standard oxygen transfer efficiency (SOTE) describes how much of the injected oxygen that becomes dissolved in water and is expressed in percent (Equation 6). SOTE is determined by the SOTR and the injected flow of oxygen (ASCE, 2007).

$$SOTE = \frac{SOTR}{W_{O_2}} \cdot 100 \quad (6)$$

where         $W_{O_2}$  = oxygen mass flow (kg/h)

### **3 PREVIOUS MODEL APPROACHES**

There are several different model approaches available in the literature. Extending the standard model is interesting because the standard model is quite simplified. An extended model would probably be a more accurate description of the aeration process and give more reliable estimated parameter values. With more reliable parameter values it is possible to get more reliable performance results. One more advantage is to get more information about the aeration process, for example how big the impact of oxygen transfer is at the water surface (McWhirter & Hutter, 1989).

There are three different model approaches that are analyzed more closely and have been as a basis for this research. They handle separated water volumes, including the oxygen transfer at the water surface and accounts for that the dissolved oxygen concentration is depth dependent.

#### **3.1 SEPARATED WATER VOLUMES**

For most aeration systems there will be water volumes that do not contain air bubbles. That can be a problem if the water mixing is small because oxygen transfer only appears from the air bubbles and at the water surface. If the mixing is small and there is a big water volume without bubbles, the main oxygen transfer will appear in the aerated water volume (Boyle, 1983).

According to Boyle (1983), there can be a difference in oxygen transfer in different places in the tank depending on the placement of aeration systems. Many systems are placed to produce a liquid flow that makes the water completely mixed. Boyle claims that the total water volume could be divided in two parts, one aerated water volume containing air bubbles and one non-aerated water volume that do not contain bubbles. There will not be any oxygen transfer in the non-aerated volume but because of a liquid flow rate, the water from the aerated volume will be mixed with the non-aerated water and vice versa. The liquid flow rate is assumed to be as big as the pumping rate from the aeration system.

Fonade et al. (2001) have built a theoretical model for systems with a jet aerator. Dividing the model into separate volumes and using known flow rates made it possible to model that case.

#### **3.2 INTRODUCING THE WATER SURFACE**

Oxygen transfer appears both by diffusion from the air bubbles and at the water surface and they should both be analyzed in a model. How big the impact of the water surface is depends on the water depth, the surface area and the type of aeration system. The bubble oxygen transfer is probably more significant in a deeper tank. (Chern et al., 2001).

A possible way of separating the overall mass transfer coefficient is to bubble a tank with nitrogen gas instead of air. Because the nitrogen strips dissolved oxygen from the water, the only factor that could affect the oxygen transfer is the water surface. The measured dissolved oxygen concentration in the tank will then be a result of oxygen



transfer at the water surface only (Wilhelms & Martin, 1992). This approach was not evaluated in this thesis.

### **3.3 DEPTH DEPENDENT SATURATION CONCENTRATION**

To evaluate this model there are two different parameters that have to be estimated, the volumetric mass transfer coefficient for both the bubbles and at the water surface (Chern & Yu, 1997). If those parameters are known, it is easier to design aeration systems which either maximize the oxygen transfer from air bubbles or maximize the oxygen transfer at the water surface (DeMoyer et al., 2003). The dissolved oxygen equilibrium concentration in this model is calculated instead of estimated, as in the standard model (Chern et al., 2001). This model approach is analyzed more in detail in this research (chapter 4.3).

There is also a similar model like the one above but that also includes the diffusion of nitrogen from the air bubbles (Schierholz et al., 2006). The transfer of other gases than oxygen and nitrogen are assumed to be negligible (DeMoyer et al., 2003).

## 4 ALTERNATIVE METHODS FOR OXYGEN TRANSFER MEASUREMENTS

The focus of this Master Thesis was to develop and evaluate alternative oxygen transfer models which include more parameters than the standard model. Most work was devoted to modeling separated water volumes, introducing the water surface and take into account that the dissolved oxygen saturation concentration is depth dependent. Attempts to combine the different model approaches were also done. Model nr 1 and 2 were developed in this project with inspiration from other authors. Ideas for model nr 3 were taken from literature but with a small modification. Model evaluations and results are presented in Chapter 6.

When a new model is introduced, there is a possibility that the measurements or the data analysis have to be different in comparison to the standard method. If there are some changes in the new methods it will become clear in this chapter.

### 4.1 METHOD NR 1

#### 4.1.1 Model nr 1

The structure and analysis of model nr 1 is based on ideas from Arbeus (personal communication, 2011) and Uby (personal communication, 2010).

Because oxygen transfer occurs due to air bubbles in the water it can be reasonable to divide the total water volume into two different parts. An extension to the standard model would be to include an aerated water volume which contains air bubbles and a water volume without air bubbles (Figure 4). The size of the aerated water volume, which is formed due to air flow from aeration devices, is quite difficult to determine (Figure 5). Depending on the type of aeration system the bubbled plume will look very different.

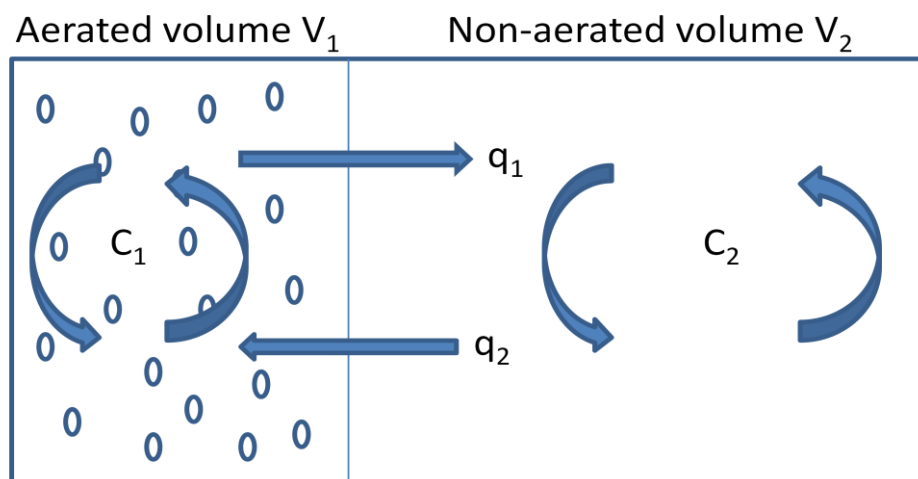


**Figure 4** Model nr 1 which contains an aerated water volume,  $V_1$ , and a water volume which is not aerated,  $V_2$ . The liquid flow between the zones is denoted  $q_1$  and  $q_2$  and the dissolved oxygen concentration in each zone is denoted  $C_1$  and  $C_2$ .

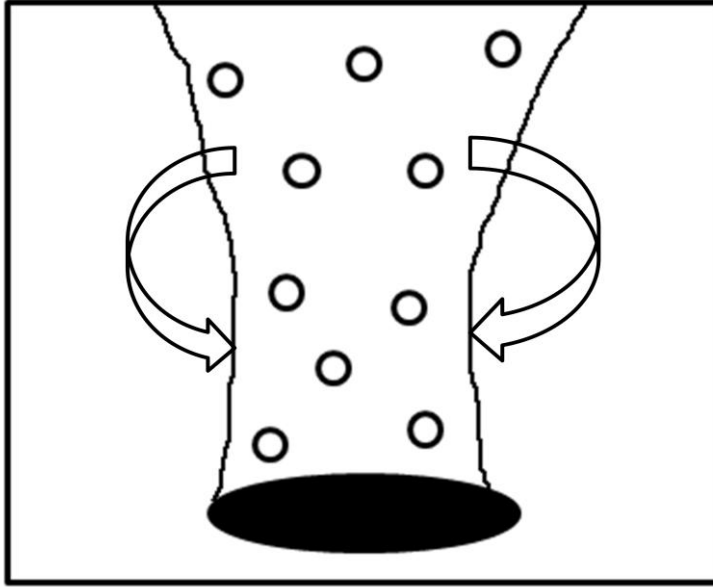


**Figure 5** Air bubbles rise vertically from a diffuser trough a column but with an expansion near the water surface. A liquid flow is induced due to drag force of the rising bubbles. Transport of water occurs continuously in and out of the two water volumes.

A liquid flow rate is introduced between the two zones due to liquid motions that appear when the bubbles rise to the water surface (Fujie, 1992). The liquid flow rates connect the two water volumes and create the mixing between them. It is assumed that the liquid flow rate in and out of the water volumes is equal (Equation 7).

$$q_1 = q_2 = q \quad (7)$$

The theory of the model is that the dissolved oxygen concentration in the aerated volume,  $C_1$ , is assumed to increase faster during the reoxygenation than the dissolved oxygen concentration in the non-aerated volume,  $C_2$ . This may be reasonable because the bubbles contribute to the oxygen transfer and they are only present in the aerated zone. Due to the liquid flow rate which mixes the two water volumes, the dissolved oxygen concentration in the non-aerated water volume,  $C_2$ , will increase during a reoxygenation, but with a delay in comparison with  $C_1$ .

The aerated water volume,  $V_1$ , is assumed to be well mixed and have air bubbles randomly distributed. The non-aerated volume,  $V_2$ , is also assumed to be well mixed but without bubbles.

More model parameters are included in the mass balance equations than in the standard model (Equation 8 and 9). The model equation is divided in two different equations, one for the aerated volume and one for the non-aerated volume. The mass transfer coefficient is only present in the equation for the aerated zone because of the bubbles. The oxygen transfer in the non-aerated water volume is assumed to be zero even if there could be oxygen transfer at the water surface.

$$\frac{dC_1}{dt} = K_L a \cdot (C_{ss} - C_1) + \frac{q \cdot C_2}{V_1} - \frac{q \cdot C_1}{V_1} \quad (8)$$

$$\frac{dC_2}{dt} = \frac{q \cdot C_1}{V_2} - \frac{q \cdot C_2}{V_2} \quad (9)$$

where  $C_1$  = dissolved oxygen concentration in a water volume with air bubbles (mg/L)  
 $C_2$  = dissolved oxygen concentration in a water volume without air bubbles (mg/L)  
 $q$  = liquid flow rate (m<sup>3</sup>/min)  
 $V_1$  = aerated water volume containing air bubbles (m<sup>3</sup>)  
 $V_2$  = non-aerated water volume without air bubbles (m<sup>3</sup>)

With derivation of Equation 8 and 9, the analytical solution is shown in Equation 10 and 11. The dissolved oxygen concentration at time zero is defined as  $C_0$ .

$$C_1 = A_1 \cdot e^{k_1 \cdot t} + A_2 \cdot e^{k_2 \cdot t} + C_{SS} \quad (10)$$

$$C_2 = A_1 \cdot e^{k_1 \cdot t} \cdot \tau_1 \left( k_1 + K_L a + \frac{1}{\tau_1} \right) + A_2 \cdot e^{k_2 \cdot t} \cdot \tau_1 \left( k_2 + K_L a + \frac{1}{\tau_1} \right) + C_{SS} \quad (11)$$

where

$$A_1 = \frac{C_{1(0)} \cdot \tau_1 (-k_1 + k_2) - C_{2(0)} + \tau_1 \left( C_{1(0)} \cdot k_1 + C_{1(0)} \cdot K_L a + \frac{C_{1(0)}}{\tau_1} - C_{SS} \cdot k_1 - C_{SS} \cdot K_L a - \frac{C_{SS}}{\tau_1} \right) + C_{SS} - C_{SS} \cdot \tau_1 (-k_1 + k_2)}{\tau_1 (-k_1 + k_2)}$$

$$A_2 = -A_1 + C_{1(0)} - C_{SS}$$

$$k_1 = \frac{-(K_L a + \frac{1}{\tau_1} + \frac{1}{\tau_2})}{2} + \sqrt{\frac{(K_L a + \frac{1}{\tau_1} + \frac{1}{\tau_2})^2}{4} - \frac{K_L a}{\tau_2}}$$

$$k_2 = \frac{-(K_L a + \frac{1}{\tau_1} + \frac{1}{\tau_2})}{2} - \sqrt{\frac{(K_L a + \frac{1}{\tau_1} + \frac{1}{\tau_2})^2}{4} - \frac{K_L a}{\tau_2}}$$

$$\tau_1 = \frac{V_1}{q}$$

$$\tau_2 = \frac{V_2}{q}$$

#### 4.1.2 Required measurements

The dissolved oxygen concentration has to be measured under a reoxygenation to evaluate model nr 1 exactly as in the standard method. At least one probe should be placed in the aerated volume and at least one probe should be placed in the non-aerated volume instead of placing the probes where it represents the total volume, as in the standard method. If most of the water is aerated it can be more accurate to place one probe in the non-aerated water volume and two probes in the aerated volume. It is also good to place the probes at different depths to ensure significant average results.

Other parameters should be measured as in the standard method.

#### 4.1.3 Data analysis

The truncation can be done as in the standard method. If it is possible, it may be more correct to analyze also lower dissolved oxygen concentrations under 20% of the

dissolved oxygen saturation concentration (Boyle, 1983). That is because the difference between the two concentrations,  $C_1$  and  $C_2$ , is probably greatest in the beginning of the reoxygenation. This could affect the results.

Parameters that have to be estimated for model nr 1 are the mass transfer coefficient,  $K_{La}$ , the dissolved oxygen saturation concentration,  $C_{ss}$ , the aerated water volume divided by the liquid flow rate,  $V_1/q$ , the non-aerated water volume divided by the liquid flow rate,  $V_2/q$ , the and the dissolved oxygen concentrations at time zero,  $C_{1(0)}$  and  $C_{2(0)}$ . By estimating  $V_1/q$  and  $V_2/q$  it is possible to calculate each of the parameters individually. That is on condition that the total water volume and the ratio between  $V_1$  and  $V_2$  are known (Equation 12 and 13).

$$V = V_1 + V_2 \quad (12)$$

$$V_1 = \frac{\frac{V_1 \cdot V}{V_2}}{1 + \frac{V_1}{V_2}} \quad (13)$$

#### 4.1.4 Calculations

Calculating the performance parameters will be a little bit different from the standard method. SOTR will be calculated only for the aerated volume (Equation 14) where the oxygen transfer is present.

$$SOTR = \frac{V_1}{n} \cdot \sum_{i=1}^n K_L a_{20} \cdot C_{ss\_20} \quad (14)$$

where  $K_L a_{20}$  = volumetric mass transfer coefficient at standard conditions (temperature 20°C and pressure 1atm) ( $\text{min}^{-1}$ )  
 $C_{ss\_20}$  = dissolved oxygen saturation concentration at standard conditions (temperature 20°C and pressure 1atm) (mg/L)

The other two performance parameters, SAE and SOTE, are to be calculated as in the standard method but with the new approach of SOTR.

## 4.2 METHOD NR 2

### 4.2.1 Model nr 2

Separating the total mass transfer,  $K_{La}$ , in two different parts makes it possible to evaluate the oxygen transfer from the air bubbles and at the water surface. The mass transfer coefficient for the air bubbles,  $K_{La,b}$ , is assumed to be present in the whole tank and the water is assumed to be completely mixed (Figure 6).  $K_{La,s}$ , which is the mass transfer coefficient at the water surface, is only present at the water surface. The more turbulence at the water surface the more oxygen is transferred and  $K_{La,s}$  increases (DeMoyer et al., 2003). How turbulent the water surface is can depend on the type of aeration system and the air flow rate.

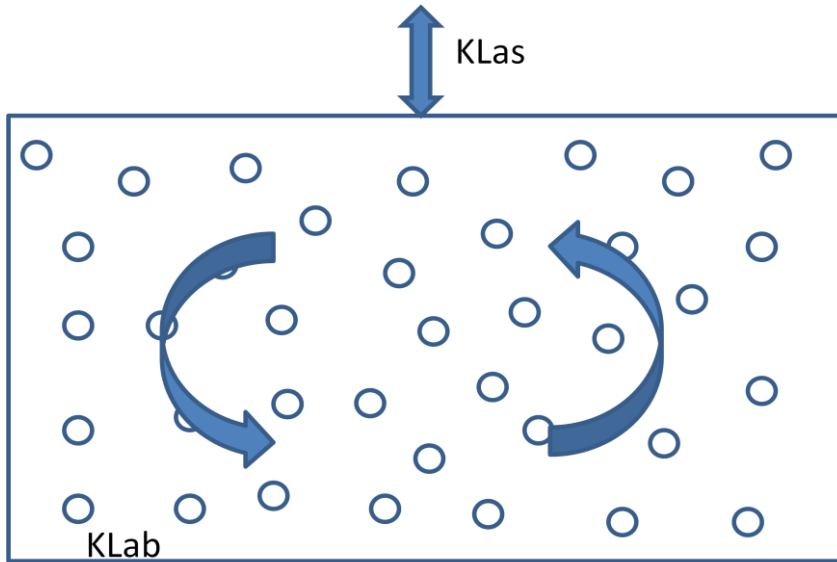


**Figure 6** Model nr 2 which includes the water surface. The mass transfer coefficient for the bubbles,  $K_{La_b}$ , is present in the whole tank and the mass transfer coefficient at the water surface,  $K_{La_s}$ , is present at the turbulent water surface.

The model is very similar to the standard model but this model includes one more term (Equation 15).

$$\frac{dc}{dt} = K_{La_b} \cdot (C_{ss} - C) + K_{La_s} \cdot (C_{surf\_sat} - C) \quad (15)$$

where  $K_{La_b}$  = volumetric mass transfer coefficient for air bubbles ( $\text{min}^{-1}$ )  
 $K_{La_s}$  = volumetric mass transfer coefficient at the water surface ( $\text{min}^{-1}$ )  
 $C_{surf\_sat}$  = dissolved oxygen saturation concentration at atmospheric pressure (mg/L)

The mass transfer coefficient at the water surface,  $K_{La_s}$ , is determined by the dissolved oxygen saturation concentration at atmospheric pressure,  $C_{surf\_sat}$ . That parameter is found in a table for given water temperatures and atmospheric pressures (Lewis, 2006).  $C_{surf\_sat}$  is lower than the dissolved oxygen saturation concentration,  $C_{ss}$ . The analytical solution of Equation 15 is shown in Equation 16.

$$C = \frac{1}{B} \cdot e^{(B \cdot t)} \cdot (A + B \cdot C_0) - \frac{A}{B} \quad (16)$$

where  $A = K_{La_b} \cdot C_{ss} + K_{La_s} \cdot C_{surf\_sat}$   
 $B = -K_{La_b} - K_{La_s}$

#### 4.2.2 Required measurements

Some parameters for performance calculations should be measured with the same conditions as in the standard method.

### 4.2.3 Data analysis

The truncation should be performed as in the standard method. Parameters that should be estimated are the dissolved oxygen saturation concentration,  $C_{ss}$ , the mass transfer coefficient for the bubbles,  $K_L a_b$ , the mass transfer coefficient at the water surface,  $K_L a_s$ , and the dissolved oxygen concentration at time zero,  $C_0$ .

### 4.2.4 Calculations

Account is taken for  $K_L a_b$  and  $K_L a_s$  in calculations of the SOTR (Equation 17).

$$SOTR = \frac{V}{n} \cdot \sum_{i=1}^n (K_L a_{b\_20i} \cdot C_{ss\_20i} + K_L a_{s\_20i} \cdot C_{surf\_sat\_20i}) \quad (17)$$

where  $K_L a_{b\_20i}$  = volumetric mass transfer coefficient for air bubbles at standard conditions for measurement probe i (temperature 20°C and pressure 1 atm) ( $\text{min}^{-1}$ )  
 $K_L a_{s\_20i}$  = volumetric mass transfer coefficient at the water surface at standard conditions for measurement probe i (temperature 20°C and pressure 1 atm) ( $\text{min}^{-1}$ )  
 $C_{surf\_sat\_20i}$  = dissolved oxygen saturation concentration at atmospheric pressure at standard conditions for measurement probe i (temperature 20°C and pressure 1 atm) (mg/L)

SAE and SOTE should be calculated as in the standard method but with the new equation for SOTR.

## 4.3 METHOD NR 3

### 4.3.1 Model nr 3

This model is quite similar to model nr 2, but in this model account has been taken to the variations of the dissolved oxygen equilibrium concentration with water depth (Figure 7). By introducing the variation with water depth it is possible to calculate it instead of estimating it like in the standard method. The reason why the dissolved oxygen equilibrium concentration varies with depth is the fact that more oxygen can be dissolved at higher pressures according to Henry's law (McWhirter & Hutter, 1989).

The equilibrium concentration is also depending on the ratio of oxygen in the air bubbles which varies with time. At infinite time when the water is saturated, no more oxygen will be dissolved and the ratio of oxygen is almost the same as in the released air (McWhirter & Hutter, 1989).

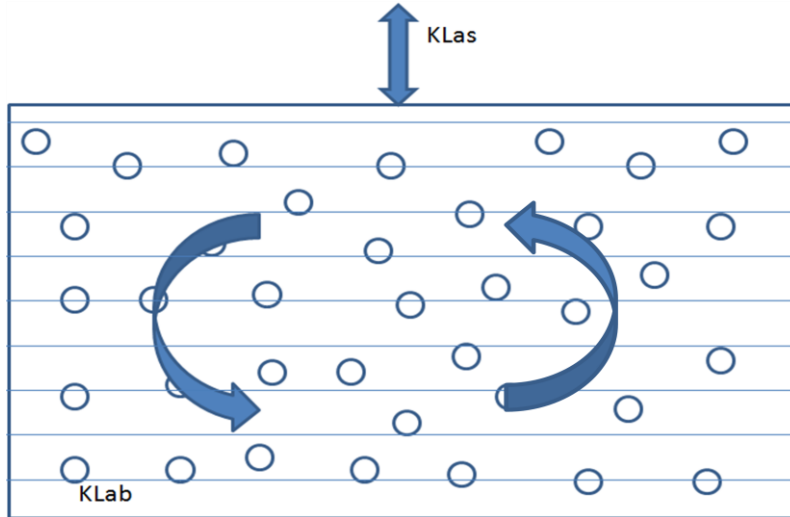


**Figure 7** Model nr 3 which includes the water surface and is depth dependent. The mass transfer coefficient for the bubbles,  $K_{La_b}$ , is present in the whole tank and the mass transfer coefficient for the water surface,  $K_{La_s}$ , is present at the water surface. The dissolved oxygen equilibrium concentration is depth and time dependent.

As the standard model and model nr 2, this model is based on the assumption that the water is well mixed. The model is based on integrating the dissolved oxygen equilibrium concentration over the water depth  $z$  (Equation 18). The integral limits of  $z$  are between zero and the actual water depth. The dissolved oxygen concentration is assumed to vary between  $C_0$  and  $C$ .

$$\frac{dC}{dt} = \frac{K_{La_b}}{h_d} \int_0^{z_s} (C_o^*(z) - C) dz + K_{La_s} \cdot (C_{surf\_sat} - C) \quad (18)$$

where  $h_d$  = depth to aeration system (m)  
 $z$  = water depth ( $z = 0$  at the tank bottom and  $z = z_s$  at the water surface) (m)  
 $C_o^*$  = dissolved oxygen equilibrium concentration (mg/L)

The dissolved oxygen equilibrium concentration,  $C_o^*$ , depends on several different parameters. One of these parameters is the concentration of oxygen in gas phase,  $y$ . (Equation 19) (McWhirter & Hutter, 1989).

$$C_o^*(z) = C_{surf\_sat} \cdot \left( \frac{P - P_{wv} + \frac{(h_d - z)}{10.33}}{1 - P_{wv}} \right) \cdot \frac{y}{0.266} \quad (19)$$

where  $P$  = atmospheric pressure (atm)  
 $P_{wv}$  = water vapor pressure (atm)  
 $y$  = concentration of oxygen in gas phase (kmol  $O_2$ /kmol  $N_2$ )

Calculating  $y$  has to be done to be able to calculate  $C_o^*$  and the actual dissolved oxygen concentration in Equation 20. The boundary value of  $y$  is 0.266 kmol  $O_2$ /kmol  $N_2$  at  $z = 0$  for all times. Because  $C_o^*$  is depth dependent,  $y$  will also become depth dependent (McWhirter & Hutter, 1989). In this case  $K_{La_b}$  should be analyzed in the unit hours because the gas flow rate,  $G$ , is given per hour or vice versa.



$$\frac{dy}{dz} = -\frac{A}{G} \cdot K_L a_b \cdot (C_o^*(z) - C) \cdot K_2 \quad (20)$$

where        A = cross sectional area of the tank (m<sup>2</sup>)  
                   G = gas flow rate (kmol N<sub>2</sub>/h)  
                   K<sub>2</sub> = conversion factor (3.13·10<sup>-5</sup>(kmol O<sub>2</sub>·L)/(m<sup>3</sup>·mg))

#### 4.3.2 Required measurements

The required measurements are the same as for the standard method.

#### 4.3.3 Data analysis

There are three different parameters that should be estimated, the mass transfer coefficient for the air bubbles, K<sub>L</sub>a<sub>b</sub>, the mass transfer at the water surface, K<sub>L</sub>a<sub>s</sub> and the dissolved oxygen concentration at time zero, C<sub>0</sub>. Unlike the standard model the saturation concentrations are calculated and not estimated. Truncation of data should be performed as in the standard method.

#### 4.3.4 Calculations

This model approach leads to changes in the calculations of the SOTR in comparison to the standard model (Equation 21). C<sub>o</sub><sup>\*</sup> is calculated with C<sub>surf\_sat\_20i</sub> which is for standard conditions. The water depth is assumed to vary between zero and z<sub>s</sub>.

$$SOTR = \frac{V}{n} \cdot \sum_{i=1}^n \left( \int_0^{z_s} \left( \frac{K_L a_{b\_20i} \cdot C_o^*(z)}{z_s} \right) dz + K_L a_{s\_20i} \cdot C_{surf\_sat\_20i} \right) \quad (21)$$

Calculating standard aeration efficiency (SAE) and standard oxygen transfer efficiency (SOTE) as in the standard method is possible with the new equation of SOTR.

### 4.4 METHOD NR 4

#### 4.4.1 Model nr 4: Combining model nr 1 and 2

By combining model nr 1 and 2 it is possible to make a model that can handle both two separate water volumes and also oxygen transfer from both air bubbles and at the water surface (Figure 8). The oxygen transfer at the water surface is also separated in two different parts, the oxygen transfer at the bubbled water surface, K<sub>L</sub>a<sub>s1</sub> and at the non-bubbled water surface, K<sub>L</sub>a<sub>s2</sub>. The bubbled water surface is straight above the bubbled plume which rises to the water surface and the non-bubbled water surface is around or besides the bubbled surface. Oxygen transfer at the bubbled water surface is normally bigger than the oxygen transfer at the non-bubbled water surface (DeMoyer et al., 2003).

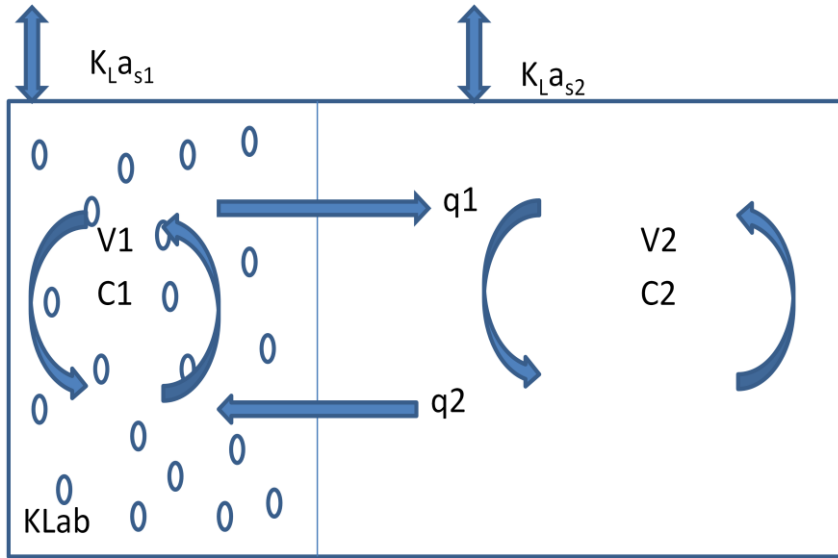


**Figure 8** Model nr 4 which includes both an aerated water volume and a non-aerated water volume. The oxygen mass transfer is separated in three different parts,  $K_{La_b}$  for the air bubbles,  $K_{La_{s1}}$  at the bubbled water surface and  $K_{La_{s2}}$  at the non-bubbled water surface.

The model equations which describe how the dissolved oxygen concentration varies with time are presented in Equation 22 and 23.

$$\frac{dC_1}{dt} = K_{La_b} \cdot (C_{ss} - C_1) + \frac{q \cdot C_2}{V_1} - \frac{q \cdot C_1}{V_1} + K_{La_{s1}} \cdot (C_{surf\_sat} - C_1) \quad (22)$$

$$\frac{dC_2}{dt} = \frac{q \cdot C_1}{V_2} - \frac{q \cdot C_2}{V_2} + K_{La_{s2}} \cdot (C_{surf\_sat} - C_2) \quad (23)$$

where  $K_{La_{s1}}$  = volumetric mass transfer coefficient at the bubbled water surface ( $\text{min}^{-1}$ )  
 $K_{La_{s2}}$  = volumetric mass transfer coefficient at the non-bubbled water surface ( $\text{min}^{-1}$ )

The derived equation which is used for model evaluation is given in Equation 24 and 25. Boundaries for the dissolved oxygen concentration is between  $C_{1(0)}$  and  $C_{2(0)}$  and to  $C$ .

$$C_1 = A_1 \cdot e^{k_1 \cdot t} + A_2 \cdot e^{k_2 \cdot t} + C_{ss} \quad (24)$$

$$C_2 = A_1 \cdot e^{k_1 \cdot t} \cdot \tau_1 \left( k_1 + K_{La_b} + \frac{1}{\tau_1} + K_{La_{s1}} \right) + A_2 \cdot e^{k_2 \cdot t} \cdot \tau_1 \left( k_2 + K_{La_b} + \frac{1}{\tau_1} + K_{La_{s1}} \right) + C_{ss} \quad (25)$$

where

$$A_2 = \frac{C_{2(0)} - \tau_1 \left( C_{1(0)} \cdot k_1 + C_{1(0)} \cdot K_{La_b} + \frac{C_{1(0)}}{\tau_1} + C_{1(0)} \cdot K_{La_{s1}} - C_{ss} \cdot k_1 - C_{ss} \cdot K_{La_b} - C_{ss} \cdot K_{La_{s1}} \right)}{\tau_1 \cdot (-k_1 + k_2)}$$

$$A_1 = -A_2 + C_{1(0)} - C_{ss}$$

$$k_1 = \frac{-\left(K_L a_b + \frac{1}{\tau_1} + K_L a_{s1} + K_L a_{s2} + \frac{1}{\tau_2}\right)}{2} +$$

$$\sqrt{\frac{\left(K_L a_b + \frac{1}{\tau_1} + K_L a_{s1} + K_L a_{s2} + \frac{1}{\tau_2}\right)^2}{4} - K_L a_b \cdot K_L a_{s2} + \frac{K_L a_b}{\tau_2} + \frac{K_L a_{s2}}{\tau_1} + K_L a_{s1} \cdot K_L a_{s2} + \frac{K_L a_{s1}}{\tau_2}}$$

$$k_1 = \frac{-\left(K_L a_b + \frac{1}{\tau_1} + K_L a_{s1} + K_L a_{s2} + \frac{1}{\tau_2}\right)}{2} -$$

$$\sqrt{\frac{\left(K_L a_b + \frac{1}{\tau_1} + K_L a_{s1} + K_L a_{s2} + \frac{1}{\tau_2}\right)^2}{4} - K_L a_b \cdot K_L a_{s2} + \frac{K_L a_b}{\tau_2} + \frac{K_L a_{s2}}{\tau_1} + K_L a_{s1} \cdot K_L a_{s2} + \frac{K_L a_{s1}}{\tau_2}}$$

$$\tau_1 = \frac{V_1}{q}$$

$$\tau_2 = \frac{V_2}{q}$$

#### 4.4.2 Required measurements

The required measurements are a combination of the measurements for model nr 1 and 2. At least one dissolved oxygen probe should be placed in the aerated water volume and at least one in the non-aerated volume.

#### 4.4.3 Data analysis

The data truncation should be performed as in the standard method, but the lower dissolved oxygen concentration that is analyzed the better.

Eight parameters are estimated using this model. The dissolved oxygen saturation concentration,  $C_{ss}$ , the mass transfer coefficient for the air bubbles,  $K_L a_b$ , the mass transfer coefficient for the bubbled water surface,  $K_L a_{s1}$ , the mass transfer coefficient for the non-bubbled water surface,  $K_L a_{s2}$ , the liquid flow rate divided by the aerated water volume,  $V_1/q$ , the liquid flow rate divided by the non-aerated water volume,  $V_2/q$ , the dissolved oxygen concentration in the aerated water volume at time zero,  $C_{1(0)}$  and the dissolved oxygen concentration in the non-aerated water volume at time zero,  $C_{2(0)}$ .

#### 4.4.4 Calculations

All three mass transfer coefficients should be corrected to standard conditions at 20°C and pressure 1atm. Also the dissolved oxygen saturation concentrations should be analyzed for standard conditions. SOTR is calculated using Equation 26.

$$SOTR = \frac{V}{n} \cdot \sum_{i=1}^n (K_L a_{b_{20i}} \cdot C_{ss_{20i}} + K_L a_{s1_{20i}} \cdot C_{surf\_sat_{20i}} + K_L a_{s2_{20i}} \cdot C_{surf\_sat_{20i}}) \quad (26)$$

where  $K_{La_{s1\_20i}}$  = volumetric mass transfer coefficient at the bubbled water surface at standard conditions for measurement probe i (temperature 20°C and pressure 1atm) ( $\text{min}^{-1}$ )  
 $K_{La_{s2\_20i}}$  = volumetric mass transfer coefficient at the non-bubbled water surface at standard conditions for measurement probe i (temperature 20°C and pressure 1atm) ( $\text{min}^{-1}$ )

Calculations of SAE and SOTE are performed as in the standard method but with the new SOTR.

#### 4.5 METHOD NR 5

##### 4.5.1 Model nr 5: Combining model nr 1 and 3

Model nr 5 is a combination of model nr 1 and 3 (Figure 9). As model nr 1, this model can handle a water volume that is separated in two parts, an aerated water volume containing air bubbles and a non-aerated water volume without bubbles. A liquid flow rate is connecting the two volumes and is assumed to be the driving force for the water mixing. To make the model even more accurate it has three different mass transfer coefficients.  $K_{La_b}$  is the mass transfer coefficient for the air bubbles,  $K_{La_{s1}}$  at the bubbled water surface above the bubbles plume and  $K_{La_{s2}}$  which is the mass transfer coefficient at the non-bubbled water surface. The dissolved oxygen saturation concentration is assumed to vary with water depth and is named the dissolved oxygen equilibrium concentration,  $C_o^*$ .

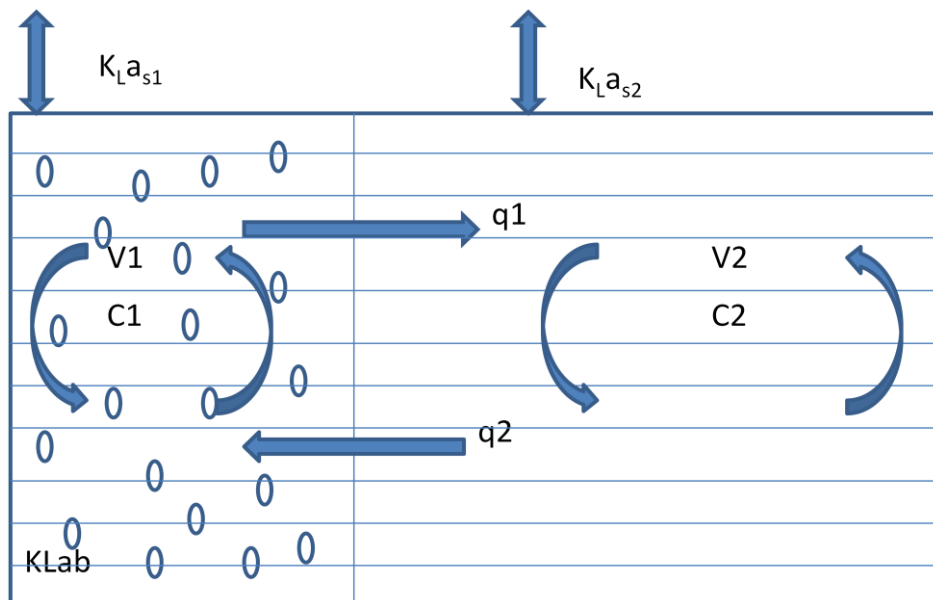


**Figure 9** Model nr 5 is the most modified and complex model in comparison to the standard model. It includes both an aerated water volume and a non-aerated water volume. The oxygen transfer is separated in three different parts,  $K_{La_b}$  for the air bubbles,  $K_{La_{s1}}$  for the bubbled water surface and  $K_{La_{s2}}$  for the non-bubbled water surface. The dissolved oxygen equilibrium concentration is also depth dependent.

This model consists of two equations that describe how the dissolved oxygen concentration in each water volume is varying with time (Equation 27 and 28).

$$\frac{dC_1}{dt} = \frac{K_L a_b}{h_d} \cdot \int_0^z (C_o^*(z) - C_1) dz + \frac{q \cdot C_2}{V_1} - \frac{q \cdot C_1}{V_1} + K_L a_{s1} \cdot (C_{surf\_sat} - C_1) \quad (27)$$

$$\frac{dC_2}{dt} = \frac{q \cdot C_1}{V_2} - \frac{q \cdot C_2}{V_2} + K_L a_{s2} \cdot (C_{surf\_sat} - C_2) \quad (28)$$

The dissolved oxygen equilibrium concentration is calculated for each water depth at ambient temperature (Equation 29). The temperature dependence is included in  $C_{surf\_sat}$ , which is a tabular value.

$$C_o^*(z) = C_{surf\_sat} \cdot \left( \frac{P - P_{wv} + \frac{(h_d - z)}{10.33}}{1 - P_{wv}} \right) \cdot \frac{y}{0.266} \quad (29)$$

The dissolved oxygen equilibrium concentration is dependent of the concentration of oxygen in gas phase,  $y$ . The initial  $y$  is assumed to be 0.266 kmol O<sub>2</sub>/kmol N<sub>2</sub>. How  $y$  is varying with water depth is presented in Equation 30.

$$\frac{dy}{dz} = -\frac{A}{G} \cdot K_L a_b \cdot (C_o^*(z) - C) \cdot K_2 \quad (30)$$

#### 4.5.2 Required measurements

The same measurements as for method nr 1 and 3 have to be done to evaluate this model. At least one probe should be placed in the aerated water volume and at least one in the non-aerated water volume to measure the dissolved oxygen concentration.

#### 4.5.3 Data analysis

Parameters that should be estimated using model nr 5 is  $K_L a_b$ ,  $K_L a_{s1}$ ,  $K_L a_{s2}$ ,  $q/V_1$ ,  $q/V_2$ ,  $C_{1(0)}$  and  $C_{2(0)}$ . The saturation concentrations are calculated instead of being estimated.

#### 4.5.4 Calculations

The equation for SOTR is separated in three terms, one for each mass transfer coefficient (Equation 31). The mass transfer coefficient is multiplied with each water volume and dissolved oxygen saturation or equilibrium concentrations. As for method nr 3,  $C_o^*$  is calculated by using the  $C_{surf\_sat\_20i}$  for standard conditions.

$$SOTR = \frac{1}{n} \cdot \sum_{i=1}^n \left( V_1 \cdot \int_0^{z_s} \left( \frac{K_L a_{b\_20i} \cdot C_o^*(z)}{z_s} \right) dz + V_1 \cdot K_L a_{s1\_20i} \cdot C_{surf\_sat\_20i} + V_2 \cdot K_L a_{s2\_20i} \cdot C_{surf\_sat\_20i} \right) \quad (31)$$

### 4.6 SUMMARY OF THE ALTERNATIVE MODELS

A summary of the alternative models is given in Figure 10.

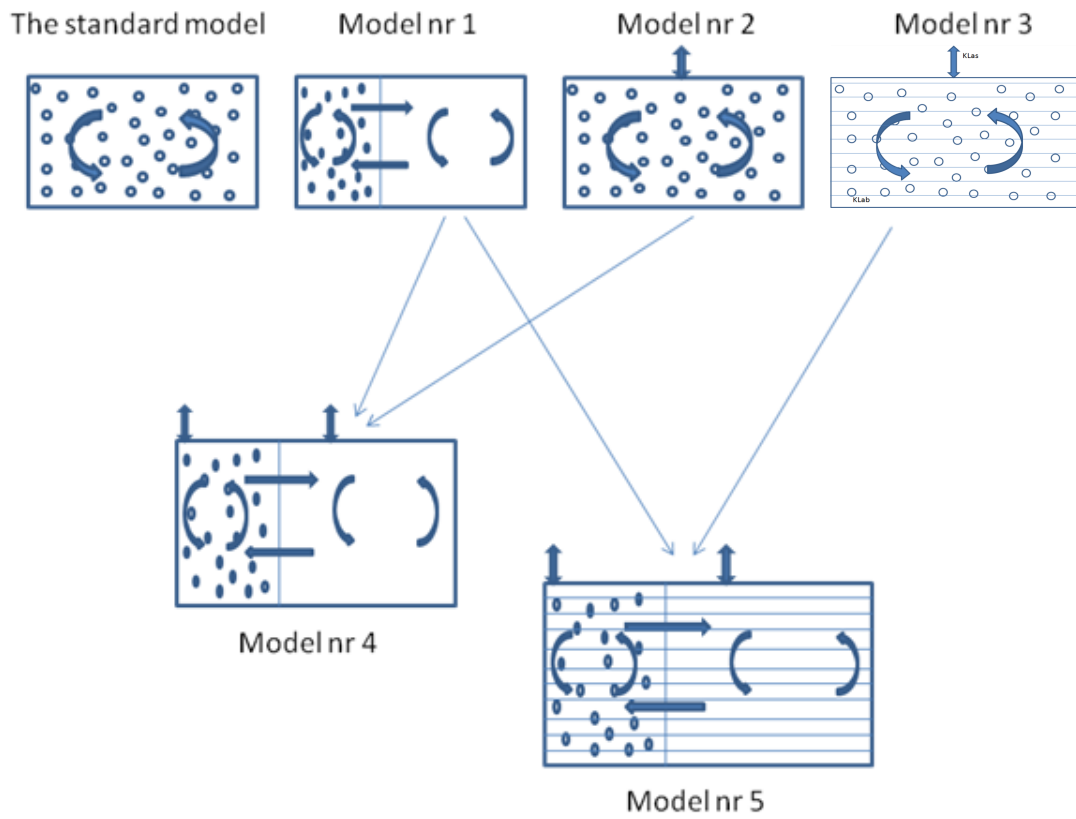


**Figure 10** All evaluated models. There are three model approaches and the standard model which can be combined in different ways.

## **5 METHODS AND MATERIALS**

Oxygen transfer data was measured to evaluate the new models. Data was analyzed from a cylinder tank and a racetrack tank which both were equipped with one or more diffusers for the air release. The measurement instruments were assumed not to affect the oxygen transfer or water velocity significantly. The two types of aeration tanks were conducted to get significant data and also to get data from two different ways of aeration. Dissolved oxygen concentration and other parameters were measured during the laboratory work and registered in a computer.

Several tests were conducted with different parameter settings, but the parameters that are presented in this chapter show the conditions for one representative test. The measurement time in the cylinder tank was 20min and in the racetrack tank 34min.

The new models were evaluated using different approaches and the most difficult part was to make the models good and reliable. A model must be validated to ensure that it is reliable. Mainly, the evaluation was to compare the systems behavior to the models (Ljung & Glad, 2004). The new models were evaluated using simulated data, plotting, calculating the residual sum of squares and controlling the parameter sensitivity.

### **5.1 THE CYLINDER TANK**

Measurements were first conducted in a cylinder tank (Figure 11) using one diffuser. The dissolved oxygen concentration was measured using five probes at different positions and depths. Two probes were positioned in the lowest part of the tank and placed in the non-aerated water volume without air bubbles. One of them was placed below the diffuser to ensure that there were no bubbles. Above them were three probes placed in the aerated water volume. The reason why all three probes were placed above the other two was to ensure that they were in a water volume containing bubbles. Four probes were attached to a steel pole which stood diagonally in the tank and the fifth probe was just hanging in a rope and attached at the top of the tank.

The diffuser was aerating the water approximately one day before any measurements started to ensure that nothing would be different by starting a dry diffuser.

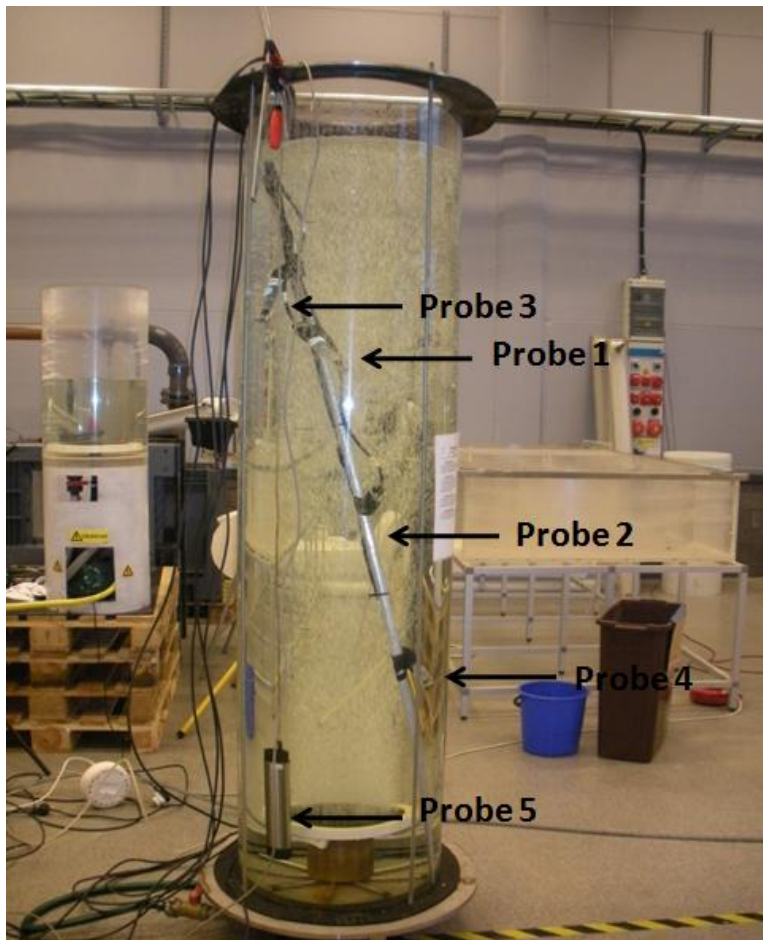


**Figure 11** The cylinder tank with five dissolved oxygen probes. The two lowest probes (probe 5 and 4) were placed in the non-aerated water volume and the three probes above (probe 2, 1 and 3) were placed in the aerated water volume with air bubbles.

The diffuser was a Sanitaire diffuser with a diameter of 0.22m (Figure 12) and positioned 0.18m above the bottom of the tank.



**Figure 12** A diffuser from Sanitaire (Figure from ITT Water & Wastewater).

The water depth was 1.95m and the cylinder tank had a diameter of 0.51m. Other parameters are summarized in Table 2. The water depth was measured after the diffuser was placed in the tank but before it was operating.



**Table 2** Cylinder tank dimensions.

| <b>Parameter</b>                      | <b>Value</b> |
|---------------------------------------|--------------|
| Water depth (m)                       | 1.95         |
| Depth to diffuser (m)                 | 1.77         |
| Cylinder diameter (m)                 | 0.51         |
| Water volume (m <sup>3</sup> )        | 0.397        |
| Number of diffusers (-)               | 1            |
| Number of dissolved oxygen probes (-) | 5            |

Some parameters were only measured before starting any tests and some were measured both before and after tests. The conductivity was measured both before and after the oxygen measurements because addition of deoxygenating chemicals should increase the conductivity (Table 3) (ASCE, 2007). Water temperature was measured using the dissolved oxygen probes.

**Table 3** Parameters for one test in the cylinder tank.

| <b>Parameter</b>             | <b>Before test</b> | <b>After test</b> |
|------------------------------|--------------------|-------------------|
| Conductivity (mS/cm)         | 0.78               | 1.03              |
| Water temperature (°C)       | 15.5               | 15.7              |
| Ambient air temperature (°C) | 20.3               | -                 |
| Ambient air pressure (hPa)   | 1015               | -                 |
| Air flow (nL/min)*           | 20.1               | -                 |
| C <sub>surf_sat</sub> (mg/L) | 10                 | 10                |

\* n = normal

## 5.2 THE RACETRACK TANK

The racetrack tank was designed like a channel (Figure 13). In the middle of the tank there was a wall. At both ends of the middle wall there are two interior walls which were formed as semicircles. They were made to reduce the water swirls which can occur due to water meeting the outer wall and to make the channel curve smoother. The forms of the outer walls were rectangular and the tank was equipped with six small diffusers which were made to fit the channel in the racetrack (Figure 14). The principle of the racetrack tank was to aerate one part of the channel and keep the rest non-aerated. Because the water was driven by a mixer the aerated water will be mixed with the non-aerated water. Theoretically, the water in the non-aerated zone will be aerated but with a delay in comparison to the water in the aerated zone.

The dissolved oxygen concentration was measured using five probes (Figure 15). Two probes were positioned in the last part of the aerated zone and three probes were placed in the last part of the non-aerated zone. All probes were placed in the last part of respectively zone to make it possible to use the data to evaluate models containing two water volumes. They were placed at the same water depth.

All the diffusers were aerating the water approximately one day before any measurements started.

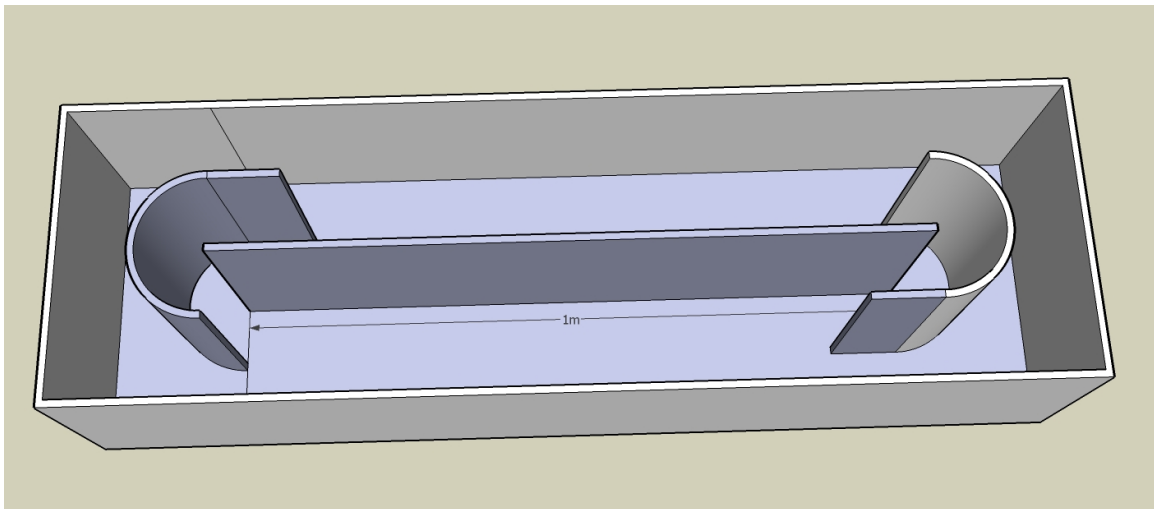


**Figure 13** The rectangular racetrack tank. An inner wall was designed to make a channel of the tank. At both ends of the inner wall there were two semicircle formed walls.

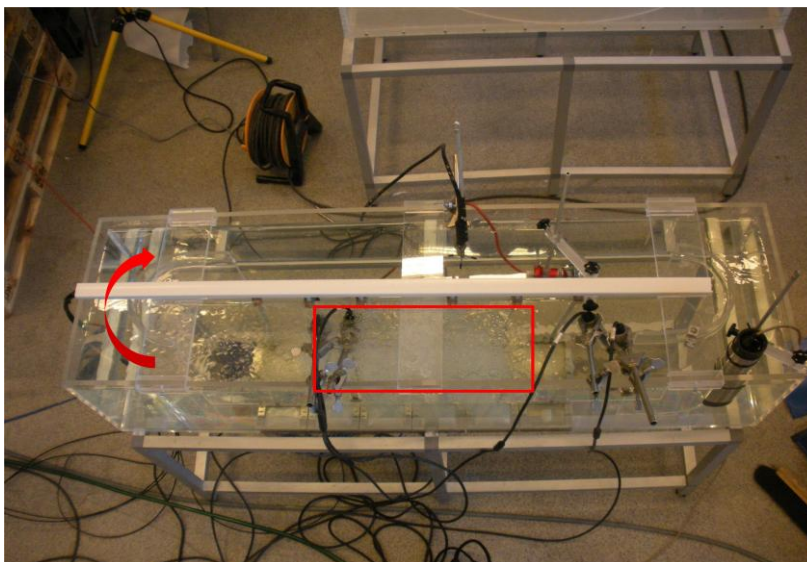


**Figure 14** The racetrack tank seen from above. The liquid flow rate was going clockwise. There was an aerated water volume in the red box and the rest of the water was non-aerated. Two dissolved oxygen probes were placed in the last part of the aerated water volume and three probes were placed in the last part of the non-aerated volume. There were also one mixer and an instrument to measure the water velocity.

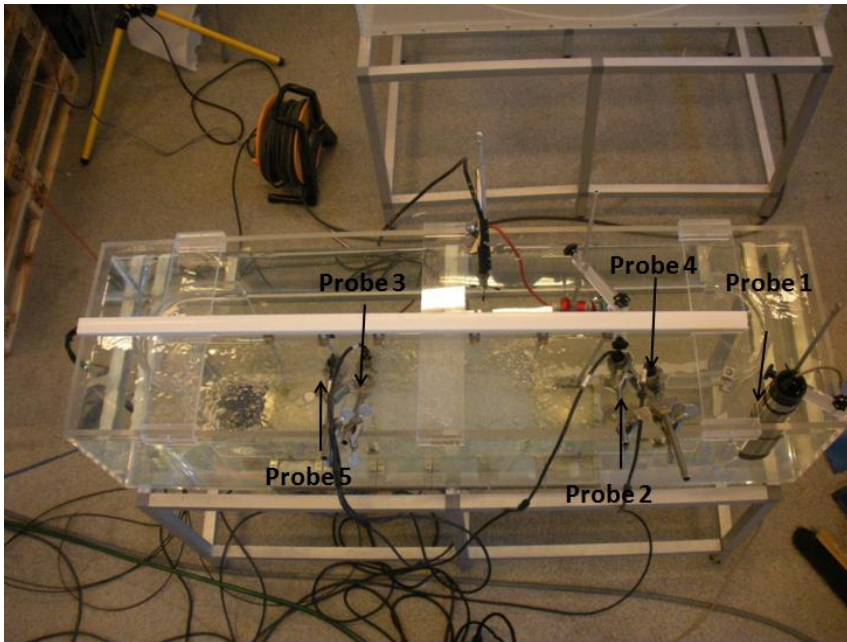


**Figure 15** Probe 5 and 3 were placed in the last part of the aerated water volume and probe 2, 4 and 1 were placed in the last part of the non-aerated water volume.

A mixer was used in the racetrack tank to produce a water flow (Figure 16). Because the tank was small the mixer was specially designed for this tank. The speed of the mixer could be regulated. The water velocity transferred the aerated water from the aerated zone to the non-aerated zone which makes the water in the whole tank aerated. The velocity was assumed to be fairly constant and was measured at six different places in a cross section of the channel just behind the mixer. That is described more detailed in chapter 5.3.2.

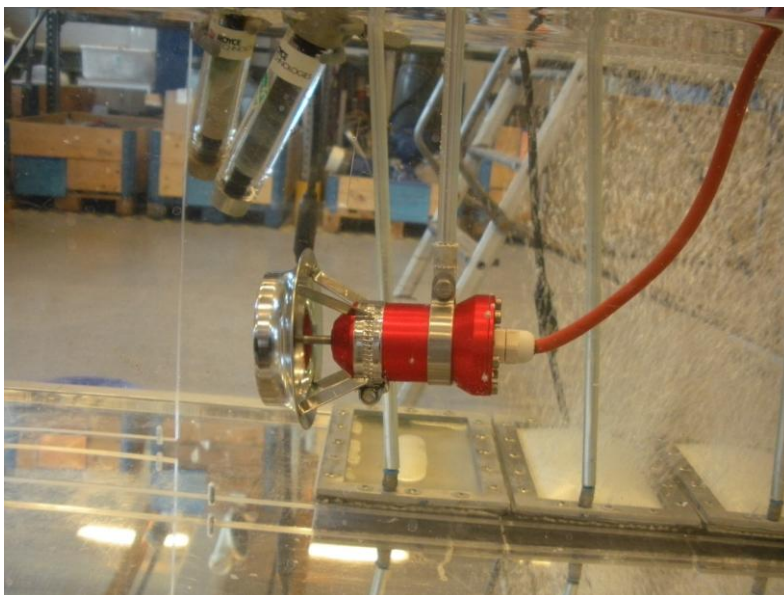


**Figure 16** The mixer which produced a liquid flow rate in the racetrack tank. Note that the inner wall is made of invisible acrylic plastic, so the diffusers on the other side can also be seen.

The diffusers were specially made to fit the channel width in the racetrack. The outer width was 0.195m and length 0.115m (Figure 17) but the diffusive material, where the bubbles were released from, was 0.16m wide and 0.08m long. Four of six diffusers were operating during all measurement tests and they were placed close to each other. The aerated water volume can then be assumed to occur in one zone.

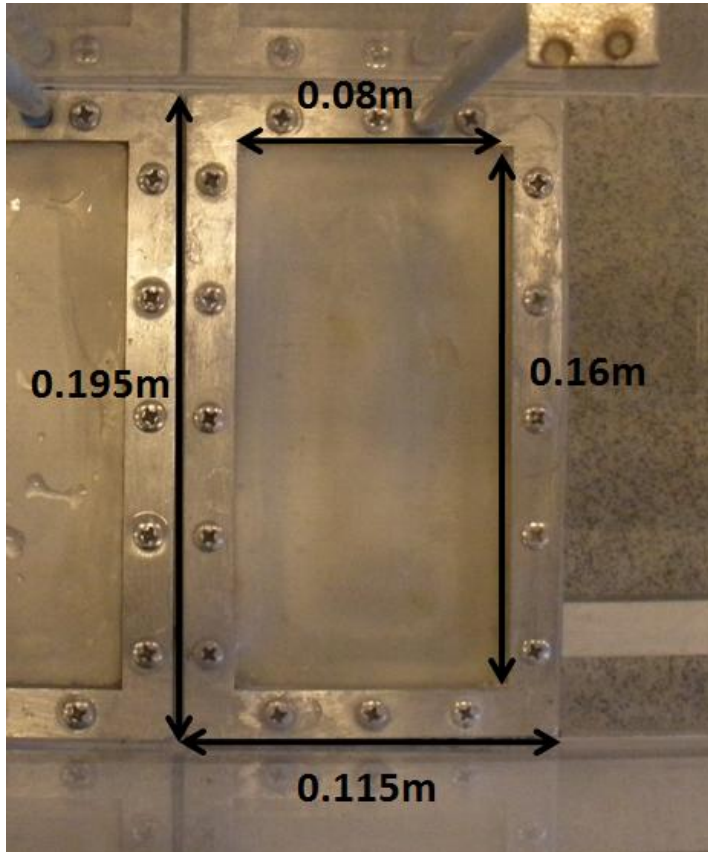


**Figure 17** Inner and outer widths of one diffuser in the racetrack tank. The air bubbles were only released from the inner part.

The water depth in the tank was 0.28m and the tank was 1.4m long and 0.4m wide. Other parameters are summarized in Table 4.

**Table 4** Racetrack tank dimensions.

| <b>Parameter</b>                      | <b>Value</b> |
|---------------------------------------|--------------|
| Water depth (m)                       | 0.28         |
| Depth to diffuser (m)                 | 0.28         |
| Tank length (m)                       | 1.4          |
| Tank width (m)                        | 0.4          |
| Water volume (m <sup>3</sup> )        | 0.146        |
| Number of diffusers (-)               | 4 operating  |
| Number of dissolved oxygen probes (-) | 5            |

As the tests in the cylinder tank, the conductivity and water temperature were measured in the racetrack tank both before and after the measurement tests (Table 5). The water

temperatures were checked at the dissolved oxygen probes controller. The liquid flow rate was measured but the average value was only briefly approximated. The dissolved oxygen concentration at atmospheric pressure was 9.5mg/L.

**Table 5** Parameters for the test in the racetrack tank.

| <b>Parameter</b>                       | <b>Before test</b> | <b>After test</b> |
|--|--------------------|-------------------|
| Conductivity (mS/cm)                   | 1.43               | 1.71              |
| Water temperature (°C)                 | 17.6               | 17.7              |
| Ambient air temperature (°C)           | 21.6               | -                 |
| Ambient air pressure (hPa)             | 1015               | -                 |
| Air flow (nL/min)*                     | 10.1               | -                 |
| Liquid flow rate (m <sup>3</sup> /min) | 0.265              | 0.265             |
| C <sub>surf_sat</sub> (mg/L)           | 9.5                | 9.5               |

\* n = normal

### 5.3 MEASUREMENT INSTRUMENTS

The measurement instruments used in the experiments were the ones which were available in the laboratory. To get even better and more accurate measurement results there are possibly better instruments or instruments with faster response time. Instructions concerning calibration and instrument placements were considered.

#### 5.3.1 Dissolved oxygen probes

Four of the dissolved oxygen probes used in the experiments was produced by Royce technologies and the indicator was a 9100D with a Royce sensor of 95A (Figure 18). The probes were made for continuous measurement of dissolved oxygen in aeration tanks of waste water treatment plants (SATRON Instruments, 2005). Both the dissolved oxygen and the water temperature were measured using these instruments.



**Figure 18** The picture to the left shows a Royce probe which was attached at a steel pole. The picture to the right shows the controller where it was possible to read the dissolved oxygen concentration and the water temperature.

At the outer end of the sensor 95A, there was a membrane which was half permeable, gases could get through it but not liquids. The dissolved oxygen in the water diffuses in to a galvanic cell of platinum and lead inside the probe. All of the oxygen was there reduced and the dissolved oxygen concentration could be read (SATRON Instruments, 2005).

Before using the probes for the first test the membrane at every probe was changed. If the probes have been dry to long the membrane could possibly be broken. Also the electrolyte liquid inside the probes, potassium chloride gel, was changed. That was done because the liquid had been there for a long time and it contained small lumps of thickened liquid. After the membrane and electrolyte was changed, the probe stayed in water without dissolved oxygen for three days.

These probes should be attached in a tank with an angle of 45°. If the angle was larger there was a risk that the electrolyte liquid did not cover the whole lead wire inside the probe and if the angle was too small there was a risk that bubbles could get stuck at the membrane.

An optical probe from Lange was also used in the tests (Figure 19). That probe was factory calibrated and was not calibrated before any test. The probe was kept in water for three days before it was used.



**Figure 19** The picture to the left shows the Lange probe. The picture to the right shows the controller where it was possible to read the dissolved oxygen concentration and the water temperature.

When all instruments were positioned in a tank, the Royce probes were to be calibrated. Using the Lange probe as a reference probe it was possible to calibrate the Royce probes. When a Royce probe was calibrated, the Lange probe was placed besides it at the same depth. The dissolved oxygen concentration was checked and the same concentration was set to the Royce probe. The same procedure followed for all four Royce probes. This was done while the diffuser or diffusers were operating and the dissolved oxygen concentration had reached steady state saturation.

The Lange probe was set straight up in both the cylinder tank and in the racetrack tank in the non-aerated water volume to prevent any bubbles to fasten underneath the probe.

Five dissolved oxygen probes were measuring during every test, but only four of them were used for model evaluation. The fifth probe was used as a backup.

### 5.3.2 Velocimeter

A Vectrino Velocimeter was used to measure the water velocity in the racetrack tank. The instrument contains a probe with four receive transducers (Figure 20). The velocity was measured using the Doppler Effect and the instrument transmits sound pulses to the water. It listens to the echoes and measures the change in the returning sound frequency. To be able to measure the Doppler Effect the water must contain small suspended particles which can reflect sound (Nortek AS, 2004). Clean water does not contain many particles, but because a deoxygenation was made before every test, the tank water contained particles. The water velocity can be assumed to be the same as for the particles (Nortek AS, 2004).



**Figure 20** Velocimeter to measure the liquid velocity in the racetrack tank. The instrument has four beams which measures the velocity in three dimensions. The beam with a red line was measuring in the X-direction which in this case was the main velocity.

The velocimeter can measure the water velocity in three dimensions with a coordinate system containing X, Y and Z (Nortek AS, 2004). Using the velocimeter in the measurements, one of the coordinates, X, were directed in the flow direction and the other coordinates, Y and Z, were perpendicular to the flow direction. They oscillated around zero and were assumed to be zero. The only interesting direction of the water was in the main direction of the channel because that water later passes the aerated water volume.

To measure the water velocity a scheme of places to measure it was determined. To get good predictions of the actual water velocity six places were chosen (Figure 21). To get as good prediction as possible the best way of doing it would be to measure at infinitely

small places but that was not feasible here. The measurement places were chosen somewhere between the middle and outer walls.

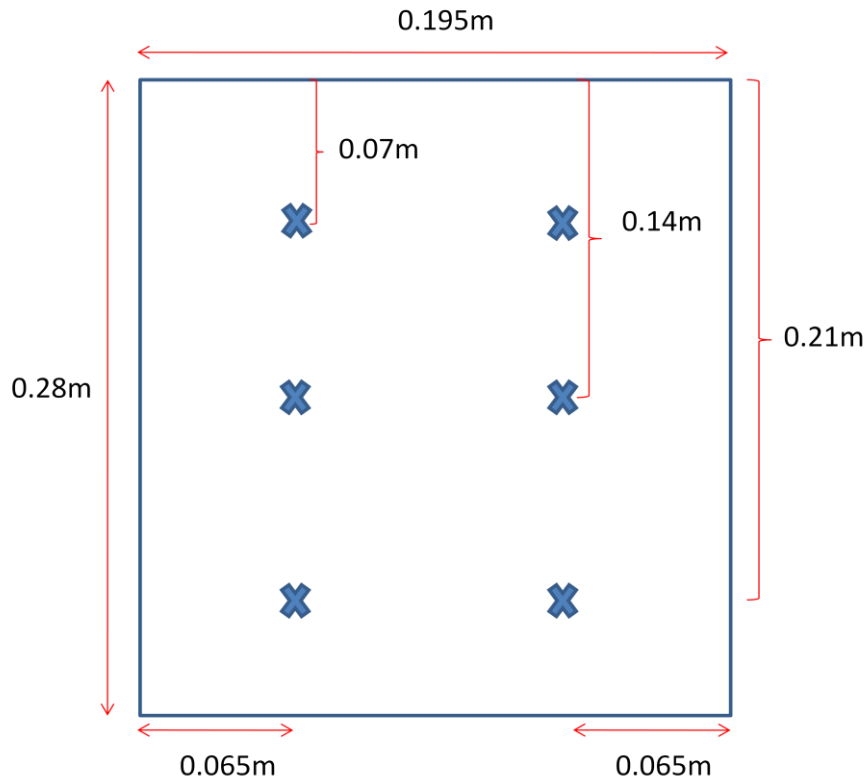


**Figure 21** Cross section area of the racetrack channel. The water velocity was measured at six points which are identified as crosses in the figure. The figure is not to scale.

### 5.3.3 Conductivity measurements

A conductivity meter HI-98312 from Hanna instruments was used for measuring the conductivity in the water. It was important to measure the conductivity both before and after chemical addition because the change was significant (ASCE, 2007). The conductivity meter was calibrated with a solution with known concentration before any measurements. During the measurements the sensor at the probe was held in the water for about ten seconds or until the conductivity at the display was constant.

### 5.3.4 Other parameters

Air temperature and air pressure was read from common temperature and pressure instruments.

## 5.4 CHEMICAL ADDITION

A concentration of approximately 0.3mg/L Cobalt salt was accomplished in both the cylinder and the racetrack tank. Before adding it to the water it was dissolved in a cup containing water. During all measurements it was only added once and that was before the first test. New cobalt addition was made if the water was changed in the tanks.

Sodium sulphite was added to the tanks before starting every new test. The chemical was dissolved in water before adding it and then evenly distributed to the tank.



Both chemicals were evenly distributed in the tanks while the aeration system and mixer operated. The dissolved oxygen concentration was recorded during the deoxygenation. It was a good way of checking that all probes were working well and that the oxygen concentration was nearly zero at all measurement point. The data from the deoxygenation was not used later in the data analysis.

After the deoxygenation, when the dissolved oxygen concentration decreased below 0.5mg/L, the reoxygenation started. If it started direct after the deoxygenation or after a while depended on how much sodium sulphite that was added. During the reoxygenation, the dissolved oxygen concentration rose to approximately the saturation value. How long time the reoxygenation takes depend among other things of the air flow.

## **5.5 DATA ANALYSIS**

A computer was used to register the dissolved oxygen concentrations over time with an interval of one second. The computer registered the concentrations the whole test even if the only interesting data was from the reoxygenation.

A program specially made for Vectrino instruments was used to register the water velocity on another computer. After finished tests the data was converted from the program to an Excel file.

The time series containing dissolved oxygen concentrations and water velocity were later used to calculate the aeration performance and to compare estimated values of the water velocity with the measured values. Calculations and estimation of model parameters were mainly made in the computer programs MATLAB and Excel. All model parameters were in this project estimated in MATLAB using the function `Lsqcurvefit` which “solve nonlinear curve-fitting problems in least-squares sense” (Mathworks, 2010a).

Some models were calculated based on the analytical solution which reduced the number of code files and also made the calculations faster in MATLAB. For the models without an analytical solution, the ordinary differential equations were solved with a function called `ode15s` which reduced the simulation time in comparison to other ordinary differential solvers. The codes for evaluating the standard model can be seen in Appendix A, model nr 1 in Appendix B, model nr 2 in Appendix C and model nr 3 in Appendix D.

## **5.6 MODEL EVALUATION**

### **5.6.1 Simulated data**

For the first model evaluations it is good to use simulated data instead of measured data because all parameter values are known and it is easy to understand how the data behaves. Creating simulated data was made without estimating parameters. Instead the parameters were set to fixed values. Then it was possible to both see how the model

behaved and also to see how sensitive the model was for changing the initial guesses for the estimated parameters. The length of the data series varied for different models.

Introducing white noise to simulated data made it more realistic and it could be interesting to see how the model behaves both with and without added noise. In this case, the noise was produced by a function called `randn` in MATLAB which produced normally distributed noises with different amplitudes depending on the inputs (Mathworks, 2010b). The variance of the noise was 0.01mg/L, the standard deviation was 0.1mg/L and the mean was zero.

### 5.6.2 Plotting

By plotting the measured data and the model in the same figure it was possible to compare how the model was behaving (Boyle, 1983). This was probably the easiest way of doing a first evaluation and was done for all models. Even if the model fits the data it does not mean that the model is a good description of the aeration process or that it is not sensitive for initial guesses for the estimated parameters.

### 5.6.3 Residual sum of squares (RSS)

A residual is the difference between a measured data and the modeled data which is calculated from a mathematical model (Nationalencyklopedin, 2010). There will be one residual for each data point which implies that a time series with data will end up with as many residuals as time steps. If the model fits the measured data correct, the residuals will be zero. The residual sum of squares (RSS) is the summarized squared residuals (Equation 32) (Mathworks, 2010a).

$$RSS = \sum_{i=1}^n (f(x_i) - y_i)^2 \quad (32)$$

There is also a possibility to evaluate the sum of residuals raised to a power higher than two. That would punish big residuals more (Carlsson, personal communication, 2010). Only the residual sum of squares was evaluated in this research.

### 5.6.4 Parameter sensitivity

Initial guesses for the estimated parameters were necessary to set before a nonlinear regression was accomplished. It was desirable that the estimated parameter values do not change even if the initial guesses change. Otherwise the parameters would be sensitive to the initial guesses and there is a risk that the estimated parameters would fasten in local minimum instead of the global minimum. No change in the estimated parameter values for different sets of initial guesses was desirable and the modeling should be reproducible.

To avoid the parameter sensitivity it was possible to set a range with lower and upper bounds for which the estimated parameters should be within. For example the volumetric mass transfer coefficient,  $K_L a$ , may not be negative, so the lower bound can then be set to zero. Only a lower bound was used in this research.

### 5.6.5 Truncation spans

Oxygen transfer measurements can take a long time depending on the tank size and the type of aeration. Reducing the measurement time can save both time and money but the results have to be significant and close to what the results had been if the whole data series had been used. Different truncation spans were evaluated for model nr 3 and compared with the results for the standard model. The truncation was performed by removing the higher concentrations. It is easy to see in Figure 22 that a reduction of the data span could save a lot of time. In this example, a truncation span between 0 and 90% of  $C_{ss}$  instead of between 0 and approximately 100% of  $C_{ss}$  would save almost 20min of the total 35min.

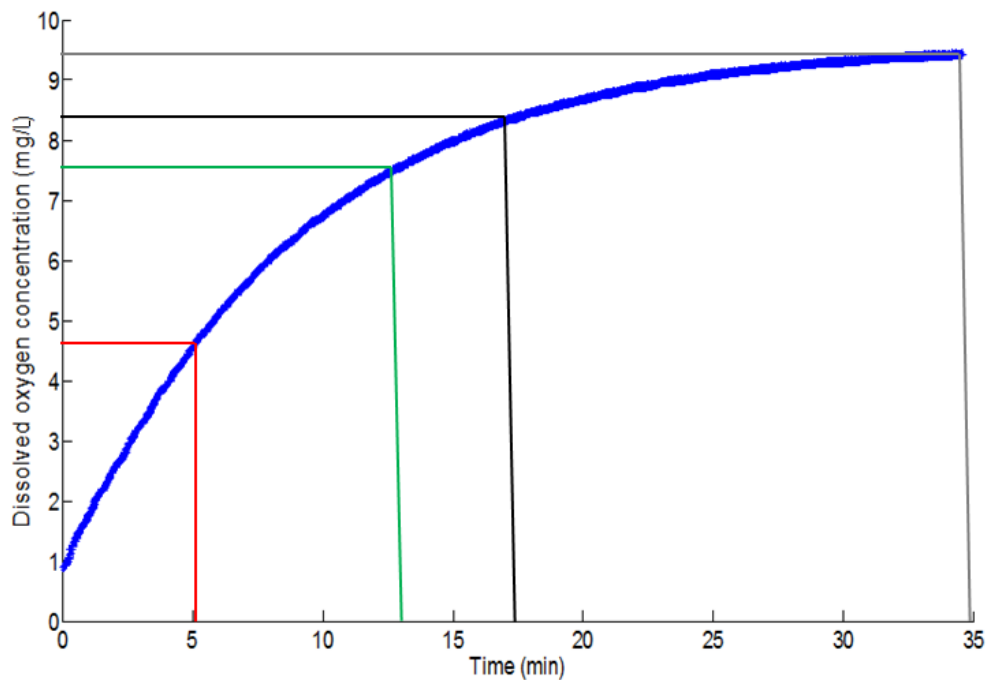


**Figure 22** Different truncation spans. The dissolved oxygen saturation concentration,  $C_{ss}$ , is approximately 9.2mg/L and the total span without truncation includes concentrations between 0 and 9.2mg/L and is denoted by the grey lines. Truncation span between 0 and 90% of  $C_{ss}$  is denoted by the black lines. The next span, the data within the green lines, is between 0 and 80% of  $C_{ss}$ . The data within the red lines represents a truncation span between 0 and 50% of  $C_{ss}$ .

## 6 RESULTS

This chapter includes evaluation of all model approaches presented in the same order as in the previous chapter. Model nr 1, 3 and the standard model were evaluated with both simulated and measured data and model nr 2 and 5 were only evaluated with simulated data. Model nr 4 was not evaluated with any data because it was assumed to behave as model nr 2. Measured data can be either data from the cylinder tank or the racetrack tank or both of them.

An easy way to discover if the estimated parameter values were sensitive to initial guesses was by estimating parameters with different combinations of initial guesses. The possibility to truncate different spans of a data series was evaluated by testing different spans and estimating the parameters. If the parameter values changed significantly it was assumed that the truncation was not satisfactory.

### 6.1 THE STANDARD MODEL

The standard model was evaluated using simulated data and data from the cylinder tank and the racetrack tank. Simulated data and racetrack data were evaluated for different truncation spans.

#### 6.1.1 Simulated data

Model parameters were estimated with simulated data using nonlinear regression. Simulated data with and without noise were evaluated with the standard model and for different initial guesses. Simulated data with added noise and the model is shown in Figure 23.

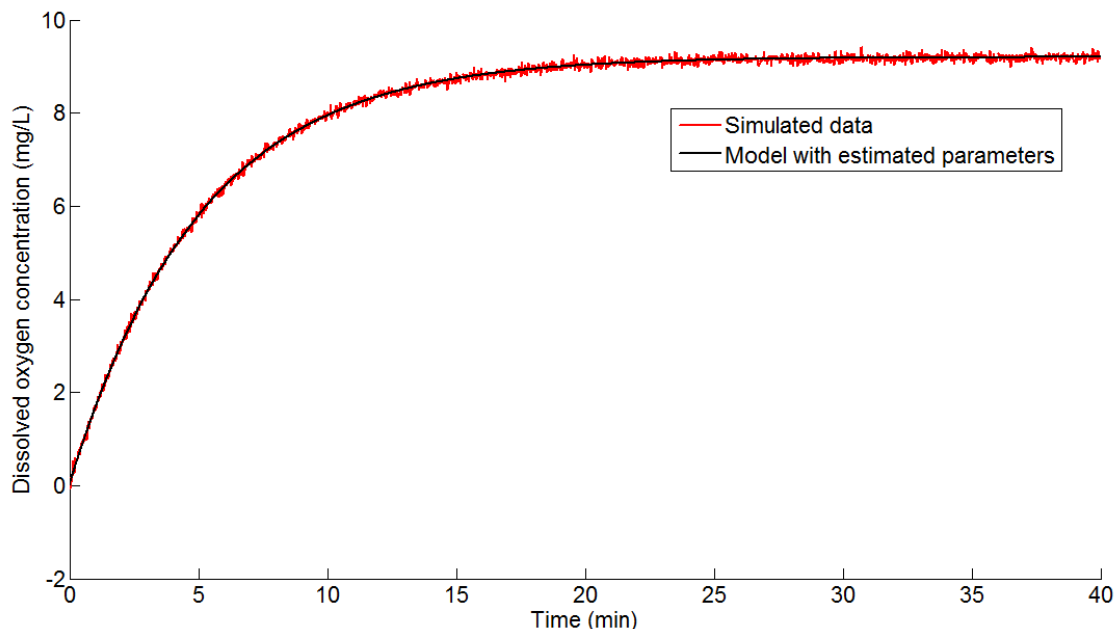


**Figure 23** Simulated data and the standard model. The dissolved oxygen saturation concentration was 9.2mg/L and  $K_L a$  was  $0.2\text{min}^{-1}$ .

Both correct and incorrect initial guesses were used for the simulated data (Table 6). The incorrect initial guesses were used to evaluate parameter sensitivity.

**Table 6** Used initial guesses for the estimated parameters.

|                                  | $C_{ss}$<br>(mg/L) | $C_0$<br>(mg/L) | $K_L a$<br>(min <sup>-1</sup> ) |
|----------------------------------|--------------------|-----------------|---------------------------------|
| <i>Correct initial guesses</i>   | 9.2                | 0               | 0.2                             |
| <i>Incorrect initial guesses</i> | 6                  | 3               | 2                               |

Results from the evaluations showed that the standard model was not sensitive for initial guesses for the estimated parameters (Table 7 and 8). The RSS and the estimated parameters were similar when simulated data was used with both correct and incorrect initial guesses and with and without added noise.

**Table 7** Results of the RSS and estimated parameter values for simulated data without noise. The results were evaluated when both correct and incorrect initial guesses were used.

|  | <b>RSS</b><br>((mg/L) <sup>2</sup> ) | $C_{ss}$<br>(mg/L) | $C_0$<br>(mg/L) | $K_L a$<br>(min <sup>-1</sup> ) |
|--|--------------------------------------|--------------------|-----------------|---------------------------------|
| <i>Using correct initial guesses</i>   | 0.00                                 | 9.20               | 0.00            | 0.200                           |
| <i>Using incorrect initial guesses</i> | 0.00                                 | 9.20               | 0.00            | 0.200                           |

**Table 8** Results of the RSS and estimated parameter values for simulated data with added noise. The results were evaluated when both correct and incorrect initial guesses were used.

|  | <b>RSS</b><br>((mg/L) <sup>2</sup> ) | $C_{ss}$<br>(mg/L) | $C_0$<br>(mg/L) | $K_L a$<br>(min <sup>-1</sup> ) |
|--|--------------------------------------|--------------------|-----------------|---------------------------------|
| <i>Using correct initial guesses</i>   | 8.85                                 | 9.20               | 0.0148          | 0.199                           |
| <i>Using incorrect initial guesses</i> | 8.85                                 | 9.20               | 0.0148          | 0.199                           |

The new data was simulated with 15000 data points during a time span of 300min (Figure 24). The values of the model parameters are presented in Table 9.

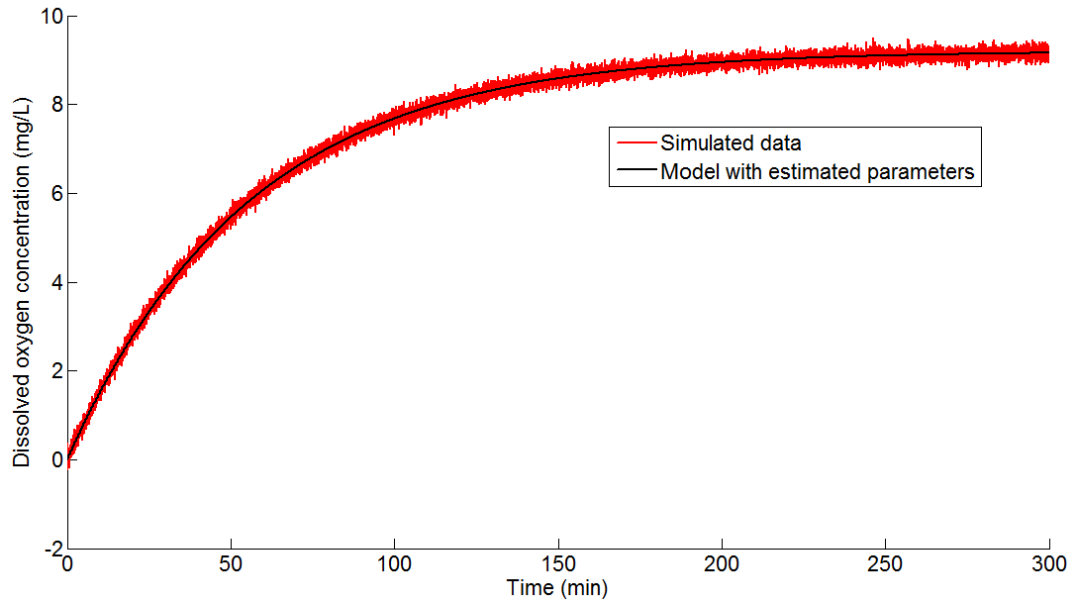


**Figure 24** Noisy simulated data with 15000 data points and the standard model. The time span was 300min. The dissolved oxygen saturation concentration,  $C_{ss}$ , was 9.2mg/L and  $K_La$  was  $0.018\text{min}^{-1}$ .

**Table 9** Used parameter values for the simulated data.

| $C_{ss}$<br>(mg/L) | $C_0$<br>(mg/L) | $K_La$<br>( $\text{min}^{-1}$ ) |
|--------------------|-----------------|---------------------------------|
| 9.2                | 0               | 0.018                           |

Different data spans of the simulated data were chosen and evaluated with nonlinear regression (Table 10). The estimated parameter values were compared with the true parameter values that are given in Table 9. Noise was added to the data to increase the difficulty and make the problem more similar to reality. Also incorrect initial guesses was used for the regression. The estimated  $K_La$  and  $C_{ss}$  for different truncations were compared and also plotted in Figure 25. It was clear that the difference was relatively small for the first truncation spans but increased with decreasing data span. It seemed that the difference between the true and the estimated parameter values increased rapidly for the time span between 0-30min. That represents a truncation between 0 and 43% of the dissolved oxygen saturation concentration, which can be seen in Figure 24.

**Table 10** Results from nonlinear regression of simulated data. The simulated data were noisy and the evaluations were made with the incorrect initial guesses. Estimated values of  $K_{La}$  and  $C_{ss}$  for different truncation spans were compared with the true values and presented in “Diff  $K_{La}$ ” and “Diff  $C_{ss}$ ”.

| Truncation span | Numer of data points (-) | RSS $((mg/L)^2)$ | $C_{ss}$ (mg/L) | $K_{La}$ ( $min^{-1}$ ) | $C_0$ (mg/L) | Diff $K_{La}$ (%) | Diff $C_{ss}$ (%) |
|-----------------|--------------------------|------------------|-----------------|-------------------------|--------------|-------------------|-------------------|
| 0-300min        | 15000                    | 65.1             | 9.20            | 0.0180                  | -0.000700    | 0.00              | 0.00              |
| 0-160min        | 8001                     | 35.1             | 9.20            | 0.0180                  | -0.0023      | 0.00              | -0.0294           |
| 0-120min        | 6001                     | 26.5             | 9.19            | 0.0181                  | -0.00420     | 0.556             | -0.113            |
| 0-80min         | 4001                     | 17.8             | 9.20            | 0.0180                  | -0.00260     | 0.00              | -0.0228           |
| 0-50min         | 2501                     | 11.0             | 9.20            | 0.0180                  | -0.00230     | 0.00              | -0.0326           |
| 0-30min         | 1501                     | 6.70             | 9.34            | 0.0177                  | 0.00100      | -1.67             | 1.57              |
| 0-10min         | 1001                     | 2.21             | 23.3            | 0.00670                 | 0.0173       | -62.8             | 153               |

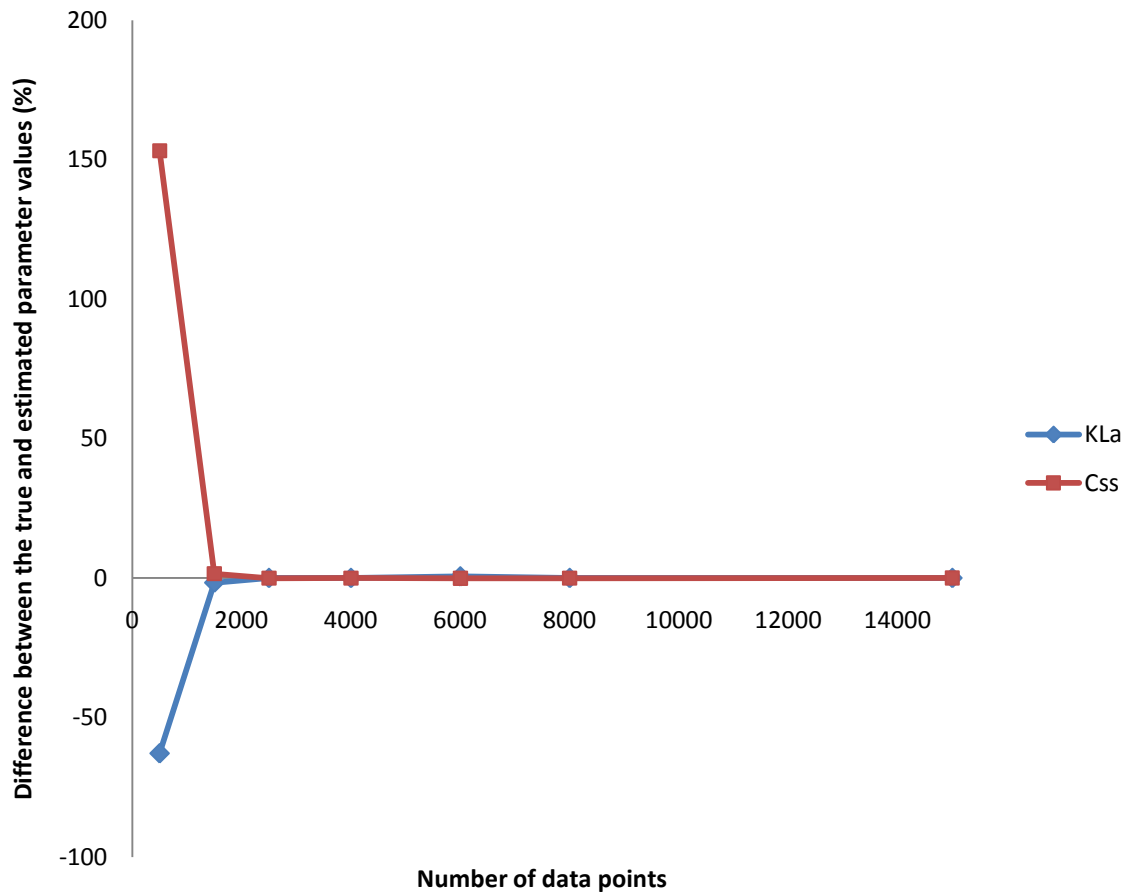


**Figure 25** The difference between the true and estimated parameter values for different truncation spans. The number of data points represents how large the truncation span was and can be seen in Table 9.  $K_{La}$  and  $C_{ss}$  were the evaluated parameters. The parameters were only evaluated at the points marked with dots.

### 6.1.2 Cylinder tank data

The data from the cylinder tank was evaluated with the standard model. Probe 5, 1, 4 and 3 were chosen (Figure 26).

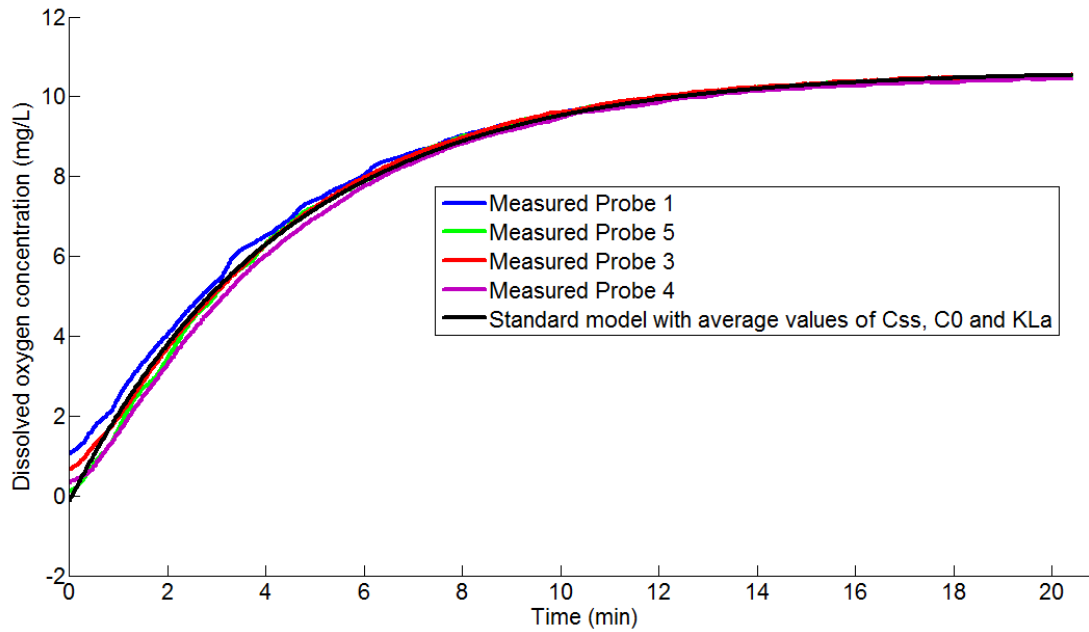


**Figure 26** The data from the cylinder tank from probe 1, 5, 3 and 4. The dashed black line represents the standard model with the average values of the estimated parameters.

Three different combinations of initial guesses were used to correctly determine the estimated parameter values and evaluate if the results changed (Table 11).

**Table 11** Used initial guesses for the estimated parameters.

|                        | $C_{ss}$<br>(mg/L) | $C_0$<br>(mg/L) | $K_L a$<br>(min <sup>-1</sup> ) |
|------------------------|--------------------|-----------------|---------------------------------|
| <i>Initial guess 1</i> | 10.5               | 0               | 0.2                             |
| <i>Initial guess 2</i> | 5                  | 2               | 2                               |
| <i>Initial guess 3</i> | 7                  | -3              | 0.002                           |

The results after nonlinear regression are presented in Table 12. The estimated parameter values and RSS did not change when the initial guesses were changed. Also the performance parameters, SOTR, SAE and SOTE were calculated with the estimated parameter values from the cylinder data (Table 13). SOTR was calculated as an average value for each data series. They did not change with changing initial guesses because they were based on the estimated parameter values.



**Table 12** Results after nonlinear regression for each probe with three different combinations of initial guesses. An average value of each parameter was calculated for each combination of initial guesses.

|                              |                | <b>RSS</b><br><i>((mg/L)<sup>2</sup>)</i> | <b>C<sub>ss</sub></b><br><i>(mg/L)</i> | <b>C<sub>0</sub></b><br><i>(mg/L)</i> | <b>K<sub>L</sub>a</b><br><i>(min<sup>-1</sup>)</i> |
|------------------------------|----------------|---|--|---------------------------------------|--|
| <i>Using initial guess 1</i> | <i>Probe 5</i> | 6.50                                      | 10.6                                   | 0.523                                 | 0.227  |
|                              | <i>Probe 1</i> | 6.85                                      | 10.7                                   | -0.487                                | 0.234  |
|                              | <i>Probe 4</i> | 10.3                                      | 10.7                                   | -0.0196                               | 0.224  |
|                              | <i>Probe 3</i> | 11.9                                      | 10.6                                   | -0.470                                | 0.221  |
|                              | <b>Average</b> | <b>8.90</b>                               | <b>10.7</b>                            | <b>-0.113</b>                         | <b>0.227</b>                                       |
| <i>Using initial guess 2</i> | <i>Probe 5</i> | 6.50                                      | 10.6                                   | 0.523                                 | 0.227  |
|                              | <i>Probe 1</i> | 6.85                                      | 10.7                                   | -0.487                                | 0.234  |
|                              | <i>Probe 4</i> | 10.3                                      | 10.7                                   | -0.0196                               | 0.224  |
|                              | <i>Probe 3</i> | 11.9                                      | 10.6                                   | -0.470                                | 0.221  |
|                              | <b>Average</b> | <b>8.90</b>                               | <b>10.7</b>                            | <b>-0.113</b>                         | <b>0.227</b>                                       |
| <i>Using initial guess 3</i> | <i>Probe 5</i> | 6.50                                      | 10.6                                   | 0.523                                 | 0.227  |
|                              | <i>Probe 1</i> | 6.85                                      | 10.7                                   | -0.487                                | 0.234  |
|                              | <i>Probe 4</i> | 10.3                                      | 10.7                                   | -0.0196                               | 0.224  |
|                              | <i>Probe 3</i> | 11.9                                      | 10.6                                   | -0.470                                | 0.221  |
|                              | <b>Average</b> | <b>8.90</b>                               | <b>10.7</b>                            | <b>-0.113</b>                         | <b>0.227</b>                                       |

**Table 13** SOTR, SAE and SOTE were calculated for the cylinder tank. Three different combinations of initial guesses were used for the estimated parameters.

|                              | <b>SOTR</b><br><i>(kg/h)</i> | <b>SAE</b><br><i>(kg/kWh)</i> | <b>SOTE</b><br><i>(%)</i> |
|------------------------------|------------------------------|-------------------------------|---------------------------|
| <i>Using initial guess 1</i> | 0.0604                       | 8.83                          | 16.0                      |
| <i>Using initial guess 2</i> | 0.0604                       | 8.83                          | 16.0                      |
| <i>Using initial guess 3</i> | 0.0604                       | 8.83                          | 16.0                      |

Truncation of the data from the cylinder tank was assumed to give approximately the same results as for the racetrack data (chapter 6.1.3) so it was not evaluated.

### 6.1.3 Racetrack data

Parameter sensitivity in the standard model was also evaluated with data from the racetrack tank. The data was collected during 34min and four data series were analyzed (Figure 27).

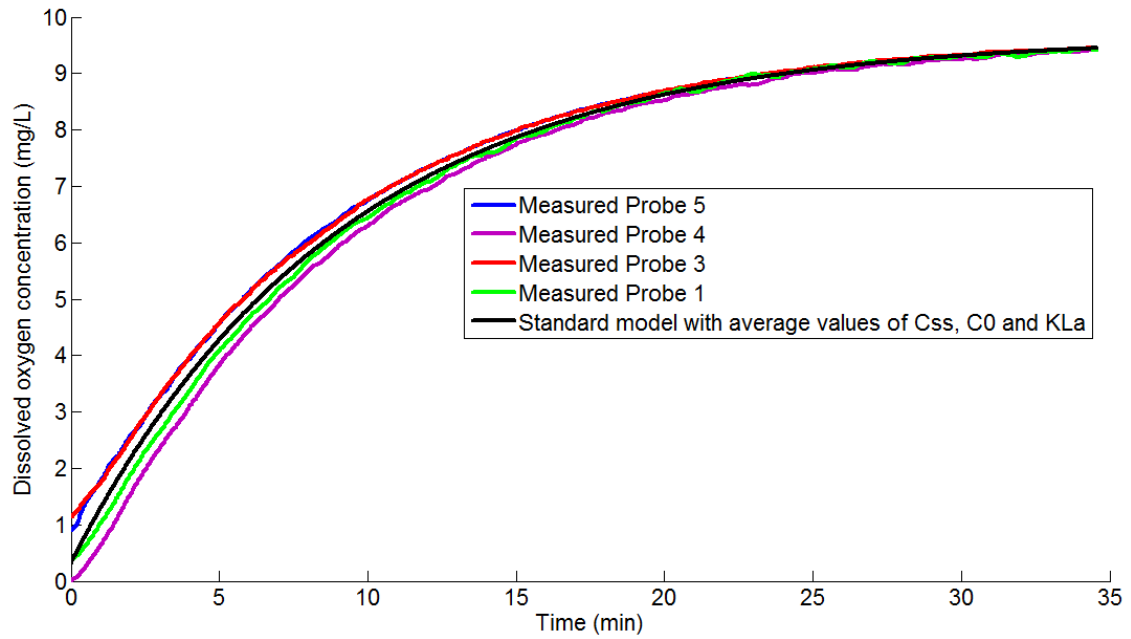


**Figure 27** The dissolved oxygen concentration over time in the racetrack tank. The dashed black line is the model with the average values of the estimated parameters,  $C_{ss}$ ,  $C_0$  and  $K_{La}$ .

Three different combinations of initial guesses (Table 14) were evaluated for the estimated parameters. The results of the estimated parameter values and RSS are presented in Table 15 for each probe and also an average value. The results were similar for all combinations of initial guesses.

**Table 14** Three combinations of initial guesses for the estimated parameters.

|                        | $C_{ss}$<br>(mg/L) | $C_0$<br>(mg/L) | $K_{La}$<br>( $min^{-1}$ ) |
|------------------------|--------------------|-----------------|----------------------------|
| <i>Initial guess 1</i> | 10.5               | 0               | 0.2                        |
| <i>Initial guess 2</i> | 5                  | 2               | 2                          |
| <i>Initial guess 3</i> | 7                  | -3              | 0.002                      |

**Table 15** The results of the estimated parameter values and RSS after nonlinear regression. Four probes were evaluated for every combination of initial guesses and an average value of all estimated parameter values was calculated.

|                              |                       | <b>RSS</b><br><i>((mg/L)<sup>2</sup>)</i> | <b>C<sub>ss</sub></b><br><i>(mg/L)</i> | <b>C<sub>0</sub></b><br><i>(mg/L)</i> | <b>K<sub>La</sub></b><br><i>(min<sup>-1</sup>)</i> |
|------------------------------|-----------------------|---|--|---------------------------------------|--|
| <i>Using initial guess 1</i> | <i>Probe 5</i>        | 0.830                                     | 9.63                                   | 0.815                                 | 0.112  |
|                              | <i>Probe 1</i>        | 3.61                                      | 9.65                                   | -0.384                                | 0.110  |
|                              | <i>Probe 4</i>        | 2.08                                      | 9.66                                   | 0.861                                 | 0.110  |
|                              | <i>Probe 3</i>        | 4.06                                      | 9.68                                   | 0.0228                                | 0.110  |
|                              | <b><i>Average</i></b> | <b><i>2.64</i></b>                        | <b><i>9.66</i></b>                     | <b><i>0.329</i></b>                   | <b><i>0.110</i></b>                                |
| <i>Using initial guess 2</i> | <i>Probe 5</i>        | 0.830                                     | 9.63                                   | 0.815                                 | 0.112  |
|                              | <i>Probe 1</i>        | 3.61                                      | 9.65                                   | -0.384                                | 0.110  |
|                              | <i>Probe 4</i>        | 2.08                                      | 9.66                                   | 0.861                                 | 0.110  |
|                              | <i>Probe 3</i>        | 4.06                                      | 9.68                                   | 0.0228                                | 0.110  |
|                              | <b><i>Average</i></b> | <b><i>2.64</i></b>                        | <b><i>9.66</i></b>                     | <b><i>0.329</i></b>                   | <b><i>0.110</i></b>                                |
| <i>Using initial guess 3</i> | <i>Probe 5</i>        | 0.830                                     | 9.63                                   | 0.815                                 | 0.112  |
|                              | <i>Probe 1</i>        | 3.61                                      | 9.65                                   | -0.384                                | 0.110  |
|                              | <i>Probe 4</i>        | 2.08                                      | 9.66                                   | 0.861                                 | 0.110  |
|                              | <i>Probe 3</i>        | 4.06                                      | 9.68                                   | 0.0228                                | 0.110  |
|                              | <b><i>Average</i></b> | <b><i>2.64</i></b>                        | <b><i>9.66</i></b>                     | <b><i>0.329</i></b>                   | <b><i>0.110</i></b>                                |

The performance parameters SOTR, SAE and SOTE calculated from the estimated parameter values are presented in Table 16. Also these results were similar and were not affected by which initial guesses that was used.

**Table 16** SOTR, SAE and SOTE calculated for the racetrack tank. Three different combinations of initial guesses were used for the estimated parameters.

|                              | <b>SOTR</b><br><i>(kg/h)</i> | <b>SAE</b><br><i>(kg/kWh)</i> | <b>SOTE</b><br><i>(%)</i> |
|------------------------------|------------------------------|-------------------------------|---------------------------|
| <i>Using initial guess 1</i> | 0.00930                      | 21.4                          | 5.46                      |
| <i>Using initial guess 2</i> | 0.00930                      | 21.4                          | 5.46                      |
| <i>Using initial guess 3</i> | 0.00930                      | 21.4                          | 5.46                      |

By evaluating how small truncation spans that could be used to get good results, only one of the four data series was analyzed. The chosen series was from probe 5 because it seemed to not contain big variations (Figure 28). The results are presented in Table 17.

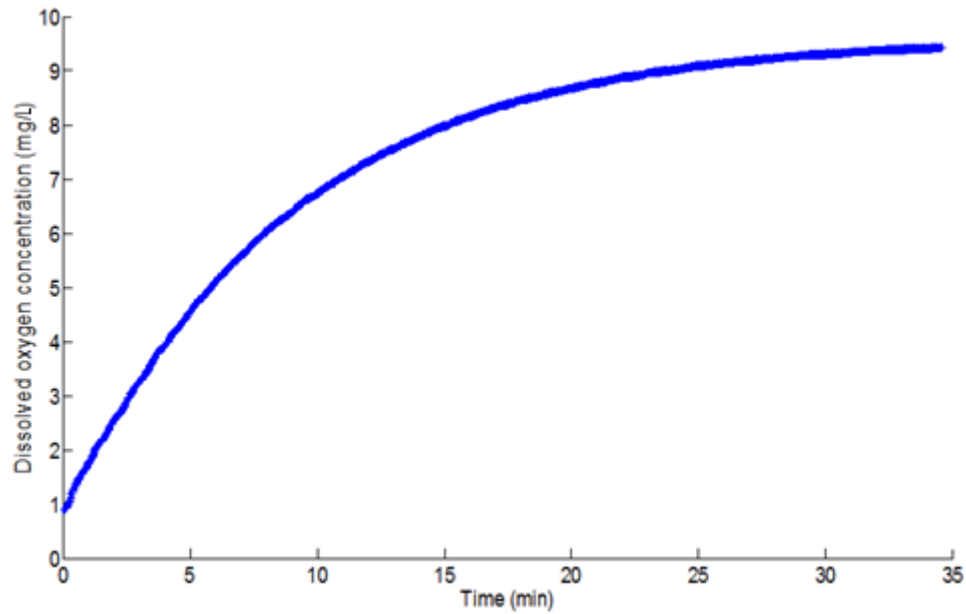


**Figure 28** Dissolved oxygen concentration measured with probe 5 in the racetrack tank.

**Table 17** Results from data truncations for probe 5. For every truncation span there were results after nonlinear regression of the estimated parameter values and RSS. The estimated parameter values for the largest truncation span with 2074 data were seen as the true values. Estimated values of  $K_{La}$  and  $C_{ss}$  for different truncation spans were compared with the true values and presented in “Diff  $K_{La}$ ” and “Diff  $C_{ss}$ ”.

| Truncation span | Number of data points (-) | RSS $((mg/L)^2)$ | $C_{ss}$ (mg/L) | $C_0$ (mg/L) | $K_{La}$ ( $min^{-1}$ ) | Diff $C_{ss}$ (%) | Diff $K_{La}$ (%) |
|-----------------|---------------------------|------------------|-----------------|--------------|-------------------------|-------------------|-------------------|
| 0-34min         | 2074                      | 0.830            | 9.63            | 0.815        | 0.112                   | 0                 | 0                 |
| 0-25min         | 1501                      | 0.772            | 9.65            | 0.823        | 0.111                   | 0.210             | -0.626            |
| 0-20min         | 1201                      | 0.696            | 9.68            | 0.833        | 0.110                   | 0.591             | -1.52             |
| 0-15min         | 901                       | 0.595            | 9.77            | 0.847        | 0.108                   | 1.49              | -3.31             |
| 0-10min         | 601                       | 0.357            | 10.2            | 0.879        | 0.100                   | 6.19              | -10.5             |

The change of the estimated parameter values was not significant for larger truncation spans but when the spans decreased, the difference between the parameter values increased. The difference between the estimated  $C_{ss}$  and  $K_{La}$  are presented in Figure 29.

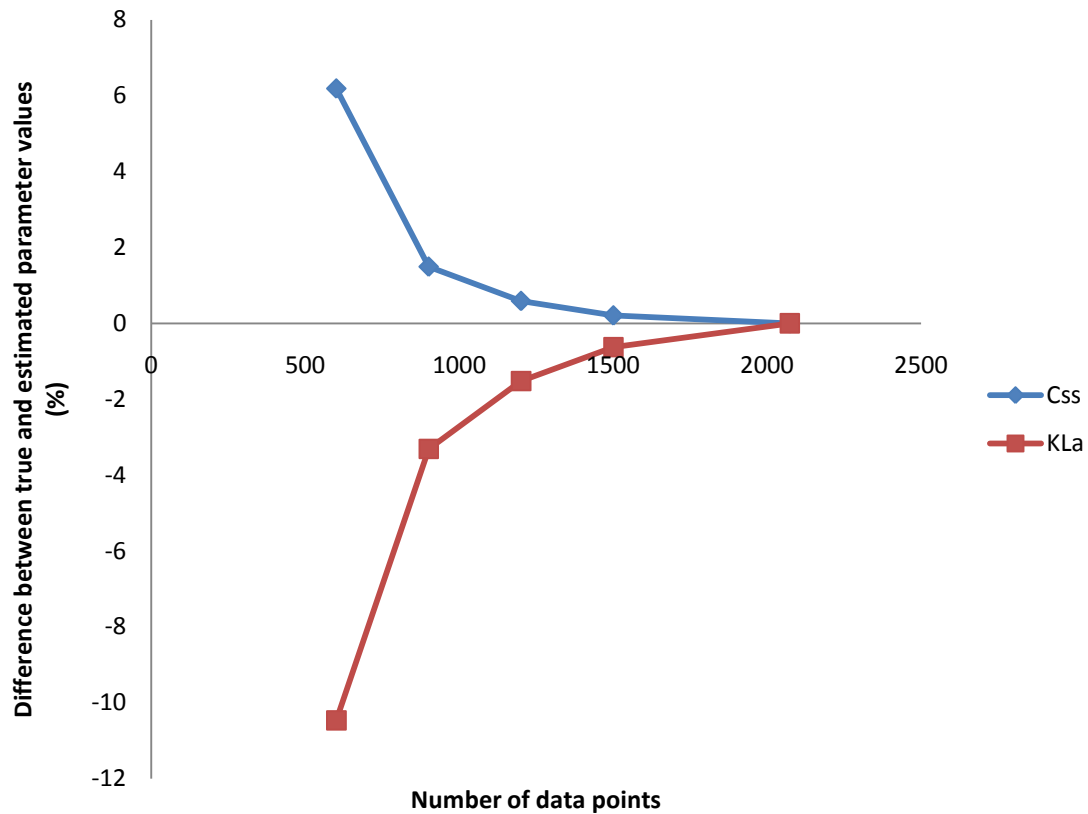


**Figure 29** Difference between true and estimated parameter values of  $C_{ss}$  and  $K_L a$  are presented as a function of the number of data points. The more points, the larger truncation spans. The parameters were only evaluated at the points marked with dots.

## 6.2 MODEL NR 1

This model was validated using both simulated data and measured data. Measured data were from both the cylinder tank and the racetrack tank.

### 6.2.1 Simulated data

Model nr 1 was evaluated with simulated data with and without added noise. The data consisted of 1225 data point over a time span of 20min. New noise realizations were produced for each simulated data series to avoid correlation between them. A plot of the simulated data with added noise and the modeled data is presented in Figure 30. Because the model consists of two different water volumes there will be two different concentration curves, one that represents the aerated water volume and one that represents the non-aerated water volume. The residual sum of squares was calculated separately for both lines that represents different volumes and then added.

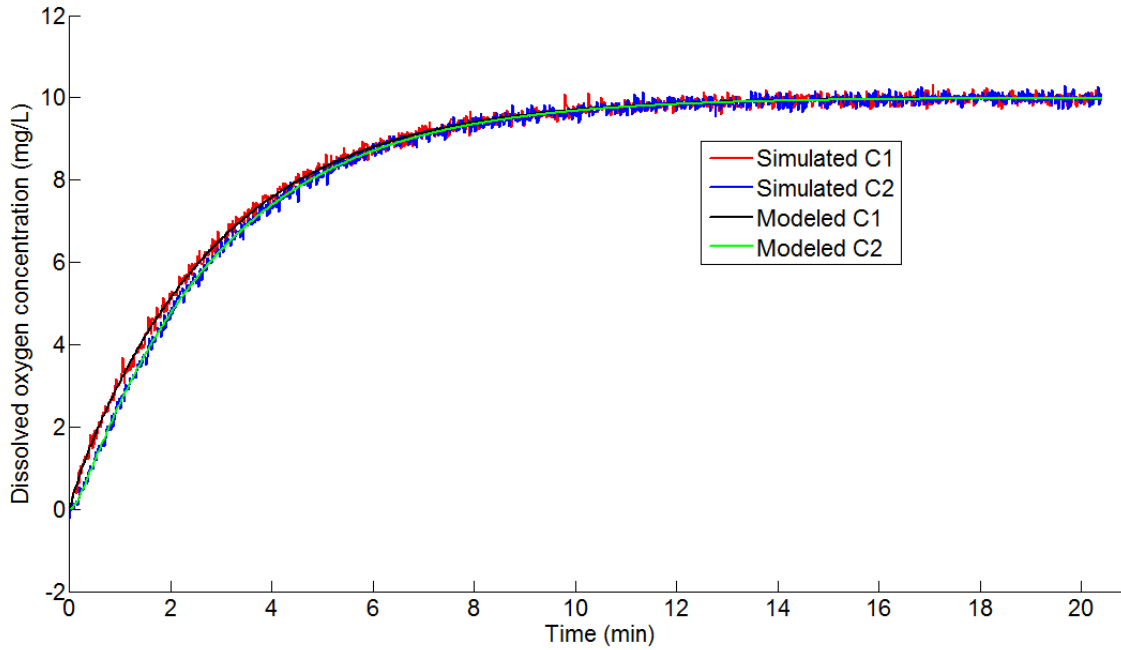


**Figure 30** Simulated data with added noise for model nr 1. The red and blue lines show the simulated data for  $C_1$  and  $C_2$ , respectively. The black line is the model for  $C_1$  and the green line is the model for  $C_2$ .

Both correct and incorrect initial guesses for the estimated parameters were used when nonlinear regression was performed (Table 18). The results from the evaluations are presented in Table 19 for simulated data without noise and in Table 20 for simulated data with added noise.

**Table 18** Used correct and incorrect initial guesses for the estimated parameters using nonlinear regression.

|                                  | $C_{ss}$<br>(mg/L) | $K_L a$<br>( $min^{-1}$ ) | $V_1/q$<br>(min) | $V_2/q$<br>(min) | $C_{1(0)}$<br>(mg/L) | $C_{2(0)}$<br>(mg/L) |
|----------------------------------|--------------------|---------------------------|------------------|------------------|----------------------|----------------------|
| <i>Correct initial guesses</i>   | 10                 | 0.5                       | 0.5              | 0.2              | 0                    | 0                    |
| <i>Incorrect initial guesses</i> | 100                | 5                         | 5                | 2                | 3                    | 3                    |

**Table 19** RSS and estimated parameter values for simulated data without noise. The estimations were done when both correct and incorrect initial guesses were used.

|  | RSS<br>( $(mg/L)^2$ ) | $C_{ss}$<br>(mg/L) | $K_L a$<br>( $min^{-1}$ ) | $V_1/q$<br>(min) | $V_2/q$<br>(min) | $C_{1(0)}$<br>(mg/L)   | $C_{2(0)}$<br>(mg/L)   |
|--|-----------------------|--------------------|---------------------------|------------------|------------------|------------------------|------------------------|
| <i>Using correct initial guesses</i>   | 0.00                  | 10.0               | 0.500                     | 0.500            | 0.200            | 0.00                   | 0.00                   |
| <i>Using incorrect initial guesses</i> | $8.40 \cdot 10^{-27}$ | 10.0               | 0.500                     | 0.500            | 0.200            | $-2.46 \cdot 10^{-16}$ | $-9.38 \cdot 10^{-16}$ |

**Table 20** RSS and estimated parameter values for simulated data with added noise. The estimations were done when both correct and incorrect initial guesses were used.

|  | RSS<br>$((\text{mg/L})^2)$ | $C_{ss}$<br>$(\text{mg/L})$ | $K_L a$<br>$(\text{min}^{-1})$ | $V_1/q$<br>$(\text{min})$ | $V_2/q$<br>$(\text{min})$ | $C_{1(0)}$<br>$(\text{mg/L})$ | $C_{2(0)}$<br>$(\text{mg/L})$ |
|--|----------------------------|-----------------------------|--------------------------------|---------------------------|---------------------------|-------------------------------|-------------------------------|
| <i>Using correct initial guesses</i>   | 59.3                       | 10.0                        | 0.503                          | 0.499                     | 0.204                     | 0.00414                       | 0.0175                        |
| <i>Using incorrect initial guesses</i> | 59.3                       | 10.0                        | 0.503                          | 0.499                     | 0.204                     | 0.00415                       | 0.0175                        |

### 6.2.2 Cylinder tank data

Measured data in the cylinder tank were evaluated using model nr 1. Figure 31 shows how the model fits the measured data. The dissolved oxygen concentration in the aerated water volume was rising faster than the dissolved oxygen concentration in the non-aerated water volume. At steady state they rose to approximately the same concentration even if the probes were placed at different water depths. In theory they should rise to different saturation concentrations and the deeper probes should measure a higher dissolved oxygen concentration because of the increasing pressure.

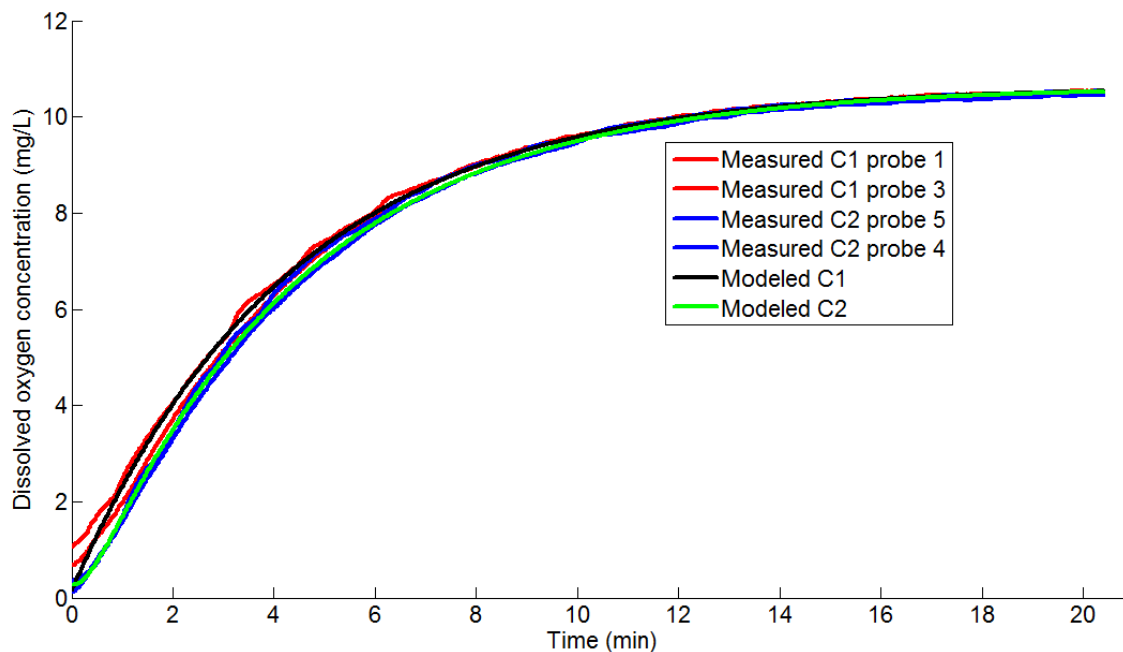


**Figure 31** Measured and modeled data for the cylinder tank with model nr 1. Red and blue lines and dashed lines show the measured data for  $C_1$  and  $C_2$ . The black and green lines show the model which represents of both  $C_1$  and  $C_2$ .

To evaluate whether the model was sensitive for initial guesses for the estimated parameters or not there were three different combinations used (Table 21).

**Table 21** Three different combinations of initial guesses for nonlinear regression.

|                        | $C_{ss}$<br>(mg/L) | $K_L a$<br>( $min^{-1}$ ) | $V_1/q$<br>(min) | $V_2/q$<br>(min) | $C_{1(0)}$<br>(mg/L) | $C_{2(0)}$<br>(mg/L) |
|------------------------|--------------------|---------------------------|------------------|------------------|----------------------|----------------------|
| <i>Initial guess 1</i> | 10.5               | 0.2                       | 0.5              | 2                | 0.5                  | 0                    |
| <i>Initial guess 2</i> | 5                  | 2                         | 0.05             | 3                | 2                    | 1                    |
| <i>Initial guess 3</i> | 7                  | 0.002                     | 5                | 0.003            | 0.2                  | -3                   |

The results from nonlinear regression of the aerated volume,  $V_1$ , the non-aerated volume,  $V_2$  and the liquid flow rate,  $q$ , were estimated as a ratio of them (Table 22) but they were also calculated individually (Table 23). There was a significant difference in the estimated values of  $V_1/q$  and also a small change in the estimated  $V_2/q$ . The performance results showed no difference depending on which initial guesses that were used (Table 24).

**Table 22** Results after nonlinear regression for model nr 1 when measured data from the cylinder tank were used. Three different combinations of initial guesses are used.

|                              | RSS<br>( $(mg/L)^2$ ) | $C_{ss}$<br>(mg/L) | $K_L a$<br>( $min^{-1}$ ) | $V_1/q$<br>(min) | $V_2/q$<br>(min) | $C_{1(0)}$<br>(mg/L) | $C_{2(0)}$<br>(mg/L) |
|------------------------------|-----------------------|--------------------|---------------------------|------------------|------------------|----------------------|----------------------|
| <i>Using initial guess 1</i> | 57.4                  | 10.6               | 0.231                     | 63300            | 0.325            | 0.165                | 0.287                |
| <i>Using initial guess 2</i> | 57.4                  | 10.6               | 0.231                     | 14900            | 0.327            | 0.165                | 0.285                |
| <i>Using initial guess 3</i> | 57.4                  | 10.6               | 0.231                     | 14200            | 0.326            | 0.163                | 0.288                |

**Table 23** Calculated  $V_1$ ,  $V_2$  and  $q$ .

|                              | $V_1$<br>( $m^3$ ) | $V_2$<br>( $m^3$ )   | $q$<br>( $m^3/min$ ) |
|------------------------------|--------------------|----------------------|----------------------|
| <i>Using initial guess 1</i> | 0.397              | $2.04 \cdot 10^{-6}$ | $6.28 \cdot 10^{-6}$ |
| <i>Using initial guess 2</i> | 0.397              | $8.74 \cdot 10^{-6}$ | $2.67 \cdot 10^{-5}$ |
| <i>Using initial guess 3</i> | 0.397              | $9.12 \cdot 10^{-6}$ | $2.80 \cdot 10^{-5}$ |

**Table 24** SOTR, SAE and SOTE calculated for the cylinder tank with three combinations of initial guesses for the estimated parameters.

|                              | SOTR<br>(kg/h) | SAE<br>(kg/kWh) | SOTE<br>(%) |
|------------------------------|----------------|-----------------|-------------|
| <i>Using initial guess 1</i> | 0.0614         | 8.98            | 16.3        |
| <i>Using initial guess 2</i> | 0.0614         | 8.98            | 16.3        |
| <i>Using initial guess 3</i> | 0.0614         | 8.98            | 16.3        |

### 6.2.3 Racetrack data

Performance evaluations were also performed for the racetrack tank. Two probes in each water volume were evaluated and the measured and modeled concentrations can be seen in Figure 32. The dissolved oxygen concentrations in the aerated water volume



were above the others in the beginning of the reoxygenation. They rose to approximately the same saturation concentration.

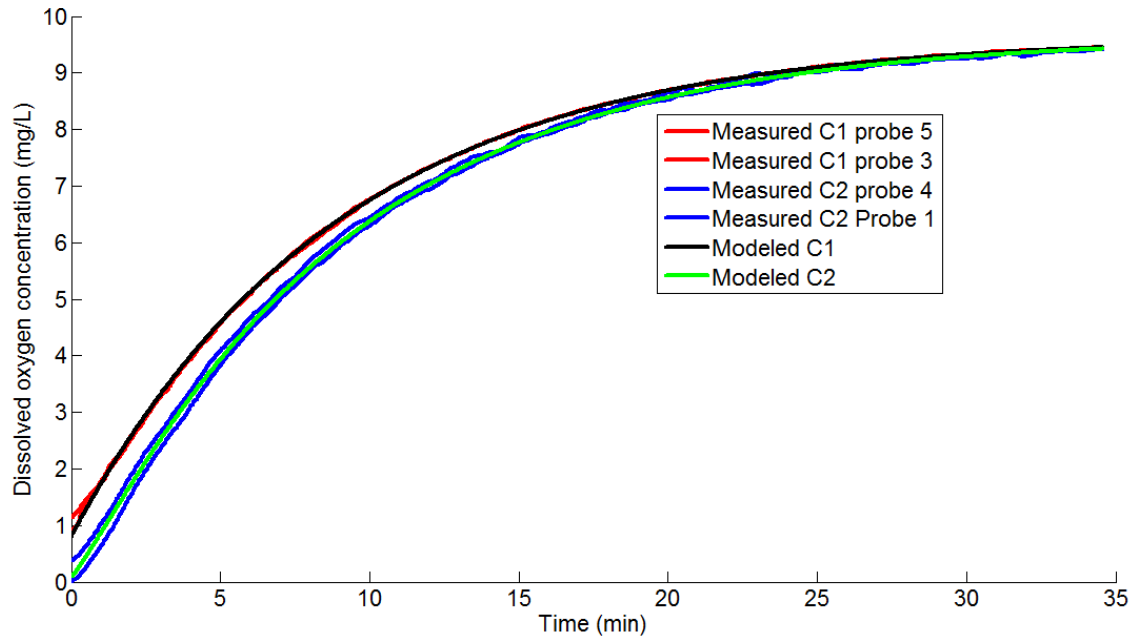


**Figure 32** Measured and modeled dissolved oxygen concentrations in the racetrack tank. The red and blue lines and dashed lines show the measured concentrations for four probes. Red represents  $C_1$  and blue represents  $C_2$ . The black and green lines show the model with  $C_1$  and  $C_2$ .

By using the same combinations of initial guesses as in Table 17, the results after nonlinear regression are given in Table 25. Some of the estimated parameters were separated and individually presented in Table 26. There was a significant change in the estimated values of  $V_1/q$  and  $V_2/q$ . Even if those parameter values were different, the performance calculations gave approximately the same results for all three different combinations of initial guesses (Table 27).

**Table 25** Results after nonlinear regression for model nr 1 when measured data from the racetrack tank were used. Three different combinations of initial guesses were used.

|                       | RSS<br>$((mg/L)^2)$ | $C_{ss}$<br>$(mg/L)$ | $K_{La}$<br>$(min^{-1})$ | $V_1/q$<br>$(min)$ | $V_2/q$<br>$(min)$ | $C_{1(0)}$<br>$(mg/L)$ | $C_{2(0)}$<br>$(mg/L)$ |
|-----------------------|---------------------|----------------------|--------------------------|--------------------|--------------------|------------------------|------------------------|
| Using initial guess 1 | 32.1                | 9.63                 | 0.112                    | 13200              | 1.03               | 0.809                  | 0.0745                 |
| Using initial guess 2 | 32.1                | 9.63                 | 0.112                    | 13700              | 1.03               | 0.809                  | 0.0744                 |
| Using initial guess 3 | 32.1                | 9.63                 | 0.112                    | 14400              | 1.03               | 0.809                  | 0.0744                 |

**Table 26** Calculated  $V_1$ ,  $V_2$  and  $q$ .

|                              | $V_1$<br>( $m^3$ ) | $V_2$<br>( $m^3$ )   | $q$<br>( $m^3/min$ ) |
|------------------------------|--------------------|----------------------|----------------------|
| <i>Using initial guess 1</i> | 0.146              | $1.13 \cdot 10^{-5}$ | $1.10 \cdot 10^{-5}$ |
| <i>Using initial guess 2</i> | 0.146              | $1.09 \cdot 10^{-5}$ | $1.06 \cdot 10^{-5}$ |
| <i>Using initial guess 3</i> | 0.146              | $1.04 \cdot 10^{-5}$ | $1.01 \cdot 10^{-5}$ |

**Table 27** SOTR, SAE and SOTE calculated for the racetrack tank with three combinations of initial guesses for the estimated parameter values.

|                              | SOTR<br>( $kg/h$ ) | SAE<br>( $kg/kWh$ ) | SOTE<br>(%) |
|------------------------------|--------------------|---------------------|-------------|
| <i>Using initial guess 1</i> | 0.00942            | 20.1                | 5.54        |
| <i>Using initial guess 2</i> | 0.00942            | 20.1                | 5.54        |
| <i>Using initial guess 3</i> | 0.00942            | 20.1                | 5.54        |

### 6.3 MODEL NR 2

Model nr 2 was only evaluated using simulated data because it was considered to be sensitive for initial guesses.

#### 6.3.1 Simulated data

Simulated data was created for model nr 2 with and without noise. The noise was created to resemble a real measurement noise. Used parameter values in the simulated data are presented in Table 28. There are also the incorrect initial guesses presented which was used for testing the parameter sensitivity.

**Table 28** Used initial guesses for parameters that were estimated using nonlinear regression. All parameter values were changed when the incorrect initial guesses were used.

|                                  | $C_{ss}$<br>( $mg/L$ ) | $K_{La_b}$<br>( $min^{-1}$ ) | $K_{La_s}$<br>( $min^{-1}$ ) | $C_0$<br>( $mg/L$ ) |
|----------------------------------|------------------------|------------------------------|------------------------------|---------------------|
| <i>Correct initial guesses</i>   | 10                     | 0.05                         | 0.01                         | 0                   |
| <i>Incorrect initial guesses</i> | 15                     | 0.5                          | 1                            | 0.5                 |

The evaluation results when noise was and was not added to the simulated data are presented in Table 29 and 30. The results were presented when both correct and incorrect initial guesses for the estimated parameters were used. The RSS was increasing when incorrect initial guesses for model evaluation were used. Also the estimated parameter values varied from the correct values when incorrect initial guesses were used.

**Table 29** RSS and estimated parameter values for evaluation of simulated data without noise. The estimations were conducted when both correct and incorrect initial guesses were used.

|  | RSS<br>((mg/L) <sup>2</sup> ) | C <sub>ss</sub><br>(mg/L) | K <sub>L</sub> a <sub>b</sub><br>(min <sup>-1</sup> ) | K <sub>L</sub> a <sub>s</sub><br>(min <sup>-1</sup> ) | C <sub>0</sub><br>(mg/L) |
|--|-------------------------------|---------------------------|---|---|--------------------------|
| <i>Using correct initial guesses</i>   | 0.00                          | 10.0                      | 0.0500  | 0.0100  | 0.00                     |
| <i>Using incorrect initial guesses</i> | 468                           | 7.11                      | 14.4  | 18.0  | -1.30·10 <sup>-14</sup>  |

**Table 30** RSS and estimated parameter values for evaluation of simulated data with added noise. The estimations were conducted when both correct and incorrect initial guesses were used.

|  | RSS<br>((mg/L) <sup>2</sup> ) | C <sub>ss</sub><br>(mg/L) | K <sub>L</sub> a <sub>b</sub><br>(min <sup>-1</sup> ) | K <sub>L</sub> a <sub>s</sub><br>(min <sup>-1</sup> ) | C <sub>0</sub><br>(mg/L) |
|--|-------------------------------|---------------------------|---|---|--------------------------|
| <i>Using correct initial guesses</i>   | 0.892                         | 10.0                      | 0.0499  | 0.0101  | 0.0116                   |
| <i>Using incorrect initial guesses</i> | 461                           | 7.08                      | 14.2  | 17.9  | 0.115                    |

A compliment to comparing the estimated parameter values for different initial guesses was to plot the simulated data and the modeled data in the same figure. The simulated data without noise and model nr 2 are plotted in Figure 33. That result was from evaluating the model with the correct initial guesses. Figure 34 shows the same data but with incorrect initial guesses for the estimated parameters. Approximately the same data fit was obtained when data with an added noise as without noise were used.

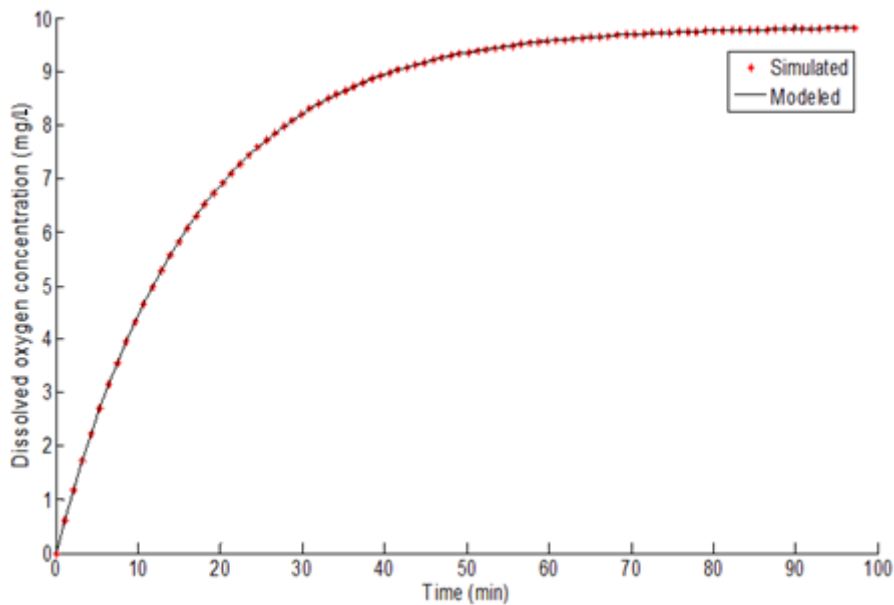


**Figure 33** Simulated data evaluated with model nr 2. The red dots show the simulated data and the black line shows the model with correct initial guesses for the estimated parameter values.

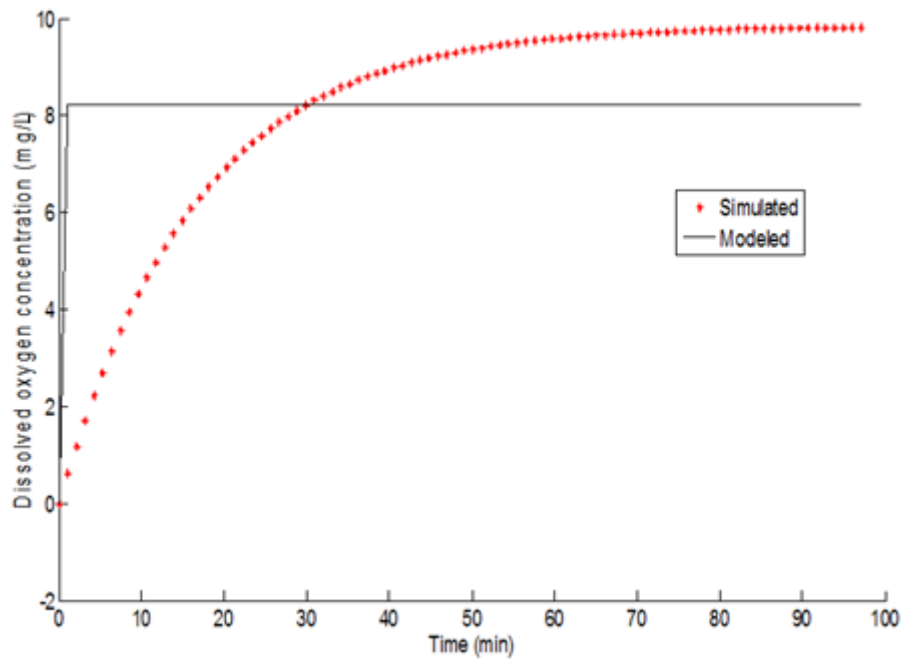


**Figure 34** Simulated data evaluated with model nr 2. The red dots show the simulated data and the black line shows the model with incorrect initial guesses for the estimated parameter values.

### 6.4 MODEL NR 3

Model nr 3 was evaluated using both simulated data and measured data from the cylinder tank and the racetrack tank.

A theory of this model is that it should be possible to truncate to a smaller span of the total reoxygenation process because the dissolved oxygen saturation concentrations are calculated and not estimated. This theory was evaluated for both simulated data and measured data in the racetrack tank. Similar tests were done with the standard model to be able to compare the results.

#### 6.4.1 Simulated data

Tests were done to evaluate whether model nr 3 was sensitive for initial guesses of the estimated parameters or not. The correct initial guesses were set to a combination which can be seen in Table 31. Another combination with incorrect initial guesses was used to compare the results from both combinations.

**Table 31** Initial guesses for the estimated parameters when simulated data were used. Correct initial guesses were known and incorrect initial guesses were set to some other values.

|                                  | $K_L a_b$<br>( $min^{-1}$ ) | $C_0$<br>( $mg/L$ ) | $K_L a_s$<br>( $min^{-1}$ ) |
|----------------------------------|-----------------------------|---------------------|-----------------------------|
| <i>Correct initial guesses</i>   | 0.1                         | 0                   | 0.2                         |
| <i>Incorrect initial guesses</i> | 10                          | 1                   | 0.5                         |

The results with simulated data without noise showed that the estimated parameter values were similar when both correct and incorrect initial guesses were used (Table

32). No big differences were discovered when simulated data with added noise were evaluated (Table 33).

**Table 32** RSS and estimated parameter values for model nr 3 when it was evaluated with simulated data without noise. The estimations were conducted when both correct and incorrect initial guesses for the estimated parameters were used.

|  | RSS<br>((mg/L) <sup>2</sup> ) | K <sub>L</sub> a <sub>b</sub><br>(min <sup>-1</sup> ) | C <sub>0</sub><br>(mg/L) | K <sub>L</sub> a <sub>s</sub><br>(min <sup>-1</sup> ) |
|--|-------------------------------|---|--------------------------|---|
| <i>Using correct initial guesses</i>   | 5.75·10 <sup>-25</sup>        | 0.100   | 0.00                     | 0.200   |
| <i>Using incorrect initial guesses</i> | 4.40·10 <sup>-9</sup>         | 0.100   | 0.00                     | 0.200   |

**Table 33** RSS and estimated parameter values for model nr 3 when it was evaluated with simulated data with noise. The estimations are conducted when both correct and incorrect initial guesses for the estimated parameters were used.

|  | RSS<br>((mg/L) <sup>2</sup> ) | K <sub>L</sub> a <sub>b</sub><br>(min <sup>-1</sup> ) | C <sub>0</sub><br>(mg/L) | K <sub>L</sub> a <sub>s</sub><br>(min <sup>-1</sup> ) |
|--|-------------------------------|---|--------------------------|---|
| <i>Using correct initial guesses</i>   | 5.31                          | 0.101   | -0.00687                 | 0.200   |
| <i>Using incorrect initial guesses</i> | 5.31                          | 0.101   | -0.00687                 | 0.200   |

The evaluation of the possibilities to truncate a smaller span of the reoxygenation was made with simulated data with added noise (Figure 35). The values of the model parameters are presented in Table 34.

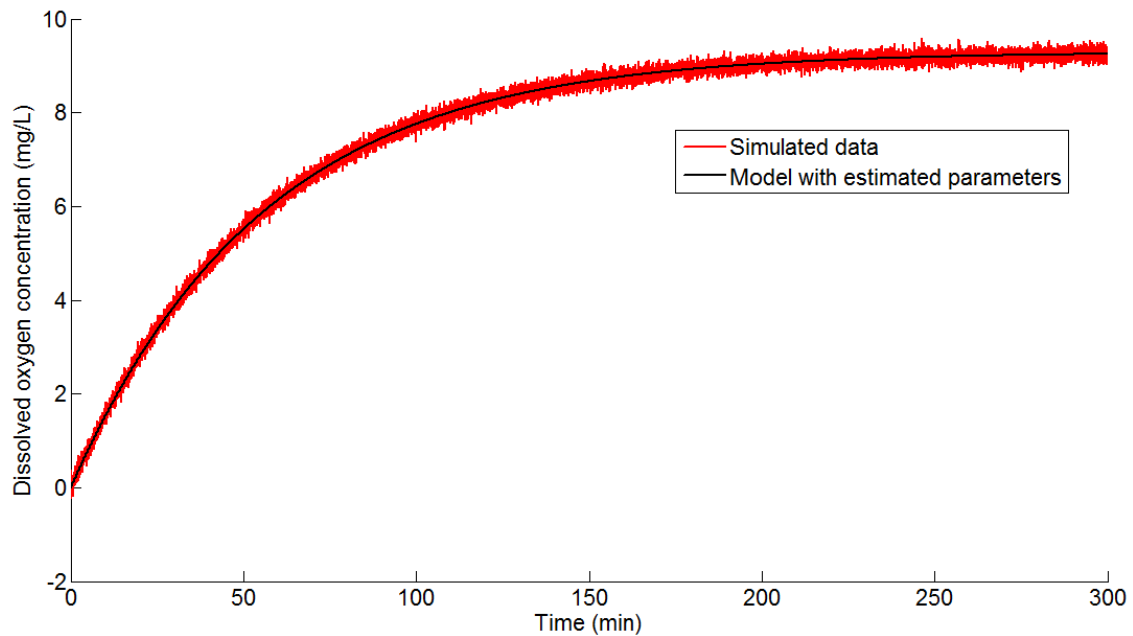


**Figure 35** Simulated data with added noise and model nr 3. The red line shows the simulated data and the black line shows the model.

**Table 34** Used parameter values for the simulated data.

| $K_{La_b}$<br>( $min^{-1}$ ) | $C_0$<br>( $mg/L$ ) | $K_{La_s}$<br>( $min^{-1}$ ) |
|------------------------------|---------------------|------------------------------|
| 0.009                        | 0                   | 0.009                        |

The standard method recommends a truncation span between 20 and 98% of the dissolved oxygen saturation concentration. In this case was the truncation for the whole data series made between 0 and 100%. Five different truncations spans were tested and all started from zero minutes (Table 35). All these tests were conducted by using incorrect initial guesses to make the case more real.

As can be seen in Table 35, the RSS decreased with smaller data series. The used parameter values (Table 34) for the simulated data were in this case seen as the true values. The estimated parameter values for other truncation spans were different from the true values. The difference of estimated  $K_{La_b}$  and  $K_{La_s}$  were approximately zero for the first truncation spans but increased when the truncation span decreased. It was also obvious that when the estimated  $K_{La_b}$  decreased, the estimated  $K_{La_s}$  increased and vice versa (Figure 36).

**Table 35** Results of RSS and the estimated parameter values after different truncations. The whole data series contained 15000 data. The difference between the true  $K_{La_b}$  and estimated  $K_{La_b}$  after different truncation spans can be seen in the column "Diff  $K_{La_b}$ " and is presented in percent. The same results are calculated for  $K_{La_s}$ .

| Truncation span | Numer of data points (-) | RSS (( $mg/L$ ) <sup>2</sup> ) | $K_{La_b}$ ( $min^{-1}$ ) | $C_0$ ( $mg/L$ ) | $K_{La_s}$ ( $min^{-1}$ ) | Diff $K_{La_b}$ (%) | Diff $K_{La_s}$ (%) |
|-----------------|--------------------------|--------------------------------|---------------------------|------------------|---------------------------|---------------------|---------------------|
| 0-300min        | 15000                    | 65.1                           | 0.00899                   | 0.0000500        | 0.00901                   | -0.0670             | -0.067              |
| 0-160min        | 8001                     | 35.1                           | 0.00896                   | -0.00226         | 0.00906                   | -0.406              | 0.700               |
| 0-120min        | 6001                     | 26.5                           | 0.00888                   | -0.00428         | 0.00918                   | -1.34               | 2.00                |
| 0-80min         | 4001                     | 17.8                           | 0.00897                   | -0.00266         | 0.00905                   | -0.309              | 0.610               |
| 0-50min         | 2501                     | 11.0                           | 0.00896                   | -0.00225         | 0.00907                   | -0.446              | 0.730               |
| 0-30min         | 1501                     | 6.70                           | 0.0107                    | 0.000960         | 0.00701                   | 18.4                | -22.2               |

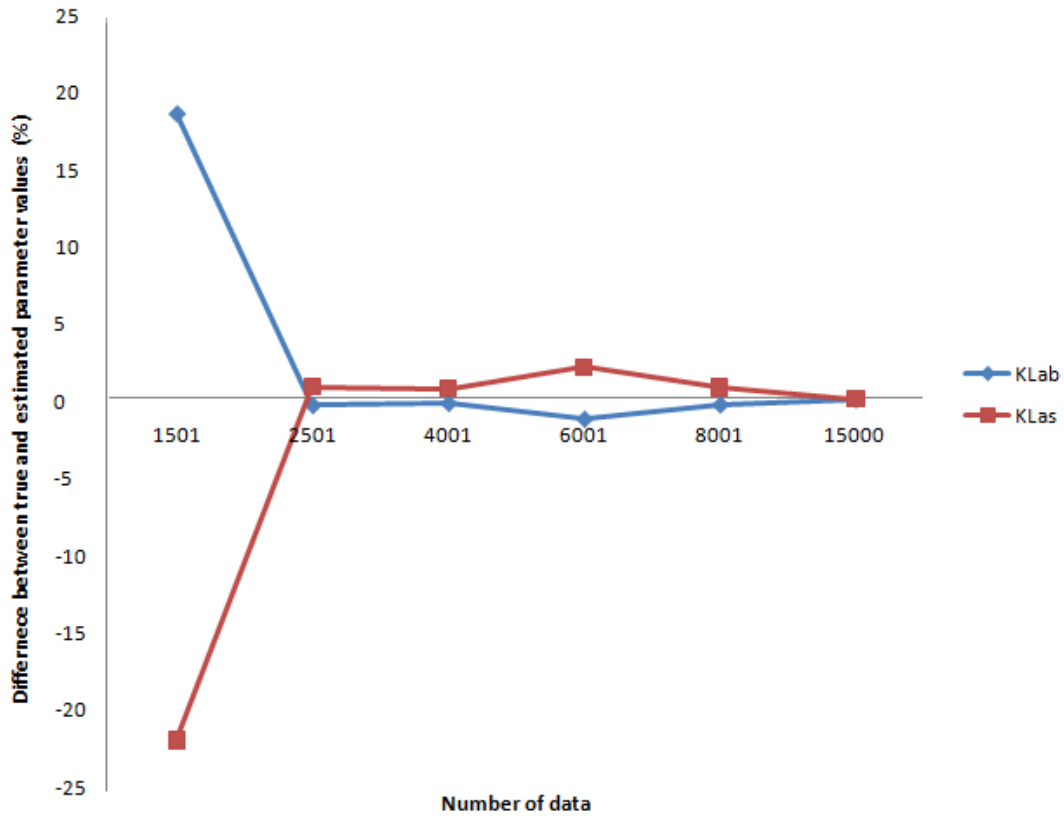


**Figure 36** The figure shows how different truncation spans of the data for model nr 3 can affect the estimated parameter values. The parameters were only evaluated at the points marked with dots.

#### 6.4.2 Racetrack data

The data from the racetrack tank was evaluated with model nr 3. How the data from probe 5 and modeled data behaved can be seen in Figure 37. The model had approximately the same fit to the rest of the data measured from the other probes.

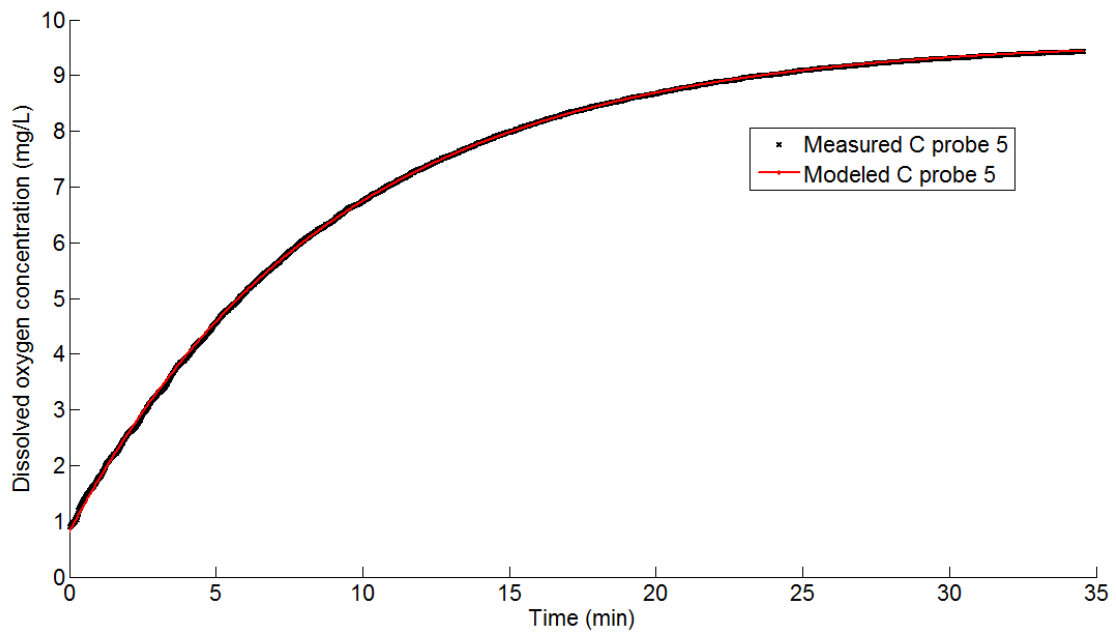


**Figure 37** Measured and modeled dissolved oxygen concentrations for probe 5 in the racetrack tank.

Two combinations of initial guesses for estimated parameters were used for nonlinear regression to ensure that the model was not sensitive for initial guesses (Table 36). Even if simulated data behave desirable is it not obvious that the model behaves in the same way for measured data. The results after nonlinear regression (Table 37) showed no significant changes in the estimated parameter values. No results of the performance parameter values were presented because the value of the used gas flow rate,  $G$ , was probably incorrect which could possibly affect the results.

**Table 36** Two different combinations of initial guesses for the estimated parameters.

|                        | $K_{La_b}$<br>( $min^{-1}$ ) | $C_0$<br>( $mg/L$ ) | $K_{La_s}$<br>( $min^{-1}$ ) |
|------------------------|------------------------------|---------------------|------------------------------|
| <i>Initial guess 1</i> | 0.6                          | 0                   | 0.5                          |
| <i>Initial guess 2</i> | 1                            | 3                   | 0.01                         |

**Table 37** Estimated parameter values and RSS after nonlinear regression. Nonlinear regression was performed for each probe. An average value for each parameter was calculated for both cases with initial guesses.

|                              |                       | RSS<br>( $(mg/L)^2$ ) | $K_{La_b}$<br>( $min^{-1}$ ) | $C_0$<br>( $mg/L$ ) | $K_{La_s}$<br>( $min^{-1}$ ) |
|------------------------------|-----------------------|-----------------------|------------------------------|---------------------|------------------------------|
| <i>Using initial guess 1</i> | <i>Probe 5</i>        | 0.830                 | 0.0516                       | 0.815               | 0.0601                       |
|                              | <i>Probe 4</i>        | 3.61                  | 0.0600                       | -0.383              | 0.0495                       |
|                              | <i>Probe 3</i>        | 2.08                  | 0.0651                       | 0.861               | 0.0447                       |
|                              | <i>Probe 1</i>        | 4.06                  | 0.0699                       | 0.0228              | 0.0396                       |
|                              | <b><i>Average</i></b> | <b>2.64</b>           | <b>0.0617</b>                | <b>0.329</b>        | <b>0.0485</b>                |
| <i>Using initial guess 2</i> | <i>Probe 5</i>        | 0.830                 | 0.0516                       | 0.815               | 0.0601                       |
|                              | <i>Probe 4</i>        | 3.61                  | 0.0600                       | -0.383              | 0.0495                       |
|                              | <i>Probe 3</i>        | 2.08                  | 0.0651                       | 0.861               | 0.0447                       |
|                              | <i>Probe 1</i>        | 4.06                  | 0.0699                       | 0.0228              | 0.0396                       |
|                              | <b><i>Average</i></b> | <b>2.64</b>           | <b>0.0617</b>                | <b>0.329</b>        | <b>0.0485</b>                |

Different truncation spans were also investigated for racetrack data. The results from a test with different truncations are presented in Table 38. Only one data series was evaluated and that was the one from probe 5 and the rest of the data series were assumed to behave similarly for different truncations. The whole data series was 34min long and the estimated parameter values from that truncation were treated as the true parameter values. The difference between the true values of  $K_{La_b}$  and  $K_{La_s}$  increased more drastically than in the case with simulated data. After truncating approximately half of the original data series, the parameter difference was almost 100%, even if the sum of  $K_{La_b}$  and  $K_{La_s}$  stayed almost the same (Figure 38). It seemed to be that a larger truncation span made the parameter values more similar to the true parameter values.



**Table 38** Estimated parameter values and RSS after different truncation spans. The whole data series is represented by the truncation between 0-34min and those estimated parameter values were seen as the true parameter values. The difference between the true  $K_{La_b}$  and the estimated  $K_{La_b}$  after other truncations are shows as “Diff  $K_{La_b}$ ”. Same thing was done for  $K_{La_s}$ .

| Truncation span | Number of data points (-) | RSS $((mg/L)^2)$ | $K_{La_b}$ $(min^{-1})$ | $C_0$ $(mg/L)$ | $K_{La_s}$ $(min^{-1})$ | Diff $K_{La_b}$ (%) | Diff $K_{La_s}$ (%) |
|-----------------|---------------------------|------------------|-------------------------|----------------|-------------------------|---------------------|---------------------|
| 0-34min         | 2074                      | 0.830            | 0.0520                  | 0.815          | 0.0600                  | 0.00                | 0.00                |
| 0-25min         | 1501                      | 0.772            | 0.0590                  | 0.823          | 0.0520                  | 15.1                | -14.1               |
| 0-20min         | 1201                      | 0.696            | 0.0730                  | 0.833          | 0.0370                  | 42.3                | -39.1               |
| 0-15min         | 901                       | 0.595            | 0.106                   | 0.847          | 0.00200                 | 106                 | -96.8               |

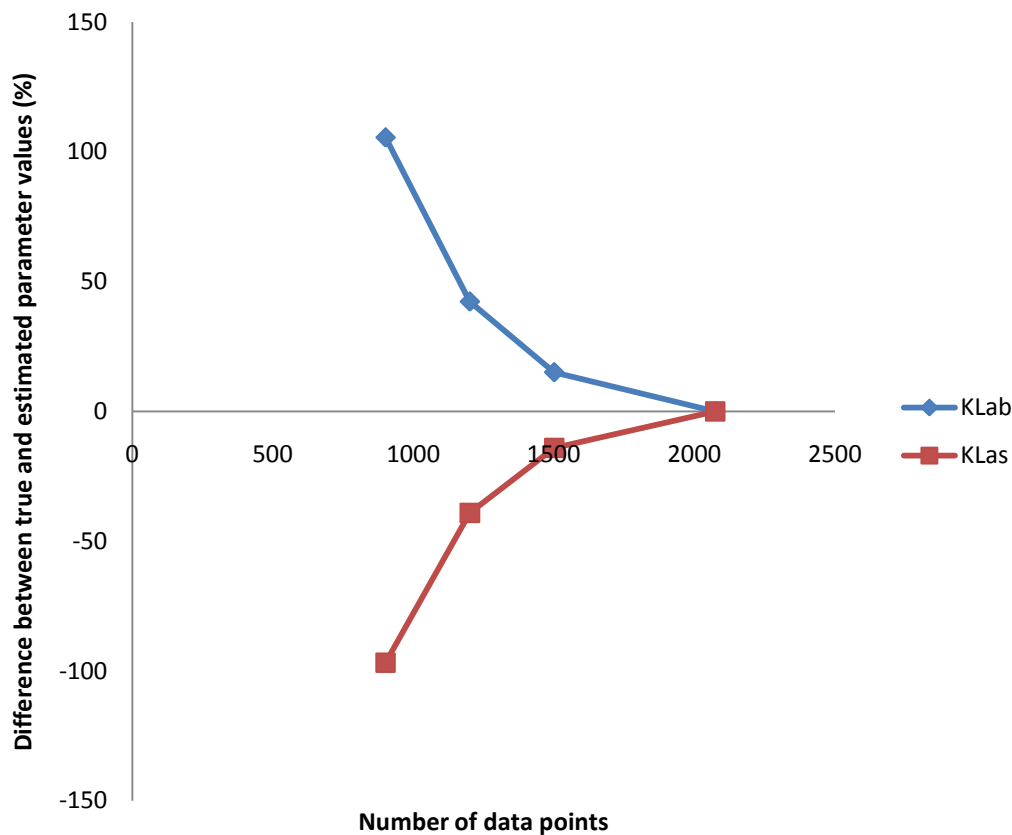


**Figure 38** Difference between the true parameter and the one which was estimated with more strictly truncation spans are shown as a function of number of data points. The more data points, the larger truncation span. The parameters were only evaluated at the points marked with dots.

## 6.5 MODEL NR 4

This model was not evaluated for either parameter sensitivity or truncation. It was assumed to behave approximately as model nr 2 concerning sensitivity for different initial guesses for the estimated parameters. Because the mass transfer coefficient  $K_{La}$  in model nr 2 is placed at the same position as  $K_{La_b}$  in model nr 4 and the mass transfer coefficient  $K_{La_s}$  in model nr 2 is stated at the same place as  $K_{La_{s1}}$  in model nr 4 they were assumed to behave approximately the same. A difference between the models had

been if the dissolved oxygen saturation concentration,  $C_{ss}$ , was known. That is almost the case in model nr 5.

## **6.6 MODEL NR 5**

Model nr 5 was not evaluated with either simulated or measured data in this project. Even if the model would not be sensitive for initial guesses for the estimated parameters it is important to see if model nr 1 is usable before combining that model with another model approaches.

## **7 DISCUSSION**

The focus of this research was to develop alternative models which describe the aeration process more accurately. To ensure that the model can be evaluated by anyone, it is necessary that the model is not sensitive for different initial guesses of the estimated parameters. Otherwise there would be a risk that the performance results would differ because of the human factor.

Another interesting thing is to consider different truncation spans and to see if the estimated parameter values changes significantly. For simulated data, the results depend on the noise levels. Reducing the measurement time leads to smaller data spans which could save both time and money but the performance results have to be trustworthy.

The simulated data used in this research were created to resemble measured data and were created both with and without added noises. The strong noises were probably not so realistic but it should be better to try the models to data with big variations than try them for only perfect data. By using perfect data it is possible to get a model which behaves perfectly but to ensure that the model could be used in reality it is important to try it for simulated data with added noise and measured data.

It is not possible to draw any conclusions about the parameter sensitivity by using only two or three different combinations of initial guesses for the estimated parameters. Because the initial guesses were set to values that were not close to each other it is possible to get an indication of the parameter sensitivity. If some of the models should be evaluated more closely it can be good to use Monte Carlo simulations and trying a large number of different initial guesses to avoid local minimums. If a model is sensitive for one combination of initial guesses it is unnecessary to evaluate it with Monte Carlo simulations because the model should not be sensitive for any combinations.

### **7.1 THE STANDARD METHOD**

The standard model assumes that the water is completely mixed in an aerated tank. That assumption is probably fairly correct for diffused aeration systems but probably less valid for mechanical aerators, such as jet aerators, where the air bubbles only distributes to a small water volume. If that assumption is not valid that could lead to estimated performance results that are not valid. Probably, the standard model is more accurate for diffused aeration systems which cover almost the whole tank bottom where the air bubbles become distributed evenly in the whole water volume than point source aeration.

Both simulated and measured data showed that the standard model was not sensitive for initial guesses for the estimated parameters. The reason why the estimated  $C_0$  changed with simulated data with added noise depends on how the noisy data around time zero was produced. Because the data was randomly produced, the noisy data can affect where the model curve should start.  $C_0$  is not an important model parameter but it is necessary to define to be able to estimate the rest of the parameters. A good

approximation of  $C_0$ , instead of an estimated value, could be to use the first measured data as the dissolved oxygen concentration at time zero. The different truncation spans that were analyzed for simulated and racetrack data showed that the model behaved desirably and gave good estimated parameter values for simulated data for almost every truncation span (Figure 25). However, when the data spans were too small with concentrations between 0 and 16% of the dissolved oxygen saturation concentration, there were significant changes of the estimated parameter values. The racetrack data showed significant changes already for truncation spans corresponding to concentrations between 0 and 85% of the dissolved oxygen saturation concentration (Figure 28 and 29). It is important to understand that the RSS decreases for decreasing truncation spans because there are smaller amounts of data.

A surprising discovery was that the estimated values of  $K_L a$  did not show any significant changes as to whether the probes were placed in the water volume with air bubbles or in a volume without air bubbles even if there is a visible difference between the measured data in each zone (Table 12 and 15). That can probably be explained by the liquid flow rate which is big in comparison to the water volume and mixes the two different zones completely. With these results it can be unmotivated to use model nr 1 for the aeration applications tested in this research.

It is desirable that all people in this business use the same method for evaluation of oxygen transfer performance and get the same results when the same equipment are used. It is possible to place the dissolved oxygen probes in the tank where it theoretically could be higher oxygen transfer. This could result in inaccurate performance results and that is why it can be difficult to compare different aeration devices if they are tested under different conditions.

## 7.2 METHOD NR 1

Model nr 1 seemed to behave desirable to simulated data. There was no significant change in the estimated parameter values and the model could fit measured data desirably. When the model was evaluated with measured data it can, by a first view, seem to be sensitive for different initial guesses for the estimated  $V_1/q$  (Table 22 and 25). That could possibly occur due to the very small  $q$ . When they are calculated individually there were differences for different initial guesses but  $V_2$  and  $q$  were very small in comparison to  $V_1$ . The relative change in  $q$  was big but the actual change was in a range of  $10^{-5} \text{m}^3/\text{min}$  which is so small that the measurement instrument is not accurate enough to give a good prediction. The expected value of  $V_1$  for the cylinder tank was approximately  $2/3$  of the total water volume which in this case is around  $0.265 \text{m}^3$ . For the racetrack tank it is easier to calculate an average  $V_1$  because the diffusers produced air bubbles in the whole channel width. The water depth, the channel area and the dimensions of the diffusers are known and  $V_1$  is approximated to  $0.0143 \text{m}^3$ . None of these estimated parameter values were even close to the calculated aerated water volumes. A possible reason is that the water is completely mixed and the model cannot see differences in  $C_1$  and  $C_2$ . The mixing in the cylinder tank is probably big because of the large amount of air bubbles and the measured liquid flow rate in the

racetrack tank shows that the tank is mixed within a minute as the volume was  $0.146\text{m}^3$  and the liquid flow rate was approximated to  $0.265\text{m}^3/\text{min}$ . Use of this model in applications with large tank volumes relative to the capacity of the aeration system can be possible. An example is aeration of a lagoon or in a racetrack where the aerated water volume is relatively small in comparison to the whole water volume or if the mixing between these volumes is small. The time it takes for mixing the water is then smaller than the time it takes to aerate a water volume in the tank to saturation (Uby, personal communication, 2010). However, no such data have been evaluated in this research which makes it difficult to draw any conclusions about this model.

Another possible reason that the model did not behave as expected can be that it is not suitable for the measured data. An additional question mark about this model is that no oxygen transfer is assumed to occur in the non-aerated water volume (Equation 8 and 9). Even if there is no oxygen transfer from air bubbles, there could possibly be some oxygen transferred at the non-bubbled water surface. However, oxygen transfer at the bubbled water surface in the aerated water volume is assumed to be bigger which could make the oxygen transfer in the non-aerated water volume negligible.

The estimated parameter values for the measured data were approximately the same for the standard model as for model nr 1. Because model nr 1 estimated the aerated water volume to almost the total volume, the model becomes similar to the standard model and the theory of it. If the aerated water volume should be estimated smaller, the  $K_{La}$  should be bigger. For smaller water volumes there should be a faster oxygenation which is represented by a bigger  $K_{La}$ . The performance parameter values show approximately the same results for both of the models when the same measured data was used.

By looking at the measured data in the racetrack tank (Figure 27) it was obvious that there was a time delay between the measured data in the aerated water volume (probe 5 and 3) and in the non-aerated water volume (probe 1 and 4). This delay cannot be explained by the uncertainty of the dissolved oxygen probes and is probably a result from the time it takes for the aerated water volume to move to the non-aerated water volume. The liquid flow rate in the racetrack tank was approximated to  $0.142\text{m}^3/\text{min}$  and can be compared with the measured flow of  $0.265\text{m}^3/\text{min}$ . There is a difference between those two flow rates but both of them are approximated. The time delay is not taken into account for in any model but could be a possible future model parameter.

By comparing the RSS for the standard model and model nr 1 for the same measured data it is easy to see that it is smaller for the standard model. That depends on the fact that RSS in the standard model is calculated for each of the four data series individually. For model nr 1, RSS is calculated at the same time for all four data series. The equations for  $C_1$  and  $C_2$  have to be calculated simultaneously because the estimated parameters are present in both equations. RSS for the cylinder tank data was calculated to  $57.4\text{mg}^2/\text{L}^2$  for model nr 1 and if all data series should be estimated simultaneously for the standard model the RSS should be calculated to  $136\text{mg}^2/\text{L}^2$ . The big difference depends on that the standard model only consists of one equation and model nr 1 consists of two

equations which reduces the RSS. The results could also be affected of that more parameters are estimated in model nr 1 than in the standard model which could help the model to fit the data better.

A disadvantage with the model is that some probes have to be placed in an aerated water volume and some in the non-aerated water volume. When the oxygen transfer should be measured in process water it can be difficult to know where the air bubbles are distributed. If it is difficult to determine where the bubbles are, maybe the probes show approximately the same trends as in these results and it does not matter exactly where they are placed.

### 7.3 METHOD NR 2

The evaluation of the simulated data for model nr 2 showed that the model was sensitive for different initial guesses for the estimated parameters. That is not desirable and could occur when the model finds a local minimum instead of a global minimum for the parameters. There are two possible reasons why the model is not identifiable and it is impossible to determine the parameter values. The first reason could be that different parameter values give the same results. The other reason could be due to different experimental conditions (Ljung & Glad, 2004). Using incorrect initial guesses increased the residual sum of squares significant and the model did not fit the measured data at all (Figure 34). Because of the parameter sensitivity the model was assumed to behave similarly to measured data.

A way of avoiding the problem with parameter sensitivity could be to calculate or measure  $K_L a_s$ . If it is known, then it is probably possible to estimate the remaining parameters needed in model nr 2. If a tank with an agitator instead of an aeration device is used, it can make the water surface turbulent. The model would be evaluated by measuring the oxygen transfer as for a usual standard measurement (Equation 33).

$$\frac{dC}{dt} = K_L a_s \cdot (C_{surf\_sat} - C) \quad (33)$$

Instead of estimating the  $K_L a$  as in the standard model, the only factor that could impact the oxygen transfer in this case is the water surface. So  $K_L a_s$  can be estimated, instead of estimating  $K_L a$ . Using Equation 33 makes it possible to standardize a value of  $K_L a_s$ . This can also be conducted by using the method with releasing nitrogen gas to a tank instead of air (Wilhelms & Martin, 1992).

### 7.4 METHOD NR 3

The difference between the originally developed model by McWhirter & Hutter (1989) and model nr 3 in this research is that  $C_0$  is estimated in model nr 3. It was considered to have a small but significant effect on the model fit. Other authors, like Schierholz et al. (2006), have advanced the model by introducing the impact of nitrogen and oxygen gas instead of only oxygen in the air bubbles. It is difficult to predict how big the impact of nitrogen is, but it can be a significant parameter to model. The reason why it was not studied in this research was because it was assumed to decrease the possibility to truncate smaller parts of the data series. Possibilities to truncation of data was predicted

to be easier for model nr 3 instead of the standard model because the saturation concentrations are calculated in model nr 3 and estimated in the standard model. Surprisingly, the standard model showed more possibilities to truncate smaller parts of the total data series because the difference of the estimated parameter values were a lot smaller than for model nr 3 (Table 10 and 35). Another interesting result was that the difference between the estimated and true  $K_{La_b}$  and  $K_{La_s}$  for model nr 3 was approximately the same but with reversed signs. Unfortunately, it is important to know the size of each of them individually when the SOTR is calculated.

The RSS seemed to be approximately the same for the standard model and model nr 3 for the measured data. It was also obvious that the estimated  $K_{La}$  for the racetrack data in the standard model was approximately the same as the sum of  $K_{La_b}$  and  $K_{La_s}$  for model nr 3. The reason why model nr 3 can separate the total  $K_{La}$  in two parts,  $K_{La_b}$  and  $K_{La_s}$  is due to the known dissolved oxygen saturation concentrations.  $K_{La_b}$  is in the model depending on  $C_o^*$  which varies with water depth and  $K_{La_s}$  is depending on the dissolved oxygen saturation concentration at atmospheric pressure,  $C_{surf\_sat}$ . Both of these saturation concentrations were calculated.  $K_{La_s}$  was relatively big in comparison to the total  $K_{La}$  but that can be explained by the small water depth and the large surface area in the racetrack tank. After an approximated calculation of the area, at which the oxygen transfer occurs, it is larger at the water surface than at the air bubbles for the racetrack tank. That was also confirmed by the results (Table 37). The area of the water surface was then calculated as the tank area and was probably an underestimation because the turbulence should increase the area. For the cylinder tank was the air bubble area approximated to 20 times larger than the water surface area which should result in larger  $K_{La_b}$  in comparison to  $K_{La_s}$ .

If a tank is 3m deep, the  $C_o^*$  can vary from approximately 8.7 to 11.3mg/L (Figure 39).

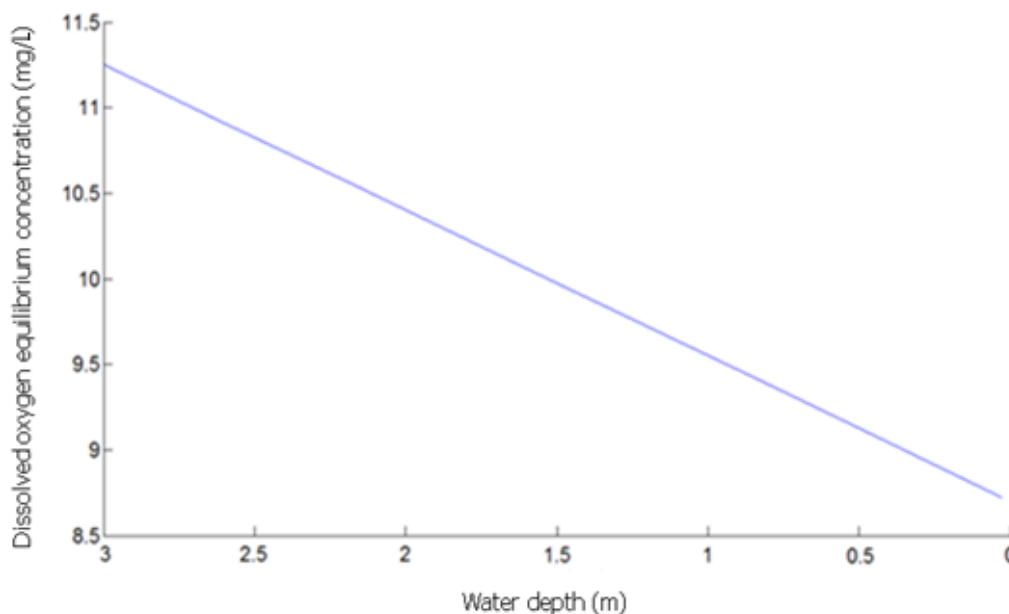


**Figure 39** The dissolved oxygen equilibrium concentration,  $C_o^*$ , versus water depth. Deeper down in the tank, the equilibrium concentration is higher due to increasing pressure.

The average value of  $C_o^*$  is then approximately 10mg/L and can be assumed to be the dissolved oxygen equilibrium concentration at the mid depth. For the standard model, the measured data is assumed to rise to the same saturation concentration,  $C_{ss}$ . If the saturation concentration is assumed to vary with water depth, the mass transfer coefficient,  $K_{La_b}$  and  $K_{La_s}$ , will have different impacts. If the dissolved oxygen concentration is measured close below the water surface, the oxygen transfer at the water surface seems to be much bigger than the oxygen transfer for the air bubbles. Air bubbles seem to have greater impact on the total oxygen transfer if the probe is placed deeper down in a tank. An example is given in Figure 40 where there are two data series with dissolved oxygen concentration over time. The dissolved oxygen concentrations represented by the blue dots are measured near the water surface and the green dots represent a probe deeper down in the tank. The mass transfer coefficient at the water surface,  $K_{La_s}$ , will then be bigger for the blue line than for the green line and the mass transfer coefficient for the air bubbles,  $K_{La_b}$  will be bigger for the green line in comparison to the blue line.

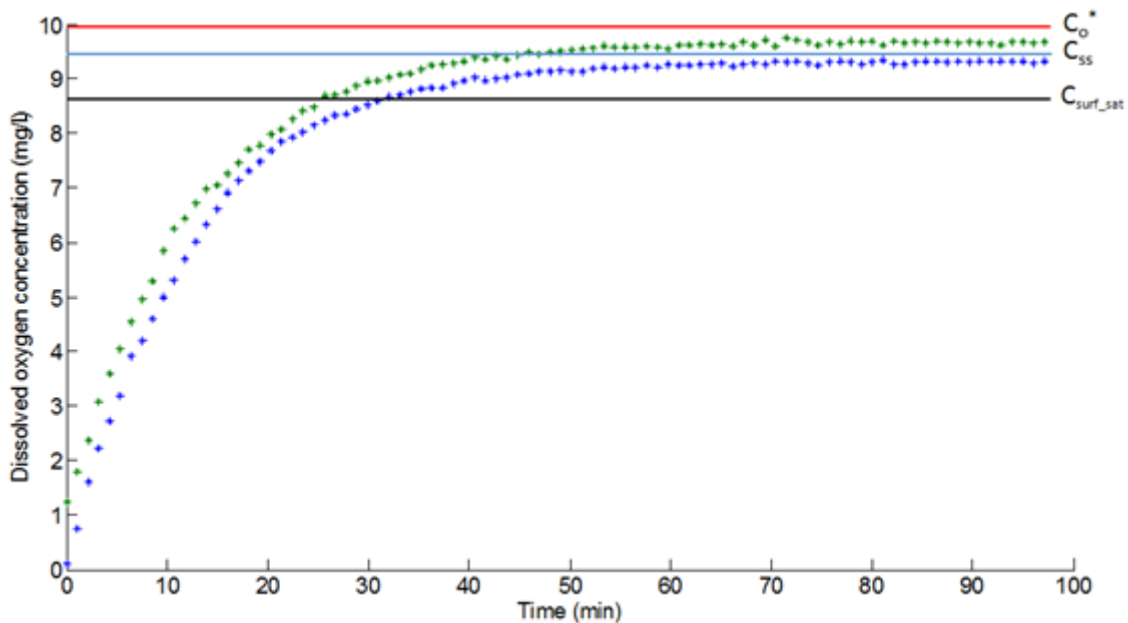


**Figure 40** Two hypothetical data series with dissolved oxygen concentrations are presented by the blue and green dots. The black line represents the dissolved oxygen saturation concentration with atmospheric pressure and the red line represents the depth average dissolved oxygen equilibrium concentration. This value, 10mg/L, is the dissolved oxygen equilibrium concentration at the mid depth. It varies from 11.3 to 8.7mg/L in the whole tank. The blue line shows how the dissolved oxygen saturation value would be estimated using the standard model but has nothing to do with model nr 3.

Whether  $C_{ss}$  or  $C_o^*$  and  $C_{surf\_sat}$  is the best parameter to describe how the water is saturated is difficult to determine. If a tank is well mixed, the dissolved oxygen saturation concentration should probably be approximately equal at any depth in the tank. In that case, maybe it is correct to use  $C_{ss}$  as in the standard model. But if the water is not well mixed and there is a big difference between the saturation concentrations in the upper and lower parts of the tank, maybe it is more correct to assume that the saturation concentration varies with water depth. In that case,  $C_o^*$  and



$C_{surf\_sat}$  should be used. If those parameters should be used it may be important to take into account how mixed the water is. How that could be done is not clear, but it may be good to analyze the possibility. Possibly it can be done by placing one dissolved oxygen probe at the bottom of a tank and another probe near the water surface. It may be a way of evaluating the water mixing if there is a difference in which saturation concentration they rise to.

The concentration of oxygen in gas phase,  $y$ , varies with water depth and time. When air is released to the water in the beginning of the reoxygenation, the dissolved oxygen concentration in the tank is approximately zero. Because the dissolved oxygen is zero, the gradient between dissolved oxygen and oxygen in the air bubbles will be bigger than if the water was saturated with oxygen. That is why the largest amount of oxygen in air bubbles will be transferred and dissolved in water when the gradient is high, which makes  $y$  decreasing the most. Figure 41 shows how the mole fraction of oxygen in gas is varying with both water depth and time. That behavior is approximately the same as for  $y$ . At steady state, when the water is completely saturated, the solution of oxygen deeper down in a tank is balanced by desorption of oxygen in the water close to the water surface and to the atmosphere. When the water is saturated, the concentration of oxygen in gas phase is increasing when it approaches the water surface. That occurs because the oxygen is desorbed from being dissolved in water and goes back to the gas phase. Some oxygen is also released to the atmosphere at the water surface (McWhirter & Hutter, 1989).

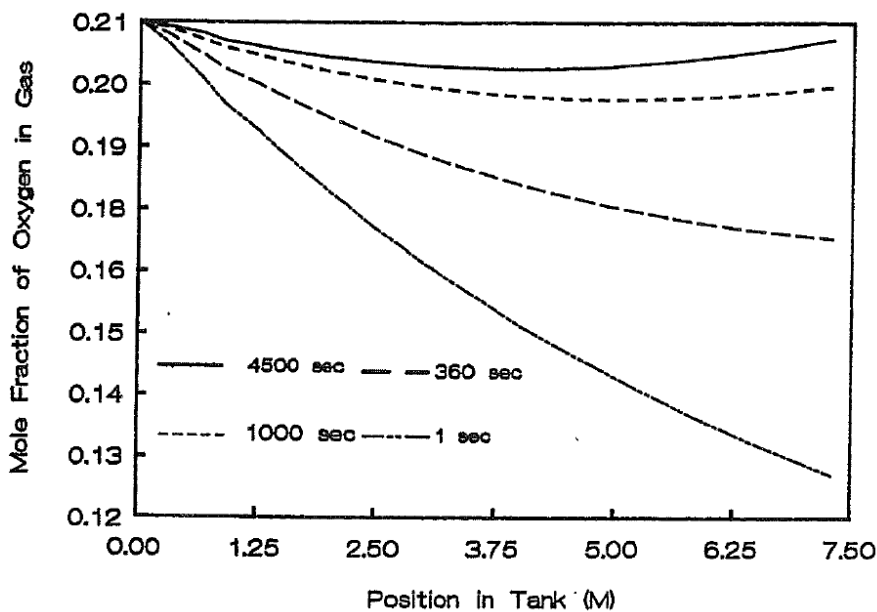


**Figure 41** The figure shows the mole fraction of oxygen in gas phase versus water depth and is presented for four different times during a reoxygenation. The lowest line represents how the mole fraction is varying after one second in a tank with water depth 7.5m. The highest line represents how it is varying 4500s after the reoxygenation started (McWhirter & Hutter, 1989).

An advantage with model nr 3 instead of using the standard model is that it is easier to predict aeration performance under changing tank and aeration properties (McWhirter & Hutter, 1989). It is easier to predict the saturation concentration because the dissolved

oxygen equilibrium concentration is calculated and not estimated. According to McWhiter & Hutter (1989), the mass transfer coefficient at the water surface,  $K_{La_s}$ , can be assumed to be somewhat equal for all aeration systems where the water surface is turbulent. The mass transfer coefficient for the air bubbles,  $K_{La_b}$ , can be assumed to vary linearly with the gas flow rate and not be dependent on the water depth. That assumption is valid for a specific type of aeration device.

## **7.5 METHOD NR 4 AND 5**

Model nr 4 was assumed to be sensitive for initial guesses for the estimated parameters. That is not a desired property for a model which could be used as in a standard method for oxygen transfer measurements.

Model nr 5 was not evaluated in this research. It is important to evaluate model nr 1 more closely before combining it with another model. It is still not totally clear if model nr 1 is usable and applicable for all aeration systems. Model nr 5 is probably a better description than the standard model of what is really occurs in an aerated water volume. Other factors that could possibly affect the oxygen transfer and could be future model parameters are the properties of the air bubbles.

Both model nr 4 and 5 contain many parameters. Probably it is not necessary to use a model which describes the oxygen transfer with more parameters than the standard model. A problem by trying to describe it with more parameters could be that the estimated parameters become sensitive for initial guesses. It can also be unmotivated to describe the dissolved oxygen curves with many parameters if it is not necessary. Simplified, the curves can be described by one parameter in the beginning of the reoxygenation that describes how fast the oxygen transfer is and another parameter that describes which value the dissolved oxygen concentration is rising against. An advantage is also to have a parameter which specifies which value the curve should start at. If the model includes more than one parameter that describes how fast the oxygen transfer is, for example as in model nr 2 and 3, it has to be motivated to use both of them. If the significance of any of them is low, it is best to leave it out.

## **7.6 POSSIBLE IMPROVEMENTS AND RECOMMENDATIONS FOR FUTURE WORK**

The measured data series were mainly produced for evaluating model nr 1 because the probes were placed in water volumes with and without air bubbles. The standard method recommends that the probes should be placed where it represents the total volume and that could be assumed to be the case when there are two probes in an aerated water volume and two in a non-aerated water volume. That is at least valid for the measured data in the cylinder tank but maybe not optimal for the racetrack tank. Maybe the probes should be placed in the middle of each water volume in the racetrack tank for evaluating the standard model, model nr 2 and model nr 3.

By performing nonlinear regression in MATLAB it is possible to set a range of upper and lower boundaries in which the estimated parameter values should be within. Only a lower boundary was set in this research to ensure that some parameters were not

estimated to a negative value. By introducing an upper boundary it is possible to capture the estimated parameter in a smaller range. The problem is that that range rarely is known and if the range is set to a large span it should probably be useless.

These alternative methods contain models with more parameters than the standard model. A positive aspect of the new methods is that they do not require any more measurements even if the models are more complicated. A possible improvement for the methods is to measure some model parameters which could reduce the number of estimated parameters. Reducing the number of estimated parameter could make it easier to develop more complicated models with more model parameters and ensure that the estimated parameters are not sensitive for initial guesses. But some parameters are difficult to measure, for example  $K_{La}$ . Maybe it cannot be justified to measure more parameters than what is done today in the standard method. The focus could instead be of reducing the measurement time. A possible way is to measure shorter parts of the reoxygenation curve and not until the dissolved oxygen concentration reaches saturation and steady state. The last part of a reoxygenation curve takes most time to measure because of the exponential form. If the measurement time should be reduced there has to be a model which does not lose its accuracy when shorter times are measured.

To be able to predict aeration performance under other operating conditions than what have been tested before it is needed to have an accurate model to be able to perform accurate predictions. These predictions are reasonable but it is desired to increase the accuracy. A possible future research would be to do several different oxygen transfer measurements in full scale tanks for different operating conditions. By predicting aeration performance for these tests it is possible to compare the predictions for the standard model and model nr 3 and see if there is a large difference. It is also possible to evaluate which of them that gives the best predictions.

An additional work could be to evaluate whether there exists some other methods for evaluating the model with measured data instead of nonlinear regression.

## 8 CONCLUSIONS

The most important and interesting conclusions of this thesis are summarized in the points below.

- The most important thing with a standard method for evaluation of oxygen transfer performance is that all investigators use the same method and at the same conditions.
- The standard method for oxygen transfer measurements which is used today seemed to be fairly good and reasonable considering usability. The standard model does not describe the whole aeration process, but if it is used for all aeration systems it is possible to get comparable results.
- Changing the standard model to another model which describes the aeration process with more parameters could be a way of getting more accurate performance results. It is also positive if an alternative model contributes to more information about the aeration, for example the oxygen transfer at the water surface.
- Model nr 1 seemed to be working as a model which describes mixing between a water volume containing air bubbles and a water volume without bubbles. It seemed to be unmotivated to use this model for the most common aeration systems in which the water was rather mixed. More research should be done and the model should be tested with data in situations where the mixing is small in comparison to the total water volume.
- Where the bubbles are distributed in a tank is not important as long as the mixing of the water is fast, relative to the oxygen transfer.
- Method nr 3 seemed to be a good alternative method to the standard method. A factor that should be more discussed is the dissolved oxygen equilibrium concentration. Which parameter that describes the saturation best is difficult to determine and it probably varies for different aeration systems.

## 9 REFERENCES

ASCE & WPCF, 1988. Aeration: A wastewater treatment process. American Society of Civil Engineers and the Water Pollution Control Federation, USA.

ASCE, 2007. Measurements of Oxygen Transfer in Clean Water. American Society of Civil Engineers, Virginia.

Boyle, W. C., 1983. Development of standard procedures for evaluating oxygen transfer devices. American Society of Civil Engineers, Oxygen Transfer Standards Subcommittee.

Chern, J-M., Chou, S-R. & Shang, C-S., 2001. Effects of impurities on oxygen transfer rates in diffused aeration systems. *Water Research*, vol. 35, no. 13, pp 3041-3048.

Chern, J-M. & Yang, S-P., 2003. Oxygen transfer rate in a coarse-bubble diffused aeration system. *Industrial & Engineering Chemistry Research*, vol. 42, pp 6653-6660.

Chern, J-M. & Yu, C-F., 1997. Oxygen transfer modeling of diffused aeration systems. *Industrial & Engineering Chemistry Research*, vol. 36, pp 5447-5453.

DeMoyer, C. D., Schierholz, E. L., Gulliver, J. S. & Wilhelms, S. C., 2003. Impact of bubble and free surface oxygen transfer on diffused aeration systems. *Water Research*, vol. 37, no. 9, pp 1890-1904.

Fonade, C., Doubrovine, N., Maranges, C. & Morchain, J., 2001. Influence of a transverse flowrate on the oxygen transfer performance in heterogeneous aeration: Case of hydro-ejectors. *Water Research*, vol. 35, no. 14, pp 3429-3435.

Fujie, K., Urano, K., Kubota, H. & Kasakura, T., 1992. Hydrodynamics and oxygen transfer characteristics in activated sludge aeration tanks. *Water science and technology*, vol. 26, no. 3-4, pp 791-800.

Larson, L., Rosso, D., Leu, S-Y. & Stenstrom, M. K., 2007. Energy-conservation in fine pore diffuser installations in activated sludge processes. University of California, Civil & Environmental Engineering Department, Los Angeles.

Lewis, M. E., 2006. Dissolved oxygen (version 2.1). Chapter A6, section 6.2. [http://water.usgs.gov/owq/FieldManual/Chapter6/6.2\\_v2.1.pdf](http://water.usgs.gov/owq/FieldManual/Chapter6/6.2_v2.1.pdf) (2011-01-11).

Ljung, L. & Glad, T., 2004. *Modellbygge och simulering*. Studentlitteratur AB, Lund.

Mathworks, 2010a. Lsqcurvefit.

<http://www.mathworks.com/help/toolbox/optim/ug/lsqcurvefit.html> (2010-11-30).

Mathworks, 2010b. Randn.

<http://www.mathworks.com/help/techdoc/ref/randn.html> (2010-12-13).

McWhirter, J. R. & Hutter, J. C., 1989. Improved Oxygen Mass Transfer Modeling for Diffused/Subsurface Aeration Systems. *American Institute of Chemical Engineers Journal*, vol. 35, no. 9, pp 1527-1534.

Nationalencyklopedin, 2010. Residual.  
<http://www.ne.se/lang/residual> (2010-11-30).

Nortek AS, 2004. Vectrino velocimeter user guide. Nortek AS, Rud.

SATRON Instruments, 2005. Driftinstruktion – O<sub>2</sub>-mätare för löst syre 9100D med mätcell typ 95A. SATRON Instruments Process & Miljö AB, Säffle.

Schierholz, E. L., Gulliver, J. S., Wilhelms, S. C. & Henneman, H. E., 2006. Gas transfer from air diffusers. *Water Research*, vol. 40, no. 5, pp 1018-1026.

Seber, G. A. F. & Wild, C. J., 2003. *Nonlinear regression*. John Wiley & Sons, Inc, New Jersey.

Svenskt Vatten, 2007. *Avloppsteknik 2 – Reningsprocessen*. Publikation U2, Svenskt Vatten AB.

Wilhelms, S. C. & Martin, S. K., 1992. Gas transfer in diffused bubble plumes. American Society of Civil Engineers, Lincoln.

### **Personal communication**

Arbeus, Ulf, 2011. Director of Product Development at ITT Water & Wastewater (2011-01-27).

Carlsson, Bengt, 2010. Professor in Automatic Control at Uppsala University (2010-10-06).

Uby, Lars, 2010. Senior Application Engineer at ITT Water & Wastewater (2010-11-24).

## APPENDIX A

### Calculation.m

```
% THE STANDARD MODEL
% ESTIMATION OF Css, C0 AND KLa USING NONLINEAR REGRESSION
% X = time and y1, y2, y3 = dissolved oxygen concentrations
beta0 = [9.5; 0; 0.08]; % Initial guess for [Css; C0; KLa]
[beta1, resnorm1] = lsqcurvefit(@DO,beta0,X,y1);
[beta2, resnorm2] = lsqcurvefit(@DO,beta0,X,y2);
[beta3, resnorm3] = lsqcurvefit(@DO,beta0,X,y3);
[beta4, resnorm4] = lsqcurvefit(@DO,beta0,X,y4);

% CALCULATIONS OF PERFORMANCE PARAMETERS
% PARAMETERS TO MEASURE
T_before = [22.7 22.7 22.7 22.7]; % Water temperature before
% measurements [°C]
T_after = [22.7 22.7 22.7 22.7]; % Water temperature after
% measurements [°C]
Conductivity = [256 581]; % Conductivity before and
% after measurements
% [µS/cm]
z = 2.975; % Liquid depth [m]
Ab = 4.1*4.5; % Bottom floor area [m2]
Qp = 18.5*10-3; % Measured air flow [m3/s]
P1 = 101.4; % Ambient atmospheric
% pressure [kPa]
Pp = (101.4*103 + 1000*9.82*z)/1000; % Gas pressure at
% measurement point [kPa]
T1 = 20+273; % Ambient air temperature
% [K]
n = 4; % Number of probes [-]

% CALCULATING THE AVERAGE WATER TEMPERATURE [°C]
T1medel = (T_before(1,1)+T_after(1,1))/2;
T2medel = (T_before(1,2)+T_after(1,2))/2;
T3medel = (T_before(1,3)+T_after(1,3))/2;
T4medel = (T_before(1,4)+T_after(1,4))/2;
T = (T1medel + T2medel + T3medel + T4medel)/4;

% FIXED PARAMETERS
Theta = 1.024; % Temperature constant [-]
R = 289; % Gas constant for air [Nm/kg*K]
k = 1.395; % Ratio of specific heats for gas.
% k = 1.395 for air with adiabatic
% compression
Ts = 293; % Temperature for standard condition
% [K]
rho = 1.2; % Density for air [kg/m3]
Ps = 101.3; % Standard barometric pressure [kPa]

% CALCULATIONS OF THE TANK VOLUME [m3]
V = Ab*z;

% CALCULATIONS OF THE MEAN CONDUCTIVITY [µS/cm]
Conductivity = (Conductivity(1)+Conductivity(2))/2;

% CALCULATIONS OF TDS (TOTAL DISSOLVED SOLIDS) [mg/L]
TDS = Conductivity*2000/3000;
```

```

% CALCULATIONS OF TEMPERATURE AT MEASUREMENT POINT Tp [°C]
Tp = T1*(Pp/P1)^((k-1)/k);

% VOLUMETRIC AIR FLOW TO THE SYSTEM, AT AMBIENT CONDITIONS [m3/s]
Q1 = Qp*(T1/Tp)*(Pp/P1);

% STANDARD CONDITIONS AIR FLOW [m3/s]
Qs = Q1*(Ts/T1)*(P1/Ps);

% CALCULATIONS OF THE DELIVERED BLOWER POWER DBP [W]
K = (k-1)/k;
w = Qs*rho; % Mass flow of gas [kg/s]
DBP = (w*R*T1)/K*((Pp/P1)^K-1);

% TEMPERATURE CORRECTION OF KLa
KLa20_1 = beta1(3)*Theta^(20-T1medel);
KLa20_2 = beta2(3)*Theta^(20-T2medel);
KLa20_3 = beta3(3)*Theta^(20-T3medel);
KLa20_4 = beta4(3)*Theta^(20-T4medel);

% TEMPERATURE CORRECTION OF STEADY STATE DO
T_1 = T1medel + 273.15;
T_2 = T2medel + 273.15;
T_3 = T3medel + 273.15;
T_4 = T4medel + 273.15;
T_20_grader = 20 + 273.15;

A1 = -173.4292; B1 = -0.033096;
A2 = 249.6339; B2 = 0.014259;
A3 = 143.3483; B3 = -0.001700;
A4 = -21.8492;
S=0;

lnDO = A1 + A2*100./T_1 + A3.*log(T_1/100) + A4.*T_1/100 + S*(B1 +
B2.*T_1/100 + B3.*(T_1/100).^2);
Csurfsat_1 = 1.4276*exp(lnDO);

lnDO = A1 + A2*100./T_2 + A3.*log(T_2/100) + A4.*T_2/100 + S*(B1 +
B2.*T_2/100 + B3.*(T_2/100).^2);
Csurfsat_2 = 1.4276*exp(lnDO);

lnDO = A1 + A2*100./T_3 + A3.*log(T_3/100) + A4.*T_3/100 + S*(B1 +
B2.*T_3/100 + B3.*(T_3/100).^2);
Csurfsat_3 = 1.4276*exp(lnDO);

lnDO = A1 + A2*100./T_4 + A3.*log(T_4/100) + A4.*T_4/100 + S*(B1 +
B2.*T_4/100 + B3.*(T_4/100).^2);
Csurfsat_4 = 1.4276*exp(lnDO);

lnDO = A1 + A2*100./T_20_grader + A3.*log(T_20_grader/100) +
A4.*T_20_grader/100 + S*(B1 + B2.*T_20_grader/100 +
B3.*(T_20_grader/100).^2);
Csurfsat_20_grader = 1.4276*exp(lnDO);

Tao_1 = Csurfsat_1/Csurfsat_20_grader;
Tao_2 = Csurfsat_2/Csurfsat_20_grader;
Tao_3 = Csurfsat_3/Csurfsat_20_grader;
Tao_4 = Csurfsat_4/Csurfsat_20_grader;

```



```

% PRESSURE CORRECTION OF STEADY STATE DO (< 6.1 m depth)
Omega = P1/Ps;

% STEADY STATE DO SATURATION CONCENTRATION CORRECTED TO 20°C ETC.
Css_20_1 = beta1(1)*(1/(Tao_1*Omega));
Css_20_2 = beta2(1)*(1/(Tao_2*Omega));
Css_20_3 = beta3(1)*(1/(Tao_3*Omega));
Css_20_4 = beta4(1)*(1/(Tao_4*Omega));

% OPTIONAL TDS NORMALIZATION OF KLa
KLa20_1000_1 = KLa20_1*exp(0.0000965*(1000-TDS));
KLa20_1000_2 = KLa20_2*exp(0.0000965*(1000-TDS));
KLa20_1000_3 = KLa20_3*exp(0.0000965*(1000-TDS));
KLa20_1000_4 = KLa20_4*exp(0.0000965*(1000-TDS));

% CALCULATIONS OF MASS FLOW OF OXYGEN AT STANDARD CONDITIONS
Wair = 1.20*Qs; % Mass flow of air, in SI units for
                % U.S. practice [kg/s]
W02 = 0.23*Wair; % Mass flow of oxygen in air stream
                % [kg/s]

% CALCULATIONS OF SOTR [kg/min]
SOTR_1 = KLa20_1000_1*Css_20_1*v*10^-3;
SOTR_2 = KLa20_1000_2*Css_20_2*v*10^-3;
SOTR_3 = KLa20_1000_3*Css_20_3*v*10^-3;
SOTR_4 = KLa20_1000_4*Css_20_4*v*10^-3;

% CALCULATIONS OF AVERAGE SOTR FOR ALL PROBES [kg/h]
SOTR = (1/n)*(SOTR_1 + SOTR_2 + SOTR_3 + SOTR_4)*60;

% CALCULATIONS OF SAE [kg/kWh]
SAE = SOTR/(DBP*10^-3);
%
CALCULATIONS OF SOTE [%]
SOTE = 100 * SOTR/(W02*3600);

```

## DO.m

```

function C = DO(b,X)
% The standard model
C = b(1)-(b(1)-b(2))*exp(-b(3)*X);
end

```

## APPENDIX B

### Calculation.m

```
% MODEL NR 1
% X = time and y1, y2, y3 = DO concentration
load workspace.mat
beta0 = [10.5; 0.2; 0.5; 2; 0.5; 0];
% Initial guesses for [Css; KLa; V1/q; V2/q; C10; C20]
[beta1, resnorm, residual] = lsqcurvefit(@DO,beta0,X,y,[0 0 0 0 -10 -
10]);
Cout = DO(beta1,X);

% Calculating V1 and V2
disp(['V1/q = ', num2str(beta1(3))])
disp(['V2/q = ', num2str(beta1(4))])
V = 0.3971;
V1V2_diff = beta1(3)/beta1(4);
V1 = V/(1+(1/V1V2_diff))
V2 = V-V1

% CALCULATIONS OF PERFORMANCE PARAMETERS
% PARAMETERS TO MEASURE
T_before = [15.5 15.5 15.5 15.5]; % Water temperature before
% measurements [°C]
T_after = [15.7 15.7 15.7 15.7]; % Water temperature after
% measurements [°C]
Conductivity = [780 1030]; % Conductivity before and
% after measurements
% [µS/cm]
z = 1.95; % Liquid depth [m]
V = 0.3971; % Water volume [m3]
Qp = 3.3500*10^-004; % Measured air flow [m3/s]
P1 = 101.5; % Ambient atmospheric
% pressure [kPa]
Pp = (P1*10^3 + 1000*9.82*z)/1000; % Gas pressure at
% measurement point [kPa]
T1 = 20.3+273; % Ambient air temperature
% [K]
n = 4; % Number of probes [-]

% CALCULATION OF THE AVERAGE WATER TEMPERATURE [°C]
T1medel = (T_before(1,1)+T_after(1,1))/2;
T2medel = (T_before(1,2)+T_after(1,2))/2;
T3medel = (T_before(1,3)+T_after(1,3))/2;
T4medel = (T_before(1,4)+T_after(1,4))/2;
T = (T1medel + T2medel + T3medel + T4medel)/n;

% FIXED PARAMETERS
Theta = 1.024; % Temperature constant [-]
R = 289; % Gas constant for air [Nm/kg*K]
k = 1.395; % Ratio of specific heats for gas.
% k = 1.395 for air with adiabatic
% compression
Ts = 293; % Temperature for standard condition
% [K]
rho = 1.2; % Density for air [kg/m3]
Ps = 101.3; % Standard barometric pressure [kPa]

% CALCULATIONS OF THE AVERAGE CONDUCTIVITY [µS/cm]
```

```

Conductivity = (Conductivity(1)+Conductivity(2))/2;

% CALCULATIONS OF TDS (TOTAL DISSOLVED SOLIDS) [mg/L]
TDS = Conductivity*2000/3000;

% CALCULATIONS OF TEMPERATURE AT MEASUREMENT POINT Tp [K]
Tp = T1*(Pp/P1)^((k-1)/k);

% VOLUMETRIC AIR FLOW TO THE SYSTEM, AT AMBIENT CONDITIONS [m3/s]
Q1 = Qp*(T1/Tp)*(Pp/P1);

% STANDARD CONDITIONS AIR FLOW [m3/s]
Qs = Q1*(Ts/T1)*(P1/Ps);

% CALCULATIONS OF THE DELIVERED BLOWER POWER DBP [W]
K = (k-1)/k;
w = Qs*rho; % Mass flow of gas [kg/s]
DBP = (w*R*T1)/K*((Pp/P1)^K-1);

% TEMPERATURE CORRECTION OF KLa
KLa20_1 = betal(2)*Theta^(20-T);

% TEMPERATURE CORRECTION OF STEADY STATE DO
T_1 = T1medel + 273.15;
T_2 = T2medel + 273.15;
T_3 = T3medel + 273.15;
T_4 = T4medel + 273.15;
T_20_grader = 20 + 273.15;

A1 = -173.4292; B1 = -0.033096;
A2 = 249.6339; B2 = 0.014259;
A3 = 143.3483; B3 = -0.001700;
A4 = -21.8492;
S=0;

lnDO = A1 + A2*100./T_1 + A3.*log(T_1/100) + A4.*T_1/100 + S*(B1 +
B2.*T_1/100 + B3.*(T_1/100).^2);
Csurfsat_1 = 1.4276*exp(lnDO);

lnDO = A1 + A2*100./T_2 + A3.*log(T_2/100) + A4.*T_2/100 + S*(B1 +
B2.*T_2/100 + B3.*(T_2/100).^2);
Csurfsat_2 = 1.4276*exp(lnDO);

lnDO = A1 + A2*100./T_3 + A3.*log(T_3/100) + A4.*T_3/100 + S*(B1 +
B2.*T_3/100 + B3.*(T_3/100).^2);
Csurfsat_3 = 1.4276*exp(lnDO);

lnDO = A1 + A2*100./T_4 + A3.*log(T_4/100) + A4.*T_4/100 + S*(B1 +
B2.*T_4/100 + B3.*(T_4/100).^2);
Csurfsat_4 = 1.4276*exp(lnDO);

lnDO = A1 + A2*100./T_20_grader + A3.*log(T_20_grader/100) +
A4.*T_20_grader/100 + S*(B1 + B2.*T_20_grader/100 +
B3.*(T_20_grader/100).^2);
Csurfsat_20_grader = 1.4276*exp(lnDO);

Tao_1 = Csurfsat_1/Csurfsat_20_grader;
Tao_2 = Csurfsat_2/Csurfsat_20_grader;
Tao_3 = Csurfsat_3/Csurfsat_20_grader;

```

```

Tao_4 = Csurfsat_4/Csurfsat_20_grader;

% PRESSURE CORRECTION OF STEADY STATE DO (< 6.1 m depth)
Omega = P1/Ps;

% STEADY STATE DO SATURATION CONCENTRATION CORRECTED TO 20°C ETC.
Css_20_1 = betal(1)*(1/(Tao_1*Omega));

% OPTIONAL TDS NORMALIZATION OF KLa [min^-1]
KLa20_1000_1 = KLa20_1*exp(0.0000965*(1000-TDS));

% CALCULATIONS OF MASS FLOW OF OXYGEN AT STANDARD CONDITIONS
Wair = 1.20*Qs;          % Mass flow of air, in SI units for U.S. practice
                        % [kg/s]
W02 = 0.23*Wair;       % Mass flow of oxygen in air stream [kg/s]

% CALCULATIONS OF SOTR [kg/min]
SOTR_1 = KLa20_1000_1*Css_20_1*V1*10^-3;

% CALCULATIONS OF AVERAGE SOTR FOR ALL PROBES [kg/h]
%SOTR = (1/n)*(SOTR_1 + SOTR_2 + SOTR_3 + SOTR_4)*60;
SOTR = SOTR_1*60;

% CALCULATIONS OF SAE [kg/kWh]
SAE = SOTR/(DBP*10^-3);

% CALCULATIONS OF SOTE [%]
SOTE = 100 * SOTR/(W02*3600);

```

## DO.m

```

function Cout = DO(b,X)
V = 0.3971;
Tao_1=b(3);          %V1/q
Tao_2=b(4);          %V2/q
k1 = (- (b(2)+(1/Tao_1)+(1/Tao_2))/2)+sqrt(((b(2)+(1/Tao_1)+(1/Tao_2))^2/4)-(b(2)/Tao_2));
k2 = (- (b(2)+(1/Tao_1)+(1/Tao_2))/2)-sqrt(((b(2)+(1/Tao_1)+(1/Tao_2))^2/4)-(b(2)/Tao_2));
C1_coeff = (b(5)*Tao_1*(-k1+k2)-b(6)+Tao_1*(b(5)*k1+b(5)*b(2)+(b(5)/Tao_1)-b(1)*k1-b(1)*b(2)-(b(1)/Tao_1))+b(1)-b(1)*Tao_1*(-k1+k2))/(Tao_1*(-k1+k2));
C2_coeff = (b(6)-Tao_1*(b(5)*k1+b(5)*b(2)+(b(5)/Tao_1)-b(1)*k1-b(1)*b(2)-(b(1)/Tao_1))-b(1))/(Tao_1*(-k1+k2));

Cout = zeros(length(X),4);
for i=1:length(X)
    %If C1-measurement
    Cout(i,1)=C1_coeff*exp(k1*X(i))+C2_coeff*exp(k2*X(i))+b(1);
    %If C2-measurement
    Cout(i,2) = C1_coeff*exp(k1*X(i))*Tao_1*(k1+b(2)+(1/Tao_1))+C2_coeff*exp(k2*X(i))*Tao_1*(k2+b(2)+(1/Tao_1))+b(1);
    %If C1-measurement
    Cout(i,3)=C1_coeff*exp(k1*X(i))+C2_coeff*exp(k2*X(i))+b(1);
    %If C2-measurement
    Cout(i,4) = C1_coeff*exp(k1*X(i))*Tao_1*(k1+b(2)+(1/Tao_1))+C2_coeff*exp(k2*X(i))*Tao_1*(k2+b(2)+(1/Tao_1))+b(1);
end
end

```

## APPENDIX C

### Calculation.m

```
% MODEL NR 2
Csat=9.1;
% X = time and y1, y2, y3 = DO concentration

% SIMULATED DATA
Csat=9.1;
b(1) = 10; % Fixed parameters
b(2) = 0;
b(3) = 0.05;
b(4) = 0.01;

A=b(3)*b(1)+b(4)*Csat;
B=-b(3)-b(4);
sim_data = zeros(length(X),1);
for i=1:length(X)
    brus = randn(92,1)/10;
    sim_data(i) = 1/B*exp(B*X(i)) * (A+B*b(2)) -A/B+brus(i);
end

% ESTIMATION OF PARAMETERS
options = optimset('MaxFunEval', 10000, 'TolFun', 1e-8);
beta0 = [15;0.5;0.5;1]; % Initial guess for [Css; C0; KLab; KLas]
[parametrar,resnorm] = lsqcurvefit(@DO,beta0,X,sim_data,[0 -10 0
0],[],options);
Cout = DO(parametrar,X);

% CALCULATIONS OF PERFORMANCE PARAMETERS
% PARAMETERS TO MEASURE
T_before = [22.7 22.7 22.7 22.7]; % Water temperature before
% measurements [°C]
T_after = [22.7 22.7 22.7 22.7]; % Water temperature after
% measurements [°C]
Conductivity = [256 581]; % Conductivity before and
% after measurements[µS/cm]
z = 2.975; % Liquid depth [m]
Ab = 4.1*4.5; % Bottom floor area [m2]
Qp = 18.5*10^-3; % Measured air flow [m3/s]
P1 = 101.4; % Ambient atmospheric
% pressure [kPa]
Pp = (101.4*10^3 + 1000*9.82*z)/1000; % Gas pressure at
% measurement point [kPa]
T1 = 20+273; % Ambient air temperature
% [K]
n = 4; % Number of probes [-]

% CALCULATING THE AVERAGE WATER TEMPERATURE [°C]
T1medel = (T_before(1,1)+T_after(1,1))/2;
T2medel = (T_before(1,2)+T_after(1,2))/2;
T3medel = (T_before(1,3)+T_after(1,3))/2;
T4medel = (T_before(1,4)+T_after(1,4))/2;
T = (T1medel + T2medel + T3medel + T4medel)/4;

% FIXED PARAMETERS
Theta = 1.024; % Temperature constant [-]
R = 289; % Gas constant for air [Nm/kg*K]
```

```

k = 1.395; % Ratio of specific heats for gas. k = 1.395 for
% air with adiabatic compression
Ts = 293; % Temperature for standard condition [K]
rho = 1.2; % Density for air [kg/m3]
Ps = 101.3; % Standard barometric pressure [kPa]

% CALCULATIONS OF THE TANK VOLUME [m3]
V = Ab*z;

% CALCULATIONS OF THE AVERAGE CONDUCTIVITY [ $\mu$ S/cm]
Conductivity = (Conductivity(1)+Conductivity(2))/2;

% CALCULATIONS OF TDS (TOTAL DISSOLVED SOLIDS) [mg/L]
TDS = Conductivity*2000/3000;

% CALCULATIONS OF TEMPERATURE AT MEASUREMENT POINT Tp [°C]
Tp = T1*(Pp/P1)^((k-1)/k);

% VOLUMETRIC AIR FLOW TO THE SYSTEM, AT AMBIENT CONDITIONS [m3/s]
Q1 = Qp*(T1/Tp)*(Pp/P1);

% STANDARD CONDITIONS AIR FLOW [m3/s]
Qs = Q1*(Ts/T1)*(P1/Ps);

% CALCULATIONS OF THE DELIVERED BLOWER POWER DBP [W]
K = (k-1)/k;
w = Qs*rho; % Mass flow of gas [kg/s]
DBP = (w*R*T1)/K*((Pp/P1)^K-1);

% TEMPERATURE CORRECTION OF KLa
KLa20_1_b = (beta1(3))*Theta^(20-T1medel);
KLa20_2_b = (beta2(3))*Theta^(20-T2medel);
KLa20_3_b = (beta3(3))*Theta^(20-T3medel);
KLa20_4_b = (beta4(3))*Theta^(20-T4medel);
KLa20_1_s = (beta1(4))*Theta^(20-T1medel);
KLa20_2_s = (beta2(4))*Theta^(20-T2medel);
KLa20_3_s = (beta3(4))*Theta^(20-T3medel);
KLa20_4_s = (beta4(4))*Theta^(20-T4medel);

% TEMPERATURE CORRECTION OF STEADY STATE DO
T_1 = T1medel + 273.15;
T_2 = T2medel + 273.15;
T_3 = T3medel + 273.15;
T_4 = T4medel + 273.15;
T_20_grader = 20 + 273.15;

A1 = -173.4292; B1 = -0.033096;
A2 = 249.6339; B2 = 0.014259;
A3 = 143.3483; B3 = -0.001700;
A4 = -21.8492;
S=0;

lnDO = A1 + A2*100./T_1 + A3.*log(T_1/100) + A4.*T_1/100 + S*(B1 +
B2.*T_1/100 + B3.*(T_1/100).^2);
Csurfsat_1 = 1.4276*exp(lnDO);

lnDO = A1 + A2*100./T_2 + A3.*log(T_2/100) + A4.*T_2/100 + S*(B1 +
B2.*T_2/100 + B3.*(T_2/100).^2);
Csurfsat_2 = 1.4276*exp(lnDO);

```

```

lnDO = A1 + A2*100./T_3 + A3.*log(T_3/100) + A4.*T_3/100 + S*(B1 +
B2.*T_3/100 + B3.*(T_3/100).^2);
Csurfsat_3 = 1.4276*exp(lnDO);

lnDO = A1 + A2*100./T_4 + A3.*log(T_4/100) + A4.*T_4/100 + S*(B1 +
B2.*T_4/100 + B3.*(T_4/100).^2);
Csurfsat_4 = 1.4276*exp(lnDO);

lnDO = A1 + A2*100./T_20_grader + A3.*log(T_20_grader/100) +
A4.*T_20_grader/100 + S*(B1 + B2.*T_20_grader/100 +
B3.*(T_20_grader/100).^2);
Csurfsat_20_grader = 1.4276*exp(lnDO);

Tao_1 = Csurfsat_1/Csurfsat_20_grader;
Tao_2 = Csurfsat_2/Csurfsat_20_grader;
Tao_3 = Csurfsat_3/Csurfsat_20_grader;
Tao_4 = Csurfsat_4/Csurfsat_20_grader;

% PRESSURE CORRECTION OF STEADY STATE DO (< 6.1 m depth)
Omega = P1/Ps;

% STEADY STATE DO SATURATION CONCENTRATION CORRECTED TO 20°C ETC.
Css_20_1 = beta1(1)*(1/(Tao_1*Omega));
Css_20_2 = beta2(1)*(1/(Tao_2*Omega));
Css_20_3 = beta3(1)*(1/(Tao_3*Omega));
Css_20_4 = beta4(1)*(1/(Tao_4*Omega));
Csat_20_1 = Csat*(1/(Tao_1*Omega));
Csat_20_2 = Csat*(1/(Tao_2*Omega));
Csat_20_3 = Csat*(1/(Tao_3*Omega));
Csat_20_4 = Csat*(1/(Tao_4*Omega));

% OPTIONAL TDS NORMALIZATION OF KLa
KLa20_1000_1_b = KLa20_1_b*exp(0.0000965*(1000-TDS));
KLa20_1000_2_b = KLa20_2_b*exp(0.0000965*(1000-TDS));
KLa20_1000_3_b = KLa20_3_b*exp(0.0000965*(1000-TDS));
KLa20_1000_4_b = KLa20_4_b*exp(0.0000965*(1000-TDS));
KLa20_1000_1_s = KLa20_1_s*exp(0.0000965*(1000-TDS));
KLa20_1000_2_s = KLa20_2_s*exp(0.0000965*(1000-TDS));
KLa20_1000_3_s = KLa20_3_s*exp(0.0000965*(1000-TDS));
KLa20_1000_4_s = KLa20_4_s*exp(0.0000965*(1000-TDS));

% CALCULATIONS OF MASS FLOW OF OXYGEN AT STANDARD CONDITIONS
Wair = 1.20*Qs;          % Mass flow of air, in SI units for U.S. practice
                        % [kg/s]
W02 = 0.23*Wair;       % Mass flow of oxygen in air stream [kg/s]

% CALCULATIONS OF SOTR [kg/min]
SOTR_1 = KLa20_1000_1_b*Css_20_1*v*10^-3;
SOTR_2 = KLa20_1000_2_b*Css_20_2*v*10^-3;
SOTR_3 = KLa20_1000_3_b*Css_20_3*v*10^-3;
SOTR_4 = KLa20_1000_4_b*Css_20_4*v*10^-3;
SOTR_5 = KLa20_1000_1_s*Csat_20_1*v*10^-3;
SOTR_6 = KLa20_1000_2_s*Csat_20_2*v*10^-3;
SOTR_7 = KLa20_1000_3_s*Csat_20_3*v*10^-3;
SOTR_8 = KLa20_1000_4_s*Csat_20_4*v*10^-3;

% CALCULATIONS OF AVERAGE SOTR FOR ALL PROBES [kg/h]

```

```
SOTR = (1/4)*(SOTR_1 + SOTR_2 + SOTR_3 + SOTR_4 + SOTR_5 + SOTR_6 +  
SOTR_7 + SOTR_8)*60;
```

```
% CALCULATIONS OF SAE [kg/kWh]  
SAE = SOTR/(DBP*10^-3);
```

```
% CALCULATIONS OF SOTE [%]  
SOTE = 100 * SOTR/(W02*3600);
```

## **DO.m**

```
function C = DO(b,X)  
Csat = 9.1;  
A=b(3)*b(1)+b(4)*Csat;  
B=-b(3)-b(4);  
C = 1/B*exp(B*X)*(A+B*b(2))-A/B;  
end
```



## APPENDIX D

### Calculation.m

```
% MODEL NR 3
% X = time and y = DO concentrations
options = optimset('TolFun',1.0e-7,'TolX',1.0e-7, 'MaxFunEvals', 1e7);
beta0 = [1; 3; 0.01]; % Initial guesses for [KLab; C0; KLas]
[beta1, resnorm1] = lsqcurvefit(@DO,beta0,X,y1,[0 -10 0]);
[beta2, resnorm2] = lsqcurvefit(@DO,beta0,X,y2,[0 -10 0]);
[beta3, resnorm3] = lsqcurvefit(@DO,beta0,X,y3,[0 -10 0]);
[beta4, resnorm4] = lsqcurvefit(@DO,beta0,X,y4,[0 -10 0]);
Cout1 = DO(beta1,X);
Cout2 = DO(beta2,X);
Cout3 = DO(beta3,X);
Cout4 = DO(beta4,X);

% CALCULATIONS OF PERFORMANCE PARAMETERS
% PARAMETERS TO MEASURE
T_before = [17.6 17.6 17.6 17.6]; % Water temperature before
% measurements [°C]
T_after = [17.7 17.7 17.7 17.7]; % Water temperature after
% measurements [°C]
Conductivity = [1430 1710]; % Conductivity before and
% after measurements [µS/cm]
z = 0.28; % Liquid depth [m]
Ab = 0.56; % Bottom floor area [m2]
Qp = 10.1/1000*60; % Measured air flow [m3/s]
P1 = 101.5; % Ambient atmospheric
% pressure [kPa]
Pp = (101.5*10^3 + 1000*9.82*z)/1000; % Gas pressure at
% measurement point [kPa]
T1 = 21.6+273; % Ambient air temperature
% [K]
n = 4; % Number of probes [-]

% CALCULATION OF THE AVERAGE WATER TEMPERATURE [°C]
T1medel = (T_before(1,1)+T_after(1,1))/2;
T2medel = (T_before(1,2)+T_after(1,2))/2;
T3medel = (T_before(1,3)+T_after(1,3))/2;
T4medel = (T_before(1,4)+T_after(1,4))/2;
T = (T1medel + T2medel + T3medel + T4medel)/n;

% FIXED PARAMETERS
Theta = 1.024; % Temperature constant [-]
R = 289; % Gas constant for air [Nm/kg*K]
k = 1.395; % Ratio of specific heats for gas. k = 1.395 for
% air with adiabatic compression
Ts = 293; % Temperature for standard condition [K]
rho = 1.2; % Density for air [kg/m3]
Ps = 101.3; % Standard barometric pressure [kPa]

% CALCULATIONS OF THE TANK VOLUME [m3]
V = Ab*z;

% CALCULATIONS OF THE AVERAGE CONDUCTIVITY [µS/cm]
Conductivity = (Conductivity(1)+Conductivity(2))/2;

% CALCULATIONS OF TDS (TOTAL DISSOLVED SOLIDS) [mg/L]
TDS = Conductivity*2000/3000;
```

```

% CALCULATIONS OF TEMPERATURE AT MEASUREMENT POINT Tp [°C]
Tp = T1*(Pp/P1)^( (k-1)/k );

% VOLUMETRIC AIR FLOW TO THE SYSTEM, AT AMBIENT CONDITIONS [m3/s]
Q1 = Qp*(T1/Tp)*(Pp/P1);

% STANDARD CONDITIONS AIR FLOW [m3/s]
Qs = Q1*(Ts/T1)*(P1/Ps);

% CALCULATIONS OF THE DELIVERED BLOWER POWER DBP [W]
K = (k-1)/k;
w = Qs*rho; % Mass flow of gas [kg/s]
DBP = (w*R*T1)/K*((Pp/P1)^K-1);

% TEMPERATURE CORRECTION OF KLa
KLab20_1_1 = beta1(1)*Theta^(20-T);
KLab20_1_2 = beta2(1)*Theta^(20-T);
KLab20_1_3 = beta3(1)*Theta^(20-T);
KLab20_1_4 = beta4(1)*Theta^(20-T);
KLas20_1_1 = beta1(3)*Theta^(20-T);
KLas20_1_2 = beta2(3)*Theta^(20-T);
KLas20_1_3 = beta3(3)*Theta^(20-T);
KLas20_1_4 = beta4(3)*Theta^(20-T);

% TEMPERATURE CORRECTION OF STEADY STATE DO
T_1 = T1medel + 273.15;
T_2 = T2medel + 273.15;
T_3 = T3medel + 273.15;
T_4 = T4medel + 273.15;
T_20_grader = 20 + 273.15;

A1 = -173.4292; B1 = -0.033096;
A2 = 249.6339; B2 = 0.014259;
A3 = 143.3483; B3 = -0.001700;
A4 = -21.8492;
S=0;

lnDO = A1 + A2*100./T_1 + A3.*log(T_1/100) + A4.*T_1/100 + S*(B1 +
B2.*T_1/100 + B3.*(T_1/100).^2);
Csurfsat_1 = 1.4276*exp(lnDO);

lnDO = A1 + A2*100./T_2 + A3.*log(T_2/100) + A4.*T_2/100 + S*(B1 +
B2.*T_2/100 + B3.*(T_2/100).^2);
Csurfsat_2 = 1.4276*exp(lnDO);

lnDO = A1 + A2*100./T_3 + A3.*log(T_3/100) + A4.*T_3/100 + S*(B1 +
B2.*T_3/100 + B3.*(T_3/100).^2);
Csurfsat_3 = 1.4276*exp(lnDO);

lnDO = A1 + A2*100./T_4 + A3.*log(T_4/100) + A4.*T_4/100 + S*(B1 +
B2.*T_4/100 + B3.*(T_4/100).^2);
Csurfsat_4 = 1.4276*exp(lnDO);

lnDO = A1 + A2*100./T_20_grader + A3.*log(T_20_grader/100) +
A4.*T_20_grader/100 + S*(B1 + B2.*T_20_grader/100 +
B3.*(T_20_grader/100).^2);
Csurfsat_20_grader = 1.4276*exp(lnDO);

```

```

Tao_1 = Csurfsat_1/Csurfsat_20_grader;
Tao_2 = Csurfsat_2/Csurfsat_20_grader;
Tao_3 = Csurfsat_3/Csurfsat_20_grader;
Tao_4 = Csurfsat_4/Csurfsat_20_grader;

% PRESSURE CORRECTION OF STEADY STATE DO (< 6.1 m depth)
Omega = P1/Ps;

% STEADY STATE DO SATURATION CONCENTRATION CORRECTED TO 20°C ETC.
% Css_20_1 = beta1(1)*(1/(Tao_1*Omega));
tolerance = 1.0e-7;
Cout = (Cout1+Cout2+Cout3+Cout4)/4;
KLab = (KLab20_1_1 + KLab20_1_2 + KLab20_1_3 + KLab20_1_4)/4;
int = quad(@integral, 0, z, tolerance,[], KLab, Acs, G, 0, P, Pwv, hd,
Csat_O2, yg0);
Css_20_1 = int*(1/(Tao_1*Omega));

% OPTIONAL TDS NORMALIZATION OF KLa [min-1]
KLab20_1000_1_1 = KLab20_1_1*exp(0.0000965*(1000-TDS));
KLab20_1000_1_2 = KLab20_1_2*exp(0.0000965*(1000-TDS));
KLab20_1000_1_3 = KLab20_1_3*exp(0.0000965*(1000-TDS));
KLab20_1000_1_4 = KLab20_1_4*exp(0.0000965*(1000-TDS));
KLas20_1000_1_1 = KLas20_1_1*exp(0.0000965*(1000-TDS));
KLas20_1000_1_2 = KLas20_1_2*exp(0.0000965*(1000-TDS));
KLas20_1000_1_3 = KLas20_1_3*exp(0.0000965*(1000-TDS));
KLas20_1000_1_4 = KLas20_1_4*exp(0.0000965*(1000-TDS));

% CALCULATIONS OF MASS FLOW OF OXYGEN AT STANDARD CONDITIONS
Wair = 1.20*Qs; % Mass flow of air, in SI units for U.S. practice
% [kg/s]
W02 = 0.23*Wair; % Mass flow of oxygen in air stream [kg/s]

% CALCULATIONS OF SOTR [kg/min]
SOTR_1 = int*KLab20_1000_1_1*V;
SOTR_2 = int*KLab20_1000_1_2*V;
SOTR_3 = int*KLab20_1000_1_3*V;
SOTR_4 = int*KLab20_1000_1_4*V;
SOTR_5 = Csat_O2*KLas20_1000_1_1*V;
SOTR_6 = Csat_O2*KLas20_1000_1_2*V;
SOTR_7 = Csat_O2*KLas20_1000_1_3*V;
SOTR_8 = Csat_O2*KLas20_1000_1_4*V;

% CALCULATIONS OF AVERAGE SOTR FOR ALL PROBES [kg/h]
SOTR = (1/4)*(SOTR_1 + SOTR_2 + SOTR_3 + SOTR_4 + SOTR_5 + SOTR_6 +
SOTR_7 + SOTR_8)*60;

% CALCULATIONS OF SAE [kg/kWh]
SAE = SOTR/(DBP*10-3);

% CALCULATIONS OF SOTE [%]
SOTE = 100 * SOTR/(W02*3600);

```

## DO.m

```

function Cout = DO(b,X)
yg0 = 0.266;
Acs = 0.56; % Cross section area [m2]
hd = 0.28; % Depth to aeration system [m]
Qp = 10.1/1000/60; % Measured air flow [m3/s]

```

```

rho_luft = 1.293; % Density for air
G = Qp*60*rho_luft*10^6*(1/yg0)*0.21; % OBS! Wrong gas flow rate
P = 101.5; % Ambient atmospheric pressure [kPa]
P = P/100; % [atm]
Pwv = 0.02; % Water vapor pressure [atm]
z = 0.28; % Water depth [m]
Csat_O2 = 9.5; % Saturation concentration at the
% water surface [mg/L]

options = odeset('RelTol',1.0e-7,'AbsTol', 1.0e-7);
KLab = b(1); % b = parameters to estimate
C0 = b(2);
KLas = b(3);
Cout = zeros(length(X),1);
options = odeset('RelTol',1.0e-7,'AbsTol', 1.0e-7);

if X(1) == 0
    [j,C] = ode15s(@fC1C2, X, C0, options, KLab, KLas, C0, Csat_O2,
    hd, z, Acs, G, P, Pwv, yg0);
    Cout(:,1) = C(:,1);
else
    [j,C] = ode15s(@fC1C2, [0 X], C0, options, KLab, KLas, C0,
    Csat_O2, hd, z, Acs, G, P, Pwv, yg0);
end
end

```

### **dC1C2.m**

```

function C1C2 = fC1C2(t, C, KLab, KLas, C0, Csat_O2, hd, z, Acs, G, P,
Pwv, yg0)
tolerance = 1.0e-7;
Q = quad(@fCO_eq, 0, z, tolerance,[], KLab, Acs, G, C(1), P, Pwv, hd,
Csat_O2, yg0);
C1=KLab/hd*(Q-C(1)*z)+KLas*(Csat_O2-C(1));
C1C2(1,1) = C1;
End

```

### **dCO\_eq.m**

```

function fCO_eq_out = fCO_eq(z, KLab, Acs, G, C1, P, Pwv, hd, Csat_O2,
yg0)

fCO_eq_out = ones(length(z),1)*yg0;
options = odeset('RelTol',1.0e-7,'AbsTol', 1.0e-7);

if z(1) == 0
    [t,yg] = ode15s(@fyg, z, yg0, options, KLab, Acs, G, C1, P, Pwv,
hd, Csat_O2);
    fCO_eq_out = Csat_O2*(P-Pwv+((hd-z)/10.33))/(1-
Pwv).*yg/0.266;
else
    [t,yg] = ode15s(@fyg, [0 z], yg0, options, KLab, Acs, G, C1, P,
Pwv, hd, Csat_O2);
    fCO_eq_out = Csat_O2*(P-Pwv+((hd-z)/10.33))/(1-
Pwv).*yg(2:end)./0.266;
end
end

```

## fyg.m

```
function dygdz = fyg(z, yg, KLab, Acs, G, C1, P, Pwv, hd, Csat_O2)
CO_eq = zeros(10000,1);
K2 = 3.13*10^-5;
CO_eq = Csat_O2*(P-Pwv+((hd-z)/10.33))/(1-Pwv)*yg/0.266;
dygdz = -KLab*(Acs/G)*((CO_eq-C1))*K2;
end
```

## integral.m

```
function fCO_eq_out = integral(z, KLab, Acs, G, C1, P, Pwv, hd,
Csat_O2, yg0)

fCO_eq_out = ones(length(z),1)*yg0;
options = odeset('RelTol',1.0e-7,'AbsTol', 1.0e-7);

if z(1) == 0
    [t,yg] = ode15s(@fyg, z, yg0, options, KLab, Acs, G, C1, P, Pwv,
hd, Csat_O2);
    fCO_eq_out = Csat_O2*(P-Pwv+((hd-z')/10.33))/(1-
Pwv).*yg/0.266./0.28.*KLab;
else
    [t,yg] = ode15s(@fyg, [0 z], yg0, options, KLab, Acs, G, C1, P,
Pwv, hd, Csat_O2);
    fCO_eq_out = Csat_O2*(P-Pwv+((hd-z')/10.33))/(1-
Pwv).*yg(2:end)./0.266./0.28.*KLab;
end
end
```